OPTIMAL SEISMIC RETROFITTING LEVEL FOR BRIDGES BASED ON BENEFIT-COST ANALYSIS

by

YULIN GAO

B.Sc., Central South University, 1987
M.Eng., Northern Jiaotong University, 1990

A THESIS SUBMITTED IN PARTIAL FULFILLMENT OF
THE REQUIREMENTS FOR THE DEGREE OF

MASTER OF APPLIED SCIENCE

in

THE FACULTY OF GRADUATE STUDIES

Department of Civil Engineering

We accept this thesis as conforming
to the required standard

THE UNIVERSITY OF BRITISH COLUMBIA

August 2001

In presenting this thesis in partial fulfillment of the requirements for an advanced degree at the University of British Columbia, I agree that the Library shall make it freely available for reference and study. I further agree that permission for extensive copying of this thesis for scholarly purposes may be granted by the head of my department or by his or her representatives. It is understood that copying or publication of this thesis for financial gain shall not be allowed without my written permission.

Department of Civil Engineering

The University of British Columbia
Vancouver, Canada

Date August 26, 2001.

ABSTRACT

There are a large number of seismically deficient bridges in British Columbia that need to be strengthened to protect public safety in future earthquakes. Many upgrading options are available for seismic rehabilitation of these bridges, such as No Retrofitting, Safety Level Retrofitting, and Functional Level Retrofitting, etc. The search of the optimal solution among various feasible options is a complicated decision problem. The big amount of money spent for seismic retrofitting needs to be justified based on the economic and safety decisions, and they involve considerations of risk and cost.

A reliability-based risk decision model is constructed in the thesis to try to facilitate an answer to the seismic retrofitting of bridges. The methodology and procedures of decision analysis are demonstrated through a case study bridge.

The global linear, elastic response spectrum analysis is undertaken to obtain seismic demand and the component capacity/demand ratios are computed to identify the critical structural components. Seismic deficiencies and failure mechanism of the identified critical components are evaluated by local inelastic push over analysis.

Two seismic retrofitting schemes are designed to counteract the seismic deficiencies. The effect of seismic retrofitting on the structural behavior during earthquake excitations is evaluated. The retrofitting costs of both schemes are calculated.

Structural failure probability during future earthquakes is calculated by the simple FORM/SORM approach. Latin Hypercube Sampling (LHS) is used to generate random variables to obtain seismic demand and seismic capacity, which are fitted to the probability distribution functions. Both the failure probabilities of original bridge and retrofitted bridge are computed. The reduced failure probability due to seismic retrofitting is obtained.

Seismic damage analysis is undertaken to compute damage indices of the bridge before and after seismic retrofitting, which are used for mapping out economic losses. Both direct and indirect economic losses are estimated. An expected value of the future

earthquake damage costs are calculated and discounted to the present year. Present values of the total costs including retrofitting cost and future seismic financial damages for all retrofitting schemes are calculated. Then a benefit-cost analysis based on the constructed decision model is undertaken to determine the optimal seismic retrofitting level for the bridge.

It concludes that for the case study bridge considered in this research, the optimal seismic retrofitting option is the level II retrofitting, which aims to keep normal or a limited traffic flow immediately after an earthquake of 10% exceedence probability in 50 years. Sensitivity analysis is made to explore the effect of change of input variables on the decision outcome.

TABLE OF CONTENTS

LIST OF TABLES

LIST OF FIGURES

ACKNOWLEDGEMENT

I would like to thank my supervisor, Dr. Robert Sexsmith, for his knowledgeable advice, not only for my research, but also for my study and life in UBC, his encouragement and his effort and time in reviewing the first draft and final draft of my thesis.

I would like to thank Dr. Richard Foschi, Dr. Donald Anderson and Dr. Peter Byrne for their suggestions and advices at the beginning of this research. Special thanks are given to Dr. Foschi for his time in reviewing the final draft of this thesis. I would also like to thank Dr. Carlos Ventura for letting me using the program SAP 2000.

Many thanks are owned to the engineers in the Ministry of Transportation and Highways, BC, including Mr. Peter Brett, Chief Bridge Engineer, Mr. Brock Radloff, Bridge Seismic Engineer and Mr. Shannon Tao, Geotechnical Engineer. They provided the bridge design drawings, seismic retrofit report, bridge cost data and geotechnical report at the bridge site.

The financial support provided by the Natural Science and Engineering Research Council of Canada (NSERC) is acknowledged. The financial support provided by the Ministry of Transportation and Highways, BC, through the sponsorship of Professional Partnership Program, is also gratefully acknowledged.

Finally, I would personally like to offer my deepest appreciation to my wife, Qingping and my daughter, Qingyi, for their love, understanding and support.

Chapter1 Introduction

1.1 Background

There has been a long recognized seismic risk to bridges in British Columbia. To minimize the seismic risks, the Ministry of Transportation and Highways (MoTH) has initiated a two-phase bridge seismic retrofit program since 1989 (BCMoTH, 2000). Phase I program includes bridges on Lifeline and Disaster Response Routes, while the bridges on Economic Sustainability Routes and some other bridges are included in the phase II program. Recognizing the different seismic hazard zones, the importance of bridges and the limited funding to the retrofit work, the bridges are being retrofitted in stages. Two levels of retrofitting have been adopted in the phase I program, i.e. Safety retrofitting and Superstructure retrofitting.

Although the effectiveness of retrofitting has not been tested for real earthquakes in BC, the recent earthquakes in California have demonstrated the improved seismic performances of bridges after retrofitting (Caltrans, 1994 & Yashinsky, 1998). There was no or only light damages to the seismic retrofitted bridges during Northridge earthquake in 1994, whist those unretrofitted deficient ones experienced severe damages or collapse. The effectiveness and efficiency of seismic strengthening in both lab tests and most importantly, in real earthquakes, have motivated and accelerated seismic retrofitting work around the world where there is a high seismic risk. In California, Caltrans has executed a three-step seismic retrofitting plan for all seismically deficient bridges (Roberts, 1990). The retrofitting has evolved from the one-level safety retrofitting in early 1980's to the current performance-based two-level upgrading; namely safety level and function level retrofitting. The new Caltran's Seismic Design Criteria (Caltrans, 1999) has explicitly set a performance-based framework for the design of new bridges and upgrading of existing ones.

Currently, the seismic retrofitting to bridges is to the safety level only in BC. The ultimate goal of the retrofit is to prevent the collapse of bridges and maintain the bridge structure integrity after an earthquake. However, recognizing the great effects on local

economy caused by moderate to large earthquakes in California, the Ministry has set possible functional service requirement to bridges in both phase one and phase two program. But, the execution of this stringent requirement will depend on the review of bridge performances in future earthquakes. The more expensive and difficult functional retrofitting will be undertaken if the warranted bridge performances can be assured in the future earthquakes (BCMoTH, 2000).

According to the Bridge Seismic Retrofit Program, more than half bridges have been retrofitted in phase I program, and the bridges in phase II program will be retrofitted starting this year. An urgent question facing the decision-maker is which level should a bridge be strengthened to. There is no easy and immediate answer to such a hard question. Adequate information is not readily available, and the high variability of seismic hazard and the uncertainty in structural properties make the problem even more complicated. The best possible solution is through a reliability-based decision model. However, considering the many engineering, economy and policy factors involved, such a decision model can in no way be elaborate and accurate. A large amount of engineering judgement is still required.

To try to facilitate an answer to the aforementioned question, a reliability-based risk analysis of both original and retrofitted bridges during possible future earthquakes will be undertaken in this research. Such an analysis will give some useful hints on the selection of seismic retrofit levels, which can best be chosen based on the trade-off between safety and economy.

1.2 Purpose of the research

Facing a big stock of bridges, a three-step procedure can be adopted for the retrofitting decision. Firstly, a preliminary screening of all bridges to prioritize the bridges is undertaken. At this stage, complicated structural analysis will normally not be preferred. Rather some empirical factors considering the seismic hazard, the importance of the structure and the structural type will be utilized. Secondly, detailed seismic analyses will be made for the prioritized bridges to determine their seismic behaviors during future earthquakes. Because of the huge cost involved in the strengthening an existing bridge,

the time-consuming analysis is usually cost-effective. The analysis results can greatly help to identify the seismic deficiencies and determine the real needs for retrofitting. Thirdly, a risk-based decision model can be constructed for the bridges identified in step 2. Having seismic deficiencies been identified, various retrofitting schemes can be realized to update the bridge to different performance levels. Then the seismic risk corresponding to different retrofitting level can be computed; hence the optimal retrofitting level can be found.

The proposed research will put emphasis on the step 3, i.e., constructing a risk-based decision model to determine the optimal seismic retrofitting level for bridges. More specifically, the purposes of the research are as follows:

- A performance-based framework will be utilized. The expected performance levels and the corresponding earthquake levels will be defined.
- The fragility curves of both original and retrofitted structure during various earthquake excitations will be computed, and therefore the decreased failure probability due to seismic strengthening can be estimated.
- The quantified seismic damages to the original and retrofitted structure will be calculated using damage indices. Subsequently the economic damage in dollars can be evaluated based on the relationship between the physical damage index and the loss in dollars.
- The seismic risk will be assessed based on the computed failure probability and the damage in dollars. Then, the decision model can be constructed following the seismic risk determination of original structure and the retrofitted structures that are updated to different performance levels.
- The optimal seismic retrofitting level will be found based on trade-off between the economy and safety. The optimal level is the retrofitting with the minimum net present value in dollars.

1.3 Scope of the research

The ultimate purpose of the research is to find the optimal seismic retrofitting level for a specific bridge. As described in section 1.2, this objective can only be realized through a

rational decision analysis, which is based on the extensive reliability analysis and in-depth seismic behavior analysis.

Ideally a complete seismic analysis can determine the deformations and forces in the structure during the process of a strong earthquake. Based on the computed actions, the seismic damages can be evaluated, and the structural performances can be evaluated as well. However, the currently available analysis technique cannot always guarantee such an aim can be met. The earthquake load is highly variable, with a coefficient of variability as high as 100% (FEMA, 1997a). And the structural capacity has a big uncertainty due to the scattered material property. Moreover, the uncertain dynamic properties, such as mass and damping, the soil-structure interaction and the modeling error, contribute to the complexity of the problem.

The reliability-based seismic analysis can help clarify the uncertainties associated with the complicated problem. A range of possible values for various parameters can be input into the analysis to determine the most probable behavior that the structure will experience in future earthquakes. The structure can be subjected to different levels of ground excitations, in the form of spectral accelerations, to represent the seismic hazard variability. An extensive reliability analysis will be made in the proposed research to construct the bridge fragility curves.

For the retrofit decision, the first and the most important step is to evaluate the seismic deficiency and possible damages to the structure during an earthquake. An in-depth seismic analysis will be undertaken in the proposed research. State-of-the-practice analysis technique will be utilized to identify the seismic deficiency and quantify the seismic damage. Efforts are put to try to simplify the modeling and analysis since the reliability analysis needs numerous repeated calculations. Also the need for applying the proposed method to other similar bridges in BC is always kept in mind. A practical methodology suitable for the practicing engineers to use will be sought. Based on the above considerations, response spectrum analysis will be used to compute the global seismic demands, and the seismic capacity is to be found through a static nonlinear push

over analysis of various components. The quantification of seismic damage is calculated by nonlinear time history analysis of isolated bents.

The scope of research can be described in detail as follows:

- The seismic hazard in the specific bridge site will be computed using a Type II maximum probability distribution function. The spectral accelerations corresponding to the 10% & 2% exceedence in 50 years will be obtained from the new seismic hazard curve developed by GSC (GSC, 1999).
- The global response spectral analysis of the whole bridge will be utilized to calculate the seismic demands.
- The nonlinear static push over analysis of component will be undertaken to compute the seismic capacity based on the inelastic sectional property analysis.
- The reliability analysis will be made to construct the fragility curves based on the computed seismic capacity and seismic demand.
- Retrofitting design using up-to-date techniques will be done to upgrade the bridge to various performance levels.
- The nonlinear time history analysis will be used to compute the seismic damages to isolated bents.
- Seismic risk to the bridge will be defined as the product of the failure probability and the damage in dollars.
- The net present values of all retrofitting options will be calculated. Then the optimal seismic retrofitting level of the bridge is found based on the benefit/cost analysis.

1.4 Thesis outline

Chapter 1 will have a general introduction to the thesis. Background of the proposed research, the research purpose and the research scope will be described.

Chapter 2 will give a literature review of researches related to seismic risk analysis and present value decision analysis. The framework of performance-based design/retrofitting will be reviewed as well. The application of performance-based design/retrofitting to bridges will be discussed in detail. For the decision making of seismic retrofitting of

bridges, a performance-based present value decision process is to be proposed. Such a risk-based decision model will be used in the following chapters to obtain the optimal seismic retrofitting level for the case study bridge.

Chapter 3 will introduce the bridge used for the case study in this research. Structural configuration, material property, soil condition and the current status of the bridge will be described in detail. The seismic hazard on the bridge site will also be discussed.

Seismic behavior assessment of the case study bridge will be the subject in Chapter 4. Seismic deficiencies will be identified through the global response spectrum analysis and local push over analysis.

A two-level seismic retrofitting, namely Safety level retrofitting and Functional level retrofitting will be designed in Chapter 5. The state-of-practice retrofitting techniques will be adopted. Seismic analyses will be undertaken to assess the effects of retrofitting on structural behaviors of the case study bridge.

An extensive reliability analysis to compute the failure probability of the bridge during future earthquakes will be the topic in Chapter 6.

Seismic damage analysis will be undertaken in Chapter 7. Damage index of isolated bent subjected to various levels of earthquake excitations will be calculated using nonlinear time history analysis. The seismic damage in dollars will be evaluated based on the relationship between the physical damage and the damage in dollars.

Chapter 8 will construct a risk-based decision model. The seismic risk is defined as the product of failure probability of the structure and the failure consequence in dollars. Various retrofitting options will be included in the decision model. The optimal retrofitting level will be determined corresponding to the minimum net present value of the total cost or the maximum benefit to cost ratio. Sensitivity analyses will also be presented in Chapter 8.

Chapter 9 will give conclusions following previous calculations and some discussions will also be presented.

Chapter 2 Seismic Risk Analysis and Present Value Decision Model

2.1 Introduction

In upgrading a deteriorated infrastructure, decisions need to be made regarding the appropriate rehabilitation schemes. Various options are available to decision-makers, such as strengthening the structure to meet the new design code requirements, retrofitting to a less demanding performance level, or simply doing nothing, leaving it as it is. For seismic retrofitting, the cost incurred at present is providing protection to existing structures for future earthquakes. The large amount of money spent, however, needs to be justified based on the economic and safety decisions, and they involve considerations of risk and cost (Sexsmith, 1994). A decision analysis model based on risk analysis is appropriate for this purpose.

Failure probability and failure consequences of structures during a given seismic event need to be evaluated before any decision analysis can be undertaken. A reliability-based seismic risk analysis can provide valuable information for the use of decision analysis.

A literature study will be made to the seismic risk analysis and performance-based seismic rehabilitation technique in this chapter firstly. Then the present value decision analysis and some related researches are to be discussed. Finally the procedures proposed for the performance-based present value decision analysis in the case of determining optimal seismic retrofitting level for bridges will be presented.

2.2 Literature study

2.2.1 Seismic risk analysis (SRA)

Seismic risk is defined as the probability that consequences of an earthquake, such as structural damage, will equal or exceed specified values in a specific period of time. The prohibitive economic loss resulting from recent earthquakes has propelled and accelerated the seismic risk analysis (SRA) of built infrastructure subjected to future earthquakes. Due to advances in earthquake engineering & technology, and improved

data collection in recent earthquakes, some sophisticated models for SRA have been constructed. They have been successfully used in the prioritisation of bridge seismic retrofitting (Basoz & Kiremidjian, 1994, Maffei & Park, 1994), regional seismic loss estimation (King & Kiremidjian, 1994, Hwang et al, 2000), and seismic assessment of specific structures (Song & Ellingwood, 1999, Seya et al, 1993).

2.2.1.1 Seismic reliability assessment of reinforced concrete frames

The reliability assessment of a structural system subjected to a seismic event is a meaningful way of accounting for the large amount of uncertainties associated with both the seismic input and the structural modelling. Numerous researches have been made to conduct such a reliability-based seismic assessment. Identifying the randomness in the earthquake excitation as the most significant source of uncertainty, some studies consider this as the only random variable (Colangelo et al, 1996 and Tzavelis & Shinozuka, 1988). Others have dealt with advanced methods of representing this uncertainty alongside some fundamental structural variables (Singhal & Kiremidjian, 1996 and Seya et al, 1993). The selection of input random variable and simulation technique is a balance between the analytical precision and computation time.

In the study by Dymiotis and his colleagues (Dymiotis et al, 1999), unlike other researches, a much greater emphasis is given to issues relating to the structural modelling, while keeping the matter of variability in the seismic input as simple as possible. The focus is on the model uncertainty and randomness in member capacity and failure criteria. The strengths of the procedure adopted are briefly described as follows.

1) Probabilistic modelling of uncertainties: uncertainties in structural property, such as member capacity and drift capacity, are explicitly accounted. The capacity is directly estimated within the structural analysis program.
2) Structural modelling: the lumped plasticity approach is used to account for the inelastic behaviour. An extended version of DRAIN-2D/90 program is selected for the dynamic, inelastic time history analysis. Local damage index computation and the capability of accounting for member failure are included in the program.

3) Seismic input: the uncertainties in seismic input are accounted through an appropriate strategy — a number of records from actual earthquakes are considered. Three earthquake records are found to be adequate for this study.
4) Simulation strategy: the random variables are generated by the Latin Hypercube Sampling (LHS) method. LHS is an approach that may achieve a certain level of accuracy with a much smaller sample size than that required for the direct Monte Carlo method. Simulation is used to compute a fragility curve from each input ground motion.

The outputs of a reliability-based seismic assessment are fragility curves, which are defined as structural failure probability versus a peak ground acceleration or spectral acceleration. Some typical fragility curves of reinforced concrete frames computed by Dymiotis et al are shown in Fig. 2.1. It can be seen that mean vulnerability curve given by appropriately selected three earthquake records is very close to the one obtained from all seven records, which are Greece earthquake (AGEL), El Centro earthquake (ELC), Loma Prieta earthquake (LPRL), Kalamata earthquake (KALW), San Fernando earthquake (SFERT), Alkyonides earthquake and Volvi earthquake. A_d is the spectrum intensity derived from the EC8 design spectrum.

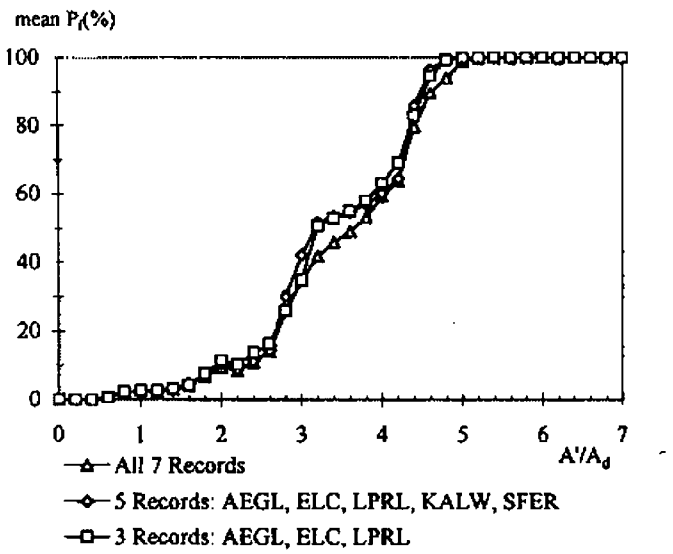

Fig 2.1 Mean vulnerability curve for reinforced concrete frames
(After Dymiotis et al, 1999)

2.2.1.2 Seismic reliability assessment of steel moment frames

Song & Ellingwood (Song & Ellingwood, 1999) used both deterministic and probabilistic approaches to evaluate seismic behaviour of weld connection in steel moment frames. Four welded special moment-resisting frames which had weld fractures during the Northridge earthquake, 1994 were taken as case studies. Firstly, a deterministic assessment was made. A new hysteretic model that incorporates the effects of connection weld fractures on building response was adopted in the analysis. The actual recorded earthquake time history was used for seismic input. The agreement of predicted and surveyed damage was relatively good for two of the frames, but generally poor for the other two. It was concluded that the ability of advanced nonlinear dynamic analysis tools to predict damage in steel frame buildings subject to strong ground motions was somewhat unpredictable. The lack of agreement may be attributed to inherent uncertainties and omissions in the modelling process. The uncertainties may be summarized as follows:

1) The structural properties (stiffness, mass, and damping) actually are random variables instead of deterministic quantities.
2) There are uncertainties in estimating the nonlinear behaviour of the connections, as well as variations in the member's mechanical properties.
3) Uncertainties in estimating the ground motions are known to be significant.

Then, an in-depth probabilistic analysis was performed. The role of inherent randomness and modelling uncertainty on building performance was considered in detail. The LHS technique was utilized to yield a probabilistic description of building performance. Roof drift angle (RDA) and inter-story drift angle (ISDA) were taken as performance indicators. Four levels of performance indications and their corresponding limit states are assumed and shown in Table 2.1. With this approach, the surveyed damage fell within the scatter of damage predicted by probabilistic modelling. The study showed that the probability analysis (computed mean damage ratios range from fractions of 1.8/16 to 2.9/16) continued to underestimate the damage observed (actual damage ratio with a fraction of 4/16), even with randomness in the structural parameters and with ground

motion taken into account. However, inclusion of the parameter uncertainties in predictions of building response indicated the variability in connection damage that was likely to occur and improved insight into building performance in comparison to a single deterministic analysis.

Table 2.1 Limit states used in the analysis (After Song & Ellingwood 1999)

Performance requirements	Structural Criterion	
	RDA (%)	ISDA (%)
LS_0 = Serviceability	0.5	0.5
LS_1 = Onset of nonstructural damage	1	1
LS_2 = Impaired function	2	2
LS_3 = Incipient collapse	5	5

To analyze seismic risk of the moment frame steel buildings with welded connections, a fragility curve, which is defined as limit state probability, conditioned on a specific spectral acceleration, was computed as follows.

$$F_R(x) = P(LS|S_a = x) \qquad \text{Equation 2.1}$$

A fragility curve for any limit state was obtained from the cumulative distribution function of the ISDA or the RDA. For example, if the limit state is 2% ISDA, then

$$P(LS|S_a = x) = 1 - P[ISDA < 2\%|S_a = x] \qquad \text{Equation 2.2}$$

The computed fragility curves for RDA and ISDA are shown in Fig. 2.2 and Fig. 2.3 respectively. They can give much more information for the potential structural damages to the building than a deterministic analysis. In Fig. 2.2 and 2.3, bilinear hysteretic model means undamaged steel connection, and degraded hysteretic model incorporates the effects of damage due to weld fracture and subsequent nonlinear response of the connection.

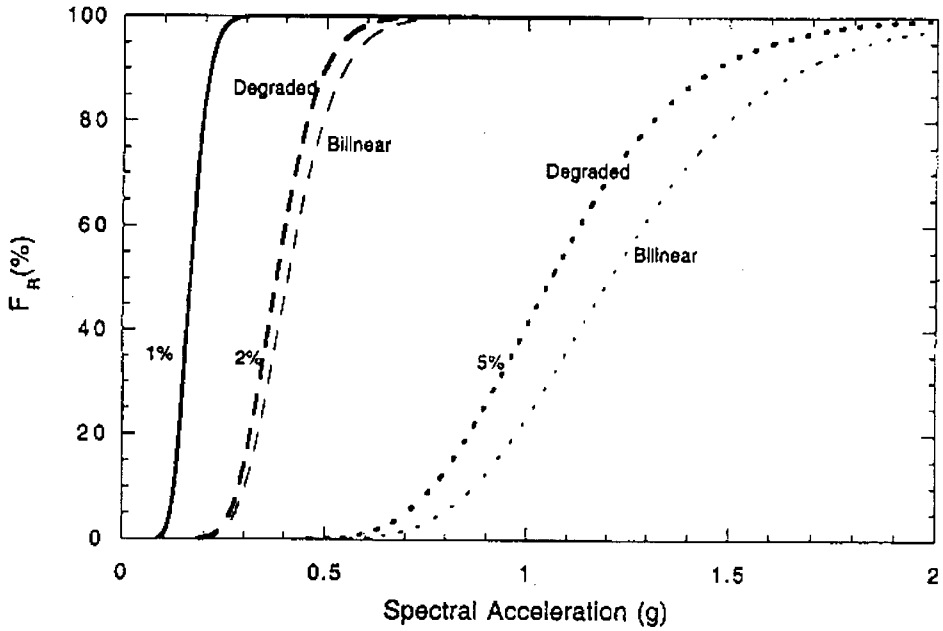

Fig. 2.2 Fragility curve for RDA of steel moment frames
(After Song & Ellingwood, 1999)

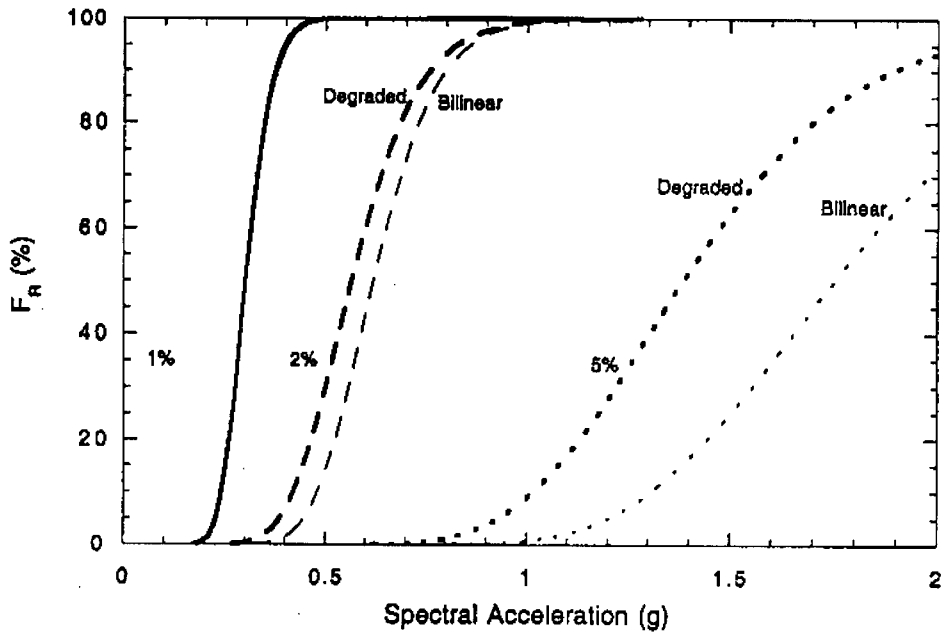

Fig. 2.3 Fragility curve for ISDA of steel moment frames
(After Song & Ellingwood, 1999)

2.2.1.3 Seismic damage estimation of bridges and highway systems

Hwang and his colleagues (Hwang et al, 2000) have used SRA to evaluate regional seismic damages to bridges and highway systems. The evaluation procedure is reproduced here as in Fig. 2.4.

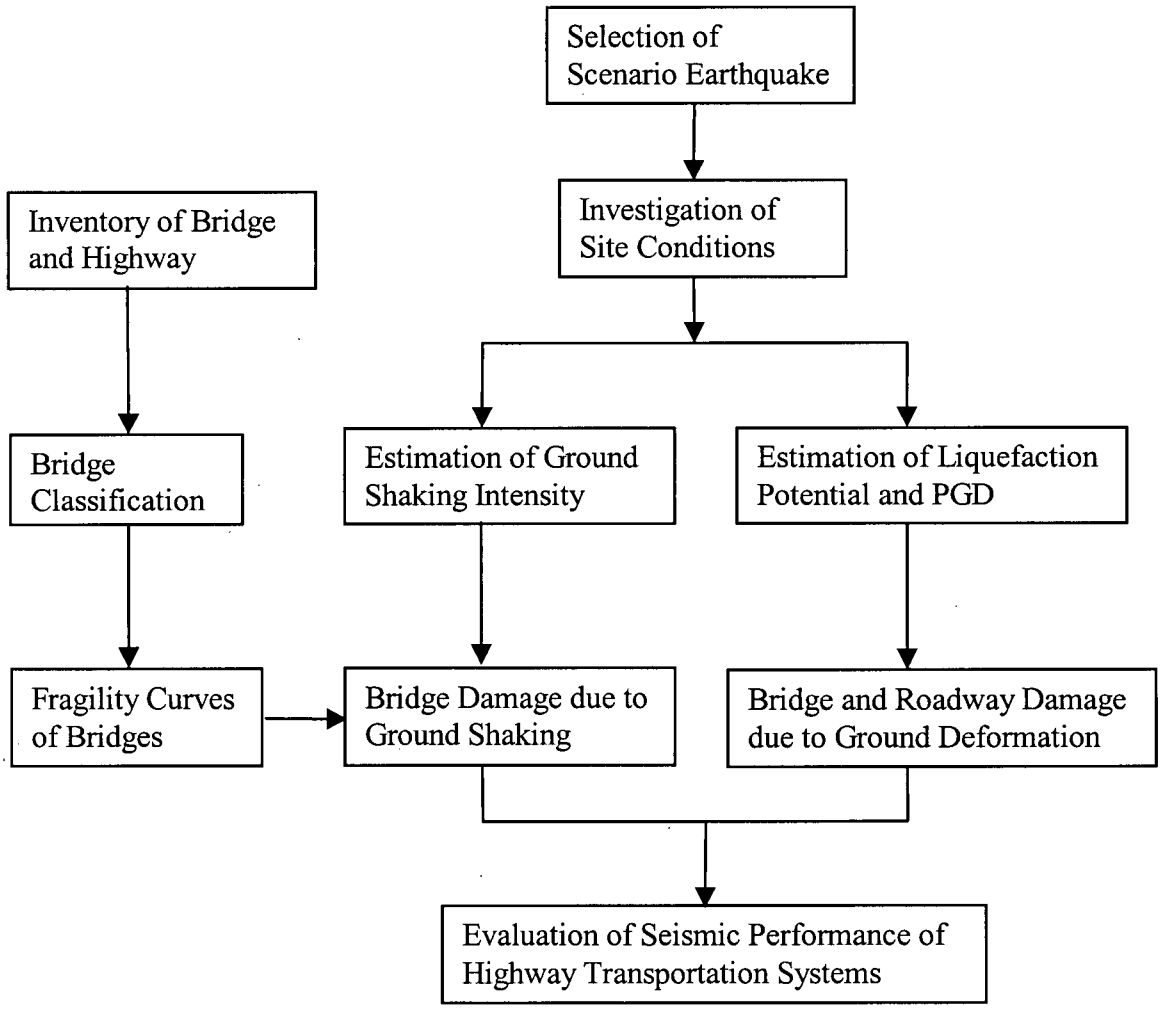

Fig. 2.4 Procedure for evaluation of seismic damage to bridge and highway transportation system (After Hwang et al, 2000)

Some features of this evaluation methodology are as follows:

1) A Geographic Information System (GIS) software is used for the development of bridge inventory.
2) The bridge classification is based on the NBIS/Federal Highway Administration recording and coding guide (FHWA, 1988). The bent or pier information is included for the classification purpose.
3) Fragility curves of specified bridge types are computed. Three structural damage states are defined in the study, namely no/minor damage, repairable damage, and significant damage. Damage states are determined according to the component capacity/demand (C/D) ratios, which are calculated using AASHTO code. Uncertainties in seismic capacity and demand are considered. The specified three damage states and corresponding C/D ratios are summarized in Table 2.2. Obviously, this is a crude estimation of structural damages during a given seismic event. For each level of peak ground acceleration, 50 calculations of bridge damage states are performed. The bridge damage data are statistically analyzed, and the results are displayed as fragility curves. Some typical fragility curves from the analysis are shown in Fig. 2.5 & Fig. 2.6. Fragility curves #1 to #6 represent different bridge classifications.
4) Seismic hazards are computed based on a scenario earthquake with the moment magnitude M of 7.0 occurring at Marked Tree, Memphis. Two hazards are considered: ground shaking and soil liquefaction. Site - specific attenuation relations, soil amplification factors, and soil liquefaction potentials are calculated. Both hazards are expressed in terms of PGA in different areas.
5) Seismic damages to bridges and roadways are determined using some simple rules. If the probability of no/minor damage or the probability of significant damage of a bridge is > 50%, then the bridge is expected to sustain no/minor or significant damage, respectively. Otherwise, the bridge is expected to sustain repairable damage. The study shows that, 160 bridges are expected to sustain significant damage; 136 bridges sustain repairable damage; and the remaining 156 bridges sustain minor or no damage, with a bridge family of 452 bridges in the area studied.

Although some crude estimates and engineering judgements are made in the seismic damage analysis and fragility curve computation, the results obtained from the study can be used to prepare a pre-earthquake preparedness plan, and to develop a post-earthquake emergency response plan.

Table 2.2 Definitions of damage states and corresponding C/D ratios (After Hwang et al 2000)

Damage state	Description	C/D ratios
No/ Minor damage (N)	Although minor inelastic response may occur, post-earthquake damage is limited to narrow cracking in concrete. Permanent deformations are not apparent.	$C/D \geq 0.5$
Repairable damage (R)	Inelastic response may occur, resulting in concrete cracking, reinforcement yield, and minor spalling of cover concrete. Extent of damage should be limited. Repair should not require closure. Permanent offsets should be avoided.	$0.5 > C/D \geq 0.33$
Significant damage (S)	Although there is minimum risk of collapse, permanent offsets may occur, and damage consisting of cracking, reinforcement yielding, and major spalling of concrete may require closure to repair. Partial or complete replacement may be required in some cases.	$C/D < 0.33$

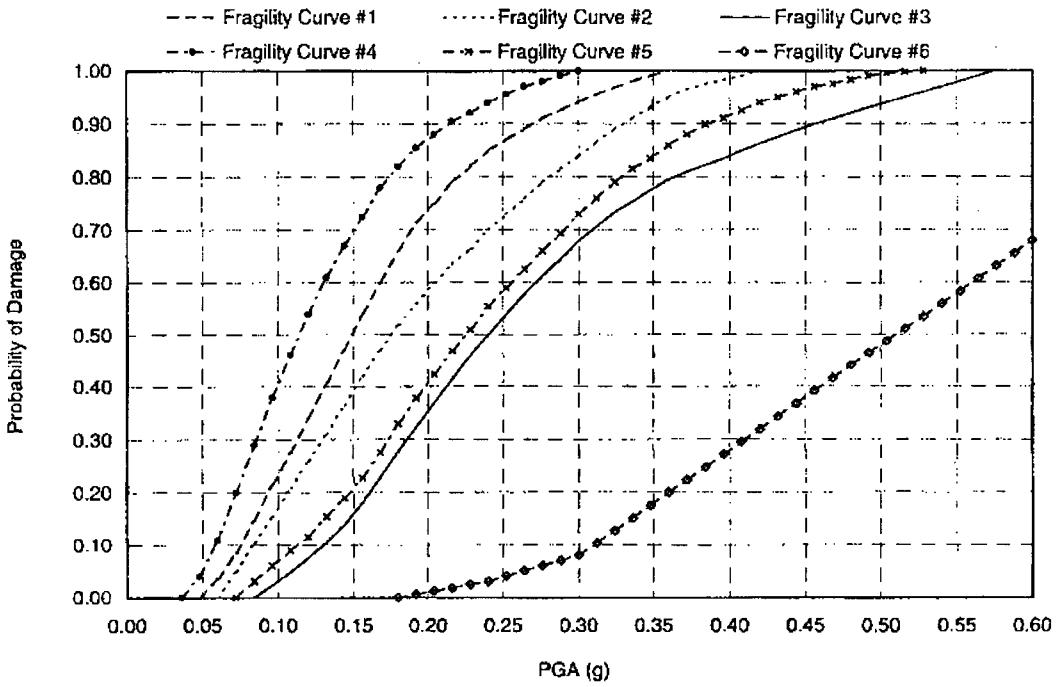

Fig. 2.5 Fragility curves for repairable damage (After Hwang et al, 2000)

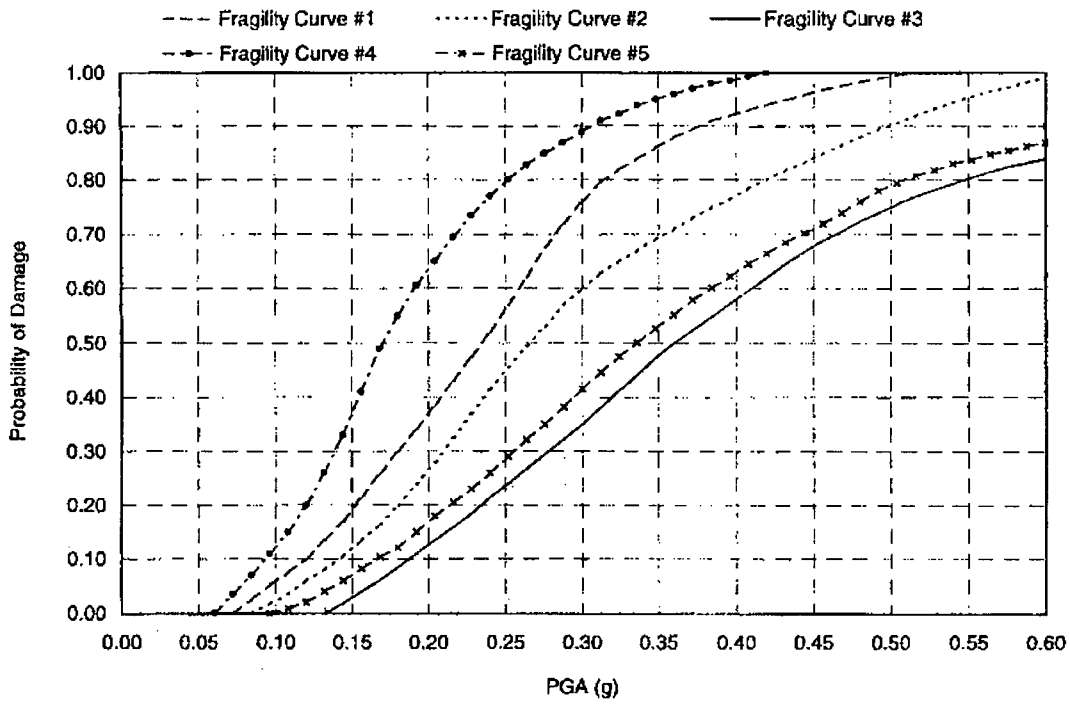

Fig. 2.6 Fragility curves for significant damage (After Hwang et al, 2000)

2.2.2 Performance-based seismic rehabilitation

Currently, most of the bridge seismic design codes, such as AASHTO (AASHTO, 1996), CAN/CSA-S6-90 (CSA, 1990), are focused mainly on life safety and preventing total collapse of the structure. Correspondingly seismic retrofitting of bridges is to the safety level only. The ultimate objective of strengthening is to maintain structural integrity and stability after an earthquake.

Seismic retrofitting practice presently in use is prescribed-based and focused on strength and capacity of structural members. The structure's overall performance during a given seismic event cannot be clearly described. Only one earthquake level is defined, i.e., the earthquake with 10% probability of exceedence in 50 years. Equivalent static force method and linear elastic analysis technique are used for the determination of forces and displacements. And the inelastic behaviour is accounted approximately by a force reduction factor, which is based on a component ductility factor for the considered bridge.

Present seismic design/retrofitting approach has many limitations, in which the most prominent one is its incapability to consider different seismic performance requirements. Although bridges designed/strengthened according to the present method are likely to survive the collapse, the significant damage suffered in recent earthquakes lead to a demand for a revised code that can predict the structure's performance in a given earthquake so as to minimum the financial damage incurred. With the development of more accurate and sophisticated structural design and analysis programs now available, great progresses have been made in the performance-based approach.

Following the milestone document on the performance-based engineering by the Structural Engineers Association of California Vision 2000 Committee (SEAOC, 1995), several standards or manuals based on performance-based approach have been developed, such as Japanese Seismic Design Method, Seismic Rehabilitation Recommendation for Buildings (FEMA-273), Caltran's Bridge Seismic Design Criteria (Caltrans, 1999) etc. In British Columbia, the Ministry of Transportation and Highways (BCMoTH, 2000) issued Bridge Seismic Retrofit Design Criteria in July 2000, which is based on the structural

performance requirements. A brief introduction to the BC Seismic Retrofit Design Criteria will be given as follows since the strategy and procedure outlined in this document will be applied in the case study bridge for this research.

As stated in the BC Seismic Retrofit Design Criteria, the level of retrofit protection is selected based on the importance of the route and the structure, the site seismicity, and the required post – earthquake performance of the structure in terms of traffic access and the acceptable damage. Four importance categories, i.e. Lifeline Bridges, Disaster Response Route Bridges, Economic Sustainability Route Bridges and Other Bridges, are classified for bridges that are currently candidates for seismic retrofitting. The classifications are made on the basis of social/survival and economic recovery requirements.

Seismic retrofitting levels for different bridge classifications are specified in Table 2.3. Three retrofit levels are defined, namely Superstructure retrofitting, Safety retrofitting and Functional retrofitting. Bridges shall be designed/retrofitted to meet one of the seismic performance criteria specified in Table 2.4, which is expressed in terms of the service levels and damage levels.

Table 2.3 Seismic retrofitting levels

Bridge Classification	Seismic Zones	Retrofit Level	
		Current Stage	Possible Ultimate Stage
Lifeline Bridges	4,5,6	Safety	Functional
	2,3	Superstructure	Safety
	0,1	Superstructure	Superstructure
Disaster Route/ Economic Route Bridges	4,5,6	Safety	Functional
	2,3	Superstructure	Safety
	0,1	None	None
Other Bridges	4,5,6	Superstructure	Safety
	2,3	Superstructure	Superstructure
	0,1	None	None

Table 2.4 Seismic performance criteria (After BCMoTH, 2000)

Retrofit Level	Seismic Performance Criteria	
	Service Level	Damage Level
Functional	Immediate	Minimal
Safety	Limited to Significantly Limited	Repairable to Significant
Superstructure	Possible complete loss of service for a prolonged period	Limited risk of collapse

Performance-based design/retrofitting is a risk-based approach. The money spent on initial structural strength currently determines the consequence the owner will take in the future. Generally, the performance-based approach will likely result in a more costly bridge (Floren & Mohammadi, 2001). However, the higher initial cost will be compensated by less damage and repair required following a seismic event. The engineer is in a better position to inform the owner the potential risk, and the latter can make a better decision as to strengthen the structure or not.

2.3 Present value decision analysis

2.3.1 Outline

Seismic risk analysis (SRA) can provide valuable information as to the possible structural behaviours during future earthquake events. The fragility curve obtained from SRA shows probability of failure against a range of earthquake excitations. However, in some special cases, such as in repair or retrofit of existing facilities with remaining life shorter than that of a new one, or in construction of temporary facilities, design based on probability alone would not be sufficient to resolve all problems. Due to the complexity of the problem and inadequate information available, they are often determined based on judgement, experience and consequences in the engineering practices. As a result, the long-term risk versus benefit implications of such design is not clear and cannot be easily quantified.

An appropriate approach should involve risk and cost considerations. Given the uncertainties in earthquake loads, structural behaviour and performance under a given earthquake loading, risk and probability must be considered when defining adequate design/retrofit criteria. Decision analysis principles can be utilized to find the most cost-effective scheme. For those difficult decisions, a more comprehensive treatment is required from a life cycle cost point of view, in which the uncertainty in the earthquake loading and structural resistance, cost versus benefit of the retrofit scheme and the time factor are all taken into consideration.

2.3.2 Previous study

2.3.2.1 ATC approach & FEMA approach

Some pioneering work has been done by Applied Technology Council (ATC) and Federal Emergency Management Agency (FEMA) to estimate the economic impact of a major earthquake. ATC-13 (ATC, 1985) provides estimates of percent physical damage versus levels of earthquake intensity for 78 existing facility classes in California, including 36 building structure classes. Damage Factor (DF), which is defined as the ratio of dollar loss to replacement, is estimated by more than 70 senior-level earthquake engineering experts. For each facility class, the experts were asked to provide a low, best, and high estimate of DF at Modified Mercalli Intensities (MMI) VI through XII. The low and high estimates were defined to be the 90% probability bounds of the DF distribution, while the best estimates was defined by the experts as the DF most likely to be observed for a given MMI and facility class.

ATC-21 (ATC, 1988) presents a Rapid Screen Procedure (RSP) to quickly identify the primary structural lateral load resisting system and significant seismic–related defects on individual buildings. Based on the field survey data, a scoring system, which relates to the probability of each building sustaining major life-threatening structural damage during a major earthquake, is introduced. Firstly, a Basic Structural Hazard (BSH) score, ranging from 1 to 8.5, is assigned to each building, depending on the building type and the NEHRP Map area. Next, each of the Performance modifiers present in a building is assigned a Performance Modification Factor (PMF), ranging from –2.5 to +2.0. Finally,

each building is assigned a Structural Score (S), equals to the BSH score plus the sum of all the PMF values for the building. Higher numbers in S mean better seismic resistance.

ATC-13 and ATC-21 can be combined to correlate Damage Factor (DF) to Structural Score (S). Therefore, estimates of structural damages due to strong earthquakes can be made. Obviously, no detailed structural analysis is needed for this approach and the estimates are very crude. It is mainly based on the expert's experience and judgments.

FEMA has always been very active in the development of methods for seismic rehabilitation of buildings so as to effectively resist the hazards imposed by earthquakes. FEMA-227 (FEMA, 1992) presents a benefit-cost analysis model for the seismic rehabilitation of hazardous buildings, which is designed to reduce expected damages and casualties from future earthquakes. Decision making about the prospective seismic rehabilitation of existing structure may be difficult because of the myriad of complex and often contentious engineering and public policy issues involved. Benefit-cost analysis can help determine whether the future benefits of prospective seismic rehabilitation are sufficient to justify the present costs of the project.

In the FEMA-227 documents, benefit-cost analysis provides estimates of the benefits and costs of a proposed seismic rehabilitation project. The seismic performance of a building before and after the proposed rehabilitation project is to be assessed. The benefits are avoided future damages and losses that are expected to accure as a result of the rehabilitation project. Costs include the engineering, construction, and other costs required to rehabilitate buildings. When the expected benefits exceed costs (i.e., benefit/cost ratio greater than one), rehabilitating existing buildings may be economically justified. Rehabilitating existing buildings may not be economically justified when the expected benefits are less than the rehabilitation costs (i.e., benefit/cost ratio less than one).

At the time when the benefit/cost analysis model was developed by FEMA in 1992, its intended use was for classes of building types or for groups of buildings of various classes and uses rather to be applied to specific, individual buildings since the model was based on typical, approximate values for building parameters and performance. More

specifically, the data including building class, damage probability matrices, retrofit effectiveness, retrofit costs and replacement cost, etc. was exclusively based on ATC-13, in which lots of crude, approximate assumptions and judgments were made.

Therefore, combining ATC-13, ATC-21 and FEMA-227 can give a rational benefit/cost analysis model to be used in the seismic retrofit decision of groups of hazardous buildings. However, in the case of specific, individual structure, local data is desirable and more refined structural analysis is required to compute seismic damage probabilities and consequences.

2.3.2.2 Research by Sexsmith and his students

Sexsmith has successfully applied decision analysis in the seismic retrofitting prioritization of bridges for the City of Vancouver (Sexsmith, 1994). In his study, the total cost for an adopted retrofitting scheme is defined as in equation 2.3,

$$C_T = C_0 + C_P \qquad \text{Equation 2.3}$$

$$C_p = C_f \times \frac{\nu}{\lambda + \nu} \qquad \text{Equation 2.4}$$

in which, C_T is the total cost, C_0 is the initial retrofitting cost, C_p is the expected present value of the consequences, C_f is the consequences due to catastrophic damage that occur at a future time t, both C_p and C_f are expressed in dollars. ν is the annual occurrence rate of earthquake and λ is real interest rate. A Poisson process of occurrence of seismic events is assumed for the derivation of equation 2.4. The most cost-effective retrofit action is that the total cost is the minimum.

Sexsmith used a present value decision model in the retrofit decisions for a set of three bridges. Firstly, the seismic risk in accordance with National Building Design Code in Vancouver is identified. Then, the probability of structural damage is calculated. It's based on the linear elastically calculated component capacity to demand ratio and various levels of peak ground velocity (PGV) on site. Annual failure probability of component is defined as half the probability of exceedence of PGV. Subjective estimates were made to

obtain different levels of failure probabilities. It concludes that, while a more refined analysis to establish the probability of damage is desirable, engineering judgement has to be applied regardless of the availability or lack of availability of accurate quantitative information. Thirdly, the consequences of damage are estimated. Again, some crude estimates are made. Finally, the decision model is constructed. Benefit-to-cost ratios of different retrofit options are computed, and the most cost-effective option is found.

Kim (Kim, 1998) applied present value decision analysis in the hypothetical seismic retrofitting prioritization of two bridges damaged in the Northridge earthquake, California, 1994. The procedures are similar to that adopted by Sexsmith (Sexsmith, 1994). The only improvement made by Kim is that a nonlinear time history analysis is used to compute damage index of an isolated bent. The failure consequence of structure is evaluated based on the relationship between the physical damage index and the damage in dollars. But, the failure probability of the bridge during an earthquake is simply defined as the occurrence probability of earthquake event itself. That is still a very crude assumption. The results inferred from the constructed present value decision model concluded that seismic retrofitting would not be economically justified for the particular bridge studied by Kim, if only direct damage costs were considered. Retrofit was justified when estimated indirect costs were included.

2.3.2.3 Research by Wen and his colleagues, University of Illinois

Wen et al (Wen & Kang, 1998) applied risk-based decision analysis in the determination of the optimal system yield force coefficient for a 9-storey steel office building located in downtown Los Angeles.

A life cycle cost analysis procedure is formulated. Uncertainties with earthquake loading and structural resistance are treated. Costs include those of initial construction, maintenance and operation, repair, damage and failure consequences (including loss of revenue, deaths and injuries, etc.) and they are discounted to a specified year. The expected total cost is expressed as a function of time t and the design variable vector X as follows,

$$E[C(t,X)] = C_0(X) + E\left[\sum_{k=1}^{N(t)}\sum_{j=1}^{l} C_j e^{-it_j} P_{kj}(X,t_k)\right] + \int_0^t C_m(X)e^{-i\tau}\,d\tau \qquad \text{Equation 2.5}$$

in which, C_0 = the construction cost for new or retrofitted facility;

C_j = cost of j-th limit state being reached at time of the loading occurrence, expressed in present dollar value. It includes costs of damage, repair, loss of service, and deaths and injuries;

C_m = operation and maintenance cost per year;

X = design variable vector, e.g., design loads and resistance;

k = number of severe loading occurrences;

N(t) = total number of severe loading occurrences in t, a random variable;

t_k = loading occurrence time, a random variable;

j = number of limit states;

l = total of number states under consideration;

i = constant discount rate per year;

P_{kj} = probability of j-th limit state being exceeded given the k-th occurrence of a single hazard or joint occurrences of different hazards;

e^{-t} = discounted factor over time t.

If hazard occurrences can be modelled by a Poisson Process with occurrence rate of ν per year and for resistance that is time-invariant, Equation (2.5) can be simplified. For the case of a single hazard, a close form can be obtained,

$$E[C(t,X)] = C_0 + (C_1P_1 + C_2P_2 + \ldots + C_kP_k)\frac{\nu}{i} \times (1 - e^{-it}) + \frac{C_m}{i}(1 - e^{-it}) \qquad \text{Equation 2.6}$$

Using the aforementioned decision analysis model, the optimal design yield force coefficient of the building is determined as in the following procedures:

1) The building is designed according to the existing building design code. Nine different designs are undertaken. Their fundamental periods and system yield

force coefficients (determined from a static push over analysis divided by the system weight) are calculated.

2) Building performance levels are defined as in Table 2.5. The corresponding limit states in terms of drift are described in Table 2.6.

3) Probabilities of failure are computed.
   - Seismic hazard is defined. Ground excitation demand for a given probability level is calculated according to the procedure recommended by FEMA 273 (FEMA, 1997).
   - An equivalent nonlinear single degree of freedom system (SDOF) is used to calculate the drift ratio. The drift ratio is then multiplied by correction factors to obtain drift ratio of multi – degree of freedom system (MDOF).
   - A generalized extreme value distribution function is used to fit the drift ratio to probability. The annual limit state exceedence probabilities for each structure are obtained.

4) The life cycle cost is estimated.
   - Initial construction cost C_0: 1996 BCCD (Building Construction Cost Data) are used. In general, the initial cost is proportion to design intensity.
   - Maintenance cost C_m: the maintenance cost is not considered.
   - Limit state cost C_j : the limit state cost includes direct damage cost, loss of contents, relocation cost, economic cost, cost of injury and cost of human fatality. Cost function is estimated based on FEMA – 227 reports (FEMA, 1992).

5) Present value life cycle expected cost C_{pv}: equation 2.6 is used to calculate the present value life cycle expected cost. A constant discount rate of 0.05 is assumed and occurrence rate of significant earthquakes of 0.1165/year is used. Fig. 2.7 shows the relationship between C_{pv} and system yield force coefficient.

6) Determination of optimal system yield force coefficient CF_y: a polynomial equation is fitted to the present value life cycle cost to determine the minimum C_{pv} and corresponding optimal CF_y. The optimal CF_y is found to be 0.188.

Table 2.5 Damage description of the performance level (After Wen & Kang, 1998)

Performance level	Performance description	Overall building damage	Permissible permanent drift
1	Fully operational	Negligible	< 0.2%
2	Operational	Light	< 0.5%
3	Life safety	Moderate	<1.5%
4	Near collapse	Severe	<2.5%
5	Collapse	Complete	>2.5%

Table 2.6 Limit states in terms of drift (After Wen and Kang, 1998)

Limit State	Drift ratio
1	$\delta<0.002$
2	$0.002<\delta<0.005$
3	$0.005<\delta<0.015$
4	$0.015<\delta<0.025$
5	$0.025<\delta$

Fig 2.7 Expected life cycle cost and system yield force coefficient (After Wen & Kang, 1998)

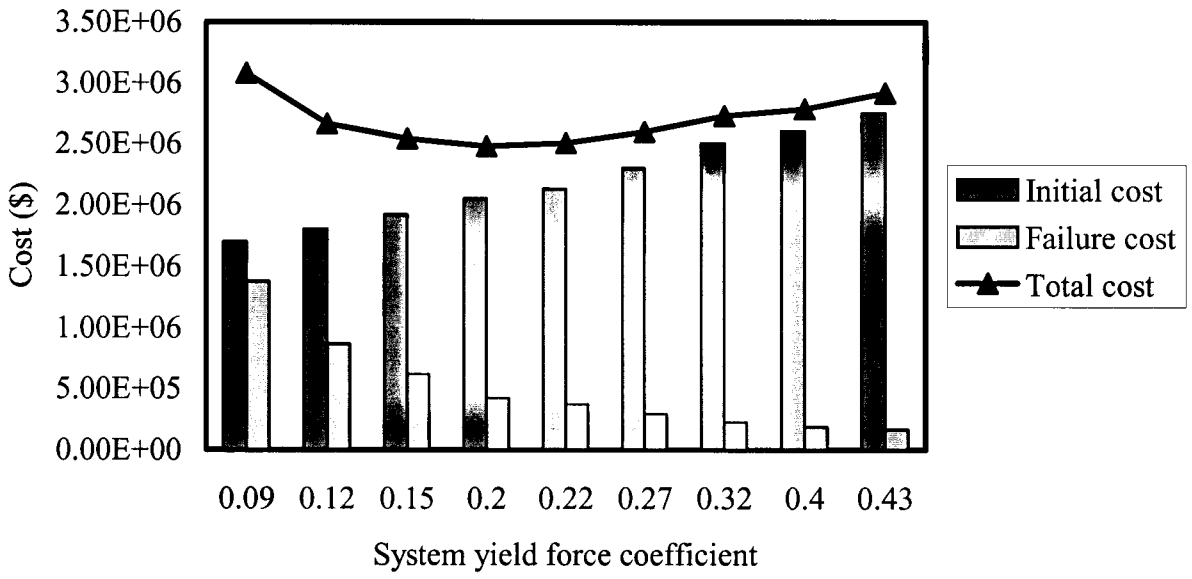

2.4 Performance-based present value decision analysis and procedures

The key elements in the present value decision analysis are evaluation of failure probability of the structure during earthquake events and the financial damage estimation, in dollars. As seen from literature study, some very crude estimates are made due to lack of adequate information and data. Also, a thorough reliability analysis for the structural responses due to earthquake loading is very time-consuming and complicated.

After review of some decision models for the practical use in the decision making regarding to the seismic event, an effort is made in this research to try to apply decision analysis principles in the determination of the optimal seismic retrofitting level for an existing concrete bridge. Decision analysis will be combined with performance-based design/retrofit requirements. A detail description of this case study bridge will be given in Chapter 3. The procedures of such a risk-based decision analysis are described here and in Fig. 2.8. Some comments and explanations are given as follows:

- Performance-based approach will be utilized in the study. The expected performance level and damage level will be defined firstly before seismic retrofitting is commenced. Different seismic retrofit level depends on the performance level expected for the bridge.
- A detailed in-depth seismic behaviour assessment and an extensive reliability analysis will be undertaken in the study. Seismic deficiencies in the existed structure will be identified and site-specific parameters will be used in the analysis. The enhanced dynamic analysis is expected to bring more confidence in the decision-making.
- Identifying the difficulties and uncertainties existed for the problem, a simple yet effective approach is developed in this study to evaluate the failure probability of the structure due to earthquake excitations. Latin Hypercube Sampling (LHS) technique is used to generate random variables for the reliability analysis input. The detail discussions of this approach are presented in Chapter 6.
- The focus of the reliability analysis will be on the uncertainty in structural property estimation, while the highly variable earthquake loadings will be treated through the use of probability-based site-specific earthquake spectrum. The spectral accelerations used in the study will be based on a probability model of Type II distribution of largest value.
- The financial damage estimations are made from the mapped-out relationships between the physical damage index and the financial damage, in dollars. This relationship is inferred from previous researches and the observations made from lab tests.

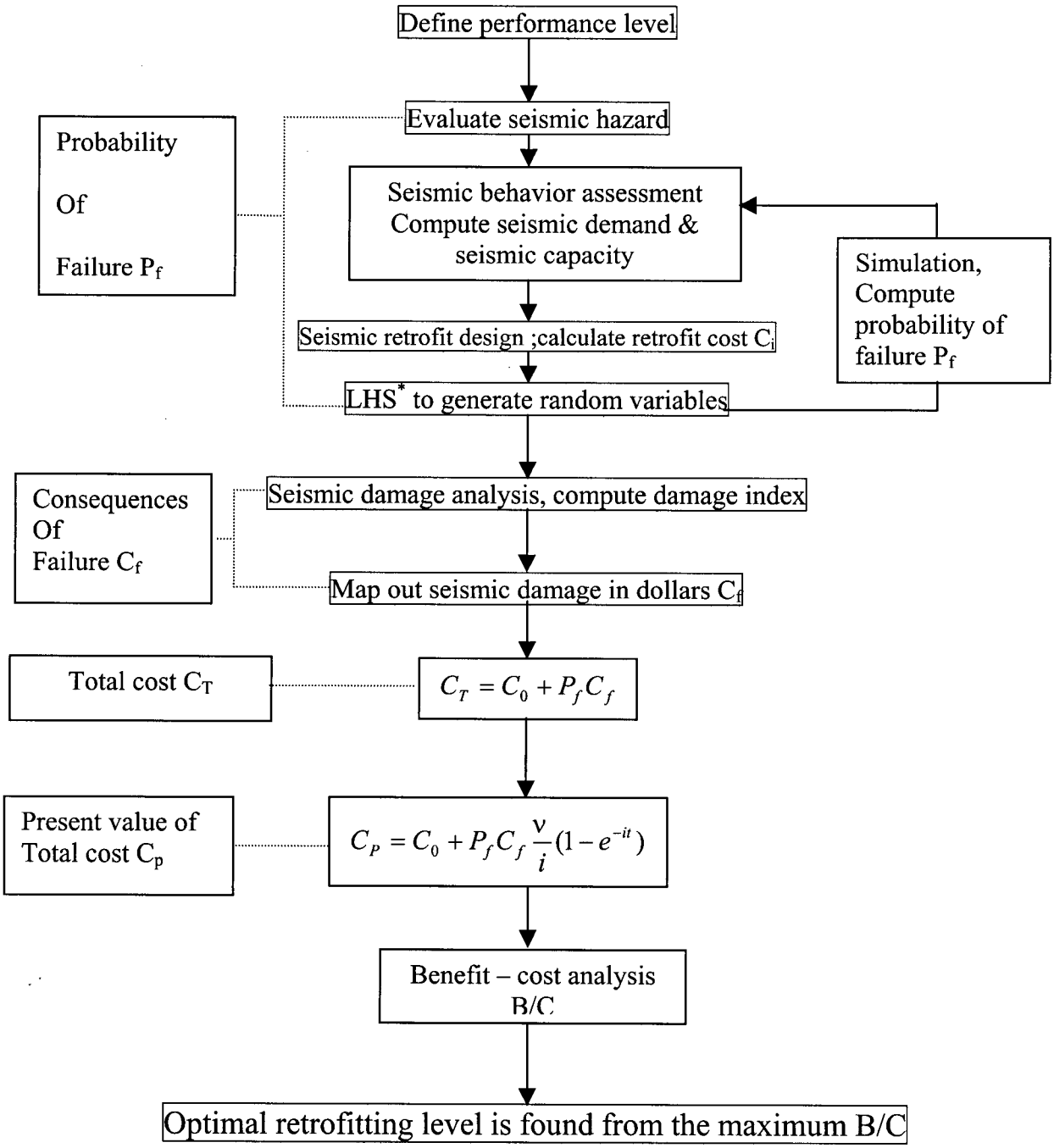

Note: 1. LHS means Latin Hypercube Sampling. It will be described in detail in Chapter 6.
2. ν is the annual occurrence rate of significant earthquakes in time t;
i is the real interest rate;
t is the time in years.

Fig. 2.8 Procedure of performance-based present value decision analysis

Chapter 3 Case Study: Colquitz River North Bridge

3.1 Introduction

The Colquitz River North Bridge will be introduced in this Chapter as a case study bridge. Detailed seismic performance analysis and reliability analysis of this bridge will be undertaken in the following chapters. Present value decision model is to be constructed to determine the optimal seismic retrofitting level for this bridge.

In this Chapter, a general description to the case study bridge will be given firstly. The bridge location, superstructure, substructure and bridge foundations will be briefly introduced. Then, soil conditions at the bridge site are to be described. Main findings of soil properties from two geotechnical reports are presented. Finally seismic hazard at the bridge site will be computed based on the new Canadian seismic hazard map from Geological Survey of Canada (GSC, 1999).

3.2 Structural configuration & bridge location

3.2.1 General description & bridge location

Colquitz River North Bridge (Colquitz Bridge) carries traffic over Colquitz river and Interurban road. It is located in the suburb of the City of Victoria, only about 15 km from downtown Victoria. The bridge is an important component in Highway 1 linking Victoria to Nanaimo. Fig. 3.1 shows the key plan of the bridge site.

The bridge was first built in 1953. In 1980, the bridge deck was upgraded. Due to the importance of the bridge to emergency response and early recovery after an earthquake, the bridge was categorized in the provincial Disaster Response Route and classified as in the Phase One seismic retrofit program by Ministry of Transportation and Highways in 1984 (BCMoTH, 2000).

The as - built drawings of Colquitz bridge (BCMoTH, 1953) are attached in Appendix A. Bridge elevations and bridge general arrangement are included. Some recent pictures of

the bridge taken during a field trip to the site (Gao & Kahn, 2000) are displayed in Fig. 3.2.

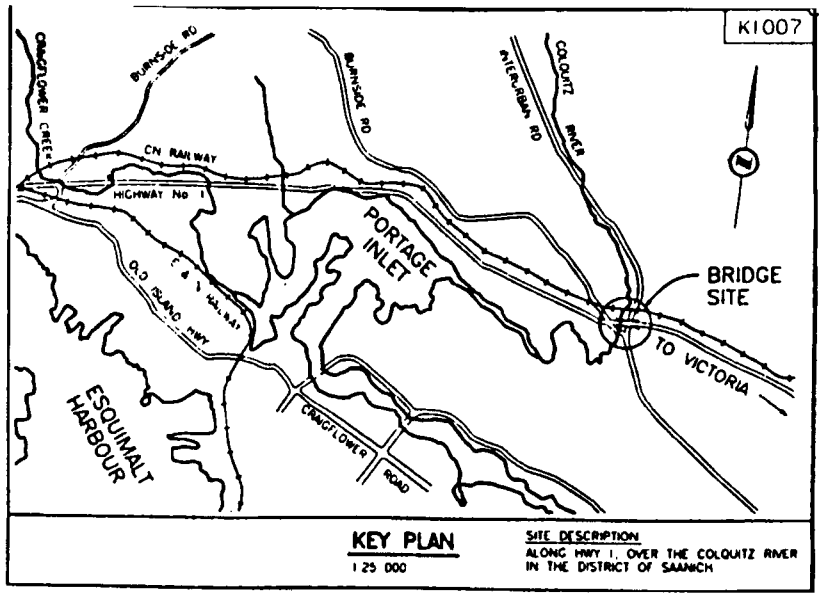

Fig 3.1 Key plan of the case study bridge

(a) Bridge overview looking to the south

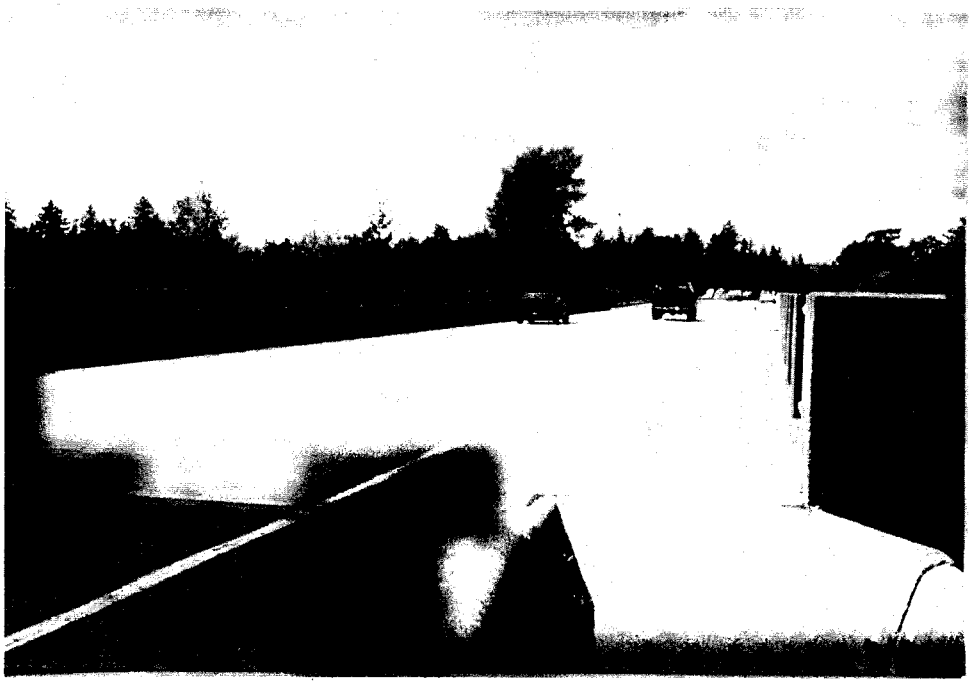

(b) Bridge deck looking to the west

Fig 3.2 Pictures of the case study bridge

3.2.2 Superstructure

Colquitz Bridge is a five span continuous steel girder bridge with reinforced concrete deck. The spans are 14.1m, 18.1m, 18.3m, 18.1m and 14.1 m with a total length of 82.7m. The superstructure consists of six steel girders spaced at 1.98 m and a 170mm thick concrete deck. Steel channel diaphragms are provided for the lateral bracing at every ¼ span and piers except at both ends of the bridge.

The asphalt deck was used when the bridge was first built in 1953. During the deck upgrading in 1980, the asphalt deck was replaced by a reinforced concrete overlay of the same dimension. However the deck was slightly changed by removing one side of sidewalk for pedestrians.

Steel bearings are used for the supports. Expansion rocker bearings, which have steel pintles engaging the upper sole plate and lower bearing plate, exist at pier 1 & 4 and both

abutments. Fixed bearings, which consist of a steel bar sandwiched between an upper sole plate and a lower bearing plate, are located at pier 2 and 3.

It is found from the drawings that no shear connectors are available between the concrete deck and the underlying steel girders. There is therefore, no direct load path, other than pure bond between the concrete and the steel girders, through which to transfer lateral forces into the underlying elements. It is also identified that there are no transverse shear keys in the concrete bents and abutments. This makes the steel bearings the only components to transfer lateral load from superstructure to substructure.

3.2.3 Substructure

3.2.3.1 Piers and abutments

Two column reinforced concrete bents are used for the four bridge piers. Column heights for bent 1 to 4 are 6.86m, 10.32m, 9.75m and 8.64m respectively. The two abutments are seat type with a straight breast wall. There are no wing walls for the abutments.

Fig. 3.3 shows geometry and general dimensions of the concrete bent, all four bents are similar in dimension and steel reinforcement arrangement. The detailed sections of cap beam and columns, as well as steel reinforcement are given in Fig. 3.4.

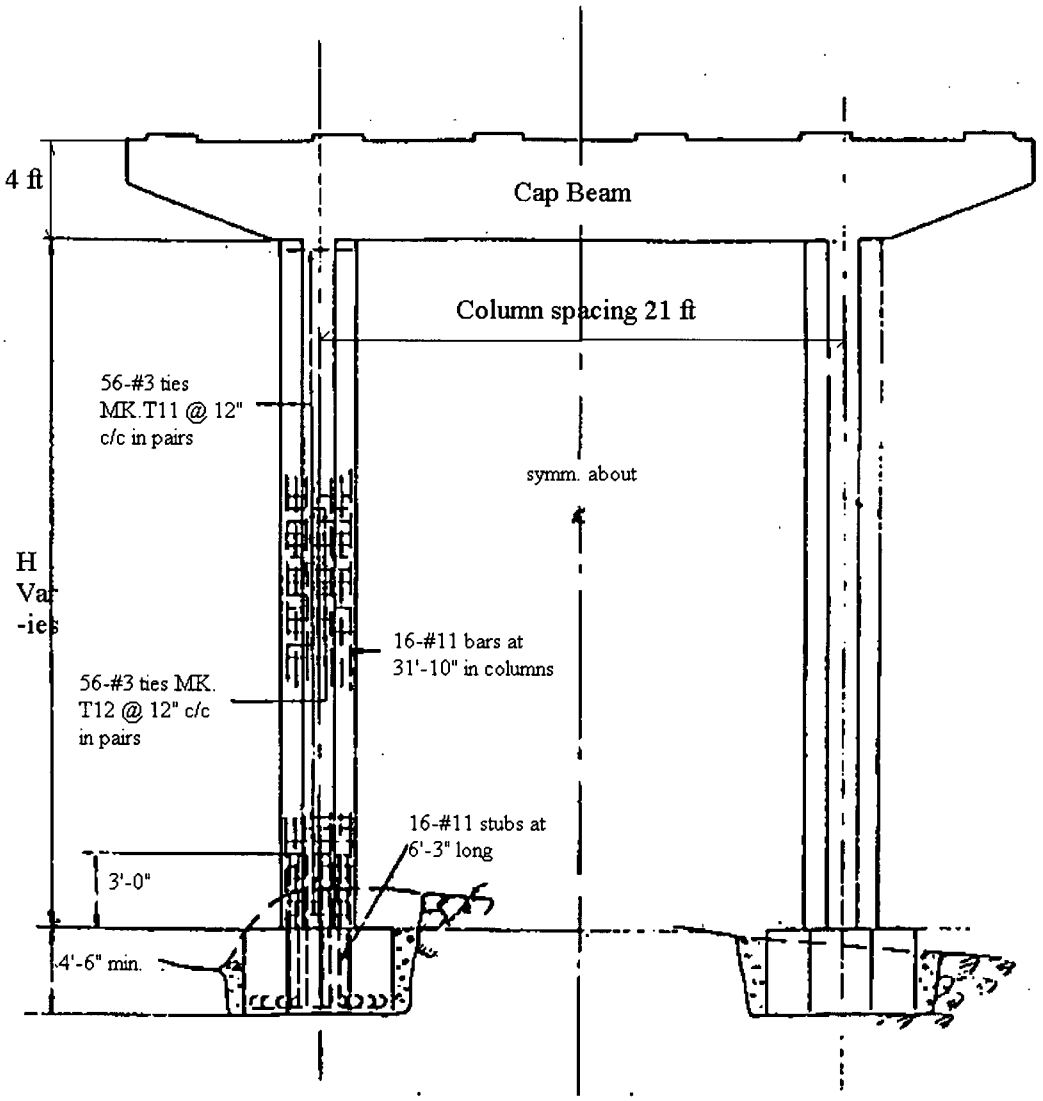

Fig. 3.3. Bent geometry and general dimensions

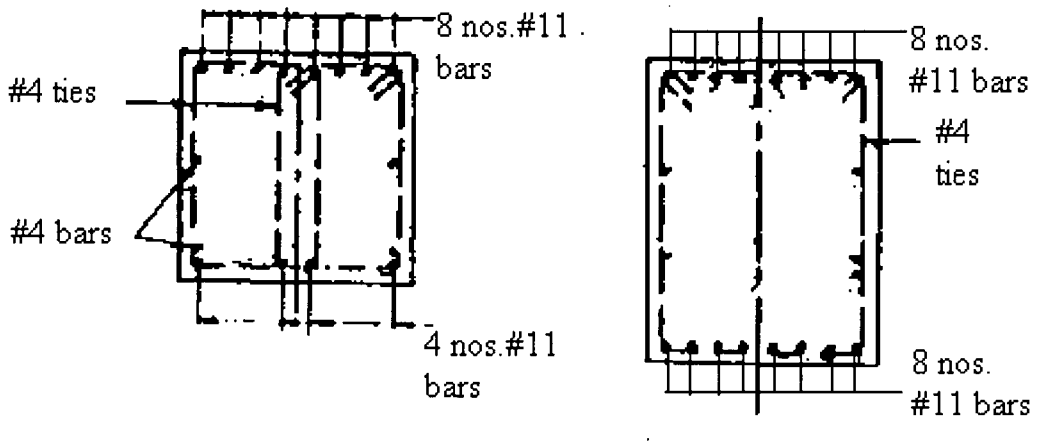

(a) Cap beam section at ends (b) Cap beam section at mid – span

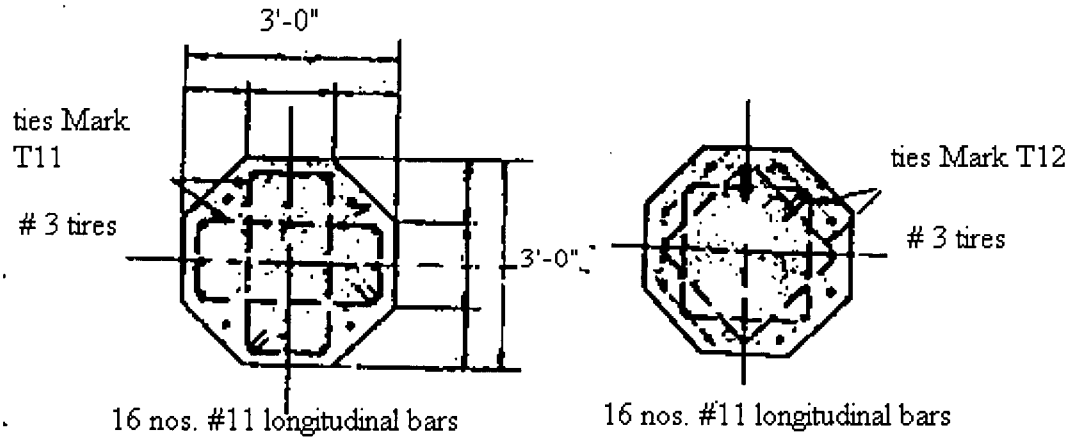

(c) Column section

Fig.3.4 Concrete sections and steel reinforcement

For the cap beam, a rectangular section is used with the dimension of 3' (915mm) width and 4' (1220mm) depth. 8 nos. #11 bars are used for the top reinforcement longitudinally; and for the bottom reinforcement, 8 nos. #11 bars are placed in the middle part of the span, in which 4 nos. bars are cut off at both ends of the cap beam. The cut off bars have a straight length of 18' (5.4m). #4 bars with a spacing of 1' (305mm) are used for the beam stirrups.

The columns have an octagonal section with the outer dimension of 3' (915mm) by 3' (315mm). 16 nos. #11 bars or #9 bars are generally used for the longitudinal reinforcement. Bar splice with a splice length of 3'6" (1065mm) is existed at bottom of the column. Lateral stirrups are #3 ties with a centre spacing of 12" (305mm).

3.2.3.2 Foundations

Footings are generally used for the foundations of west abutment and bent 2 to bent 4. Steel H piles are used for east abutment and bent 1.

The pile cap for bent 1 has a plan dimension of 6' (1830mm) wide and 9' (2745mm) long with a depth of 4'6" (1370mm). Only bottom reinforcements are provided for the pile cap. No top bars are available in the section.

Footings for other bents have an octagonal shape with the outer dimensions of 6' (1830mm) by 6' (1830mm). Similar to pile cap in bent 1, only bottom reinforcements are available for the section.

3.3 Soil conditions

Three soil reports at different times are available for the case study bridge. One (BCMoTH, 1953) was made in 1953, when the Colquitz bridge was first built. Then in 1976, in order to build the Colquitz South bridge, another soil test (BCMoTH, 1976) was undertaken at a location about 20 m south of the interested bridge. Six boreholes were driven and borehole logs were prepared. In 1994, the other soil test (BCMoTH, 1994) was made to evaluate soil properties for the purpose of seismic retrofitting of Colquitz bridge. Both soil log and shear wave velocities of the soil were made available by two Cone Penetration Tests. A brief introduction to the findings from the last two geotechnical reports will be given as follows.

The general average ground level is at +5m. At the top five meters below ground, the soil is firm to stiff brown silty clay. The soil at this level has a undrained shear strength of

more than 60kpa. At some locations, it is up to about 100kpa. The blowcount is over 20. Underneath the top layer soil, from the elevation of 0m to about –10m, is the soft to firm soil and grey sand. The soil has a undrained shear strength of around 20 to 30 kpa. The obtained shear wave velocities V_s from the two CPT tests are given in Table 3.1. The average shear wave velocity in the table 3.1 is calculated according to the definition given in ATC – 32 (ATC, 1996).

Based on soil properties described as in the above, the soil at the bridge site may be classified as Type E Soil according to ATC – 32 (ATC, 1996). Values of soil amplification factor F are taken from table RC3 – 2 in ATC – 32 (ATC, 1996).

The detailed soil data is attached as in Appendix B.

3.4 Seismic hazard

3.4.1 General description

Seismic hazard assessment is very important for the seismic damage estimation of structures subjected to future earthquakes. Various methodologies are available for a seismic hazard assessment at a particular bridge site. However, a thorough and well – defined seismic hazard evaluation for the bridge in this case study is not possible within the time and scope of this work. In this research, seismic hazard at the bridge site will be computed based on the Uniform Hazard Spectra (UHS) presented in the new seismic hazard map by Geological Survey of Canada in 1999(GSC, 1999). Also, a probabilistic seismic hazard model will be presented in this study to calculate spectral accelerations corresponding to different probabilities of exceedence.

Table 3.1 Soil shear wave velocity

Test Hole No.	Elevation (m)	Soil layer depth below the ground elevation (m)	Average depth (m)	Vs (m/s)	Average Vs (m/s)
TH94 - 3	11.84	0.00			191.9
		5.25	2.63	180	
		6.25	5.75	192	
		7.25	6.75	227	
		8.25	7.75	238	
TH94 - 2	4.98	0.00			153.7
		2.30	1.15	198	
		3.30	2.80	221	
		4.30	3.80	268	
		5.30	4.80	276	
		6.30	5.80	159	
		7.30	6.80	145	
		8.30	7.80	141	
		9.30	8.80	124	
		10.30	9.80	123	
		11.30	10.80	124	
		12.30	11.80	126	
		13.30	12.80	126	
		14.30	13.80	126	
		15.30	14.80	137	
		16.30	15.80	145	

3.4.2 Seismic hazard at the bridge site

The new seismic hazard map for Canadian cities is made available by Geological Survey of Canada in 1999(GSC, 1999). Many improvements are made in this new map compared to the old 1985 map. In the 1985 map, only national values for peak ground velocity (PGV) and peak ground acceleration (PGA) were provided. While in the new seismic hazard map, spectral acceleration values for the range of periods important for common engineered structures are given for major cities in Canada. Also tables of hazard values for most of the larger population centres exposed to seismic hazards, as well as Uniform Hazard Spectra (UHS), are presented. Spectral acceleration values corresponding to both 10% and 2% probabilities of exceedence in 50 years are provided in the new map. Table 3.2 gives spectral acceleration values at different structural periods for the city of Victoria.

Table 3.2 Spectral acceleration values (g) at different periods

Period (s)	10% in 50 years	2% in 50 years
0.1	0.59	1.10
0.15	0.69	1.20
0.2	0.68	1.20
0.3	0.58	1.10
0.4	0.50	0.92
0.5	0.45	0.83
1.0	0.20	0.38
2.0	0.096	0.19

3.4.3 Probabilistic seismic hazard model

The probability distribution of annual extreme spectral acceleration can be described by a Type II distribution of the largest values (Cornell, 1968):

$$H(x) = P[S_a > x] = 1 - \exp\left[-(x/\mu)^{-k}\right] \qquad \text{Equation 3.1}$$

in which, S_a is the annual extreme spectral acceleration, μ represents location of the distribution, and k is the slope of the distribution.

For the case study bridge in Victoria, the spectral accelerations at 10% and 2% probabilities of exceedenxe in 50 years given in the new seismic hazard map (GSC, 1999) can be used to anchor the values of μ and k. After μ and k are obtained, equation 3.1 can be utilized to compute spectral accelerations at different occurrence rates.

With the two spectral acceleration values S_a = 0.45g and S_a = 0.83g at period T = 0.5 s with a 10% and 2% probability of exceedence in 50 years respectively, the parameters μ = 0.0458 and k = 2.70 are estimated. The seismic hazard curve thus obtained is shown in Fig. 3.5.

Table 3.3 gives the spectral accelerations at period T = 0.5 s with various probabilities of exceedence. These spectral values will be used in the following computations of structural failure probabilities and seismic damages.

Fig. 3.5 Seismic hazard curve

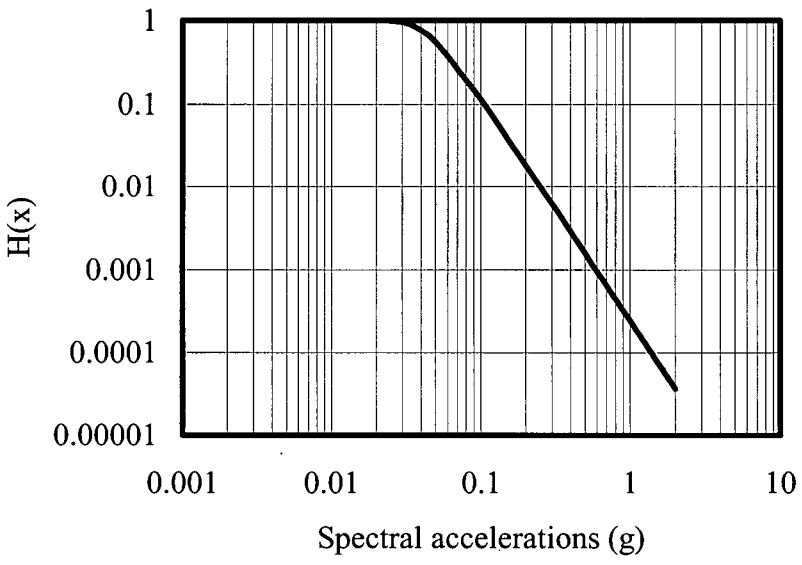

Table 3.3 Spectral accelerations at different occurrence rates

Probability of exceedence in 50 years	Annual occurrence rate	Spectral acceleration (g)
70%	0.0233	0.185
50%	0.0139	0.22
10%	0.0021	0.45
5%	0.0010	0.59
2%	0.0004	0.83
1%	0.0002	1.075

Chapter 4 Seismic Behaviour Assessment: Global Response Spectrum Analysis and Local Push Over Analysis

4.1 Introduction

In this Chapter, a seismic behaviour assessment of the case study bridge will be undertaken to identify structural seismic deficiencies and to evaluate structural behaviours. First, a global model of the whole bridge will be constructed to study dynamic properties. The calculated mode shape and corresponding period will be compared with the ambient vibration test and the computer model will be verified. Then, a deterministic response spectrum analysis of the global model will be made to calculate seismic demands and the component capacity to demand ratio will be computed. The most vulnerable components will be identified based on capacity to demand ratios. Lastly, the non-linear static push over analysis of isolated bridge bents will be utilized to identify seismic deficiencies.

4.2 Structural dynamic properties

4.2.1 Modelling

4.2.1.1 Outline

The general procedure set out in the ATC – 32 (1996) and in the book of " Seismic Design and Retrofit of Bridges" (Priestley et al, 1996) will be followed for the modeling of the whole bridge. The model should represent the geometry, boundary conditions, gravity load, mass distribution and behaviour of the components. An effort is made here to try to catch the structural dynamic property using a relatively simple model.

4.2.1.2 Superstructure

Superstructure of the existing bridge is made up six steel stringers with reinforced concrete deck. The total width of the bridge deck is about 12m. Different models can be built to analyze the structural dynamic property, such as the simple stick model to model

the stringer and the deck together as a single beam element, or the complicated hybrid model with steel girder being modelled as beam element and the concrete deck as shell element. Both models can be used under different circumstances. In this study, a grillage model (Hambly, 1991) normally used in the bridge deck analysis is developed to capture the superstructure dynamic behaviour. Previous research and the calculated results shown below have demonstrated the effectiveness and efficiency of the grillage model.

Three longitudinal beams are used to model the structure property along the span direction, with four beam elements for each span. Ten transverse beams in every span are utilized to capture the structure property in transverse direction. The strong concrete deck is modelled with the bracing elements. The superstructure model and corresponding elements are depicted in Fig. 4.1. In total, 54 beam elements are used for the longitudinal beam, 38 beam elements for the transverse beam, and 72 truss elements for the bracing.

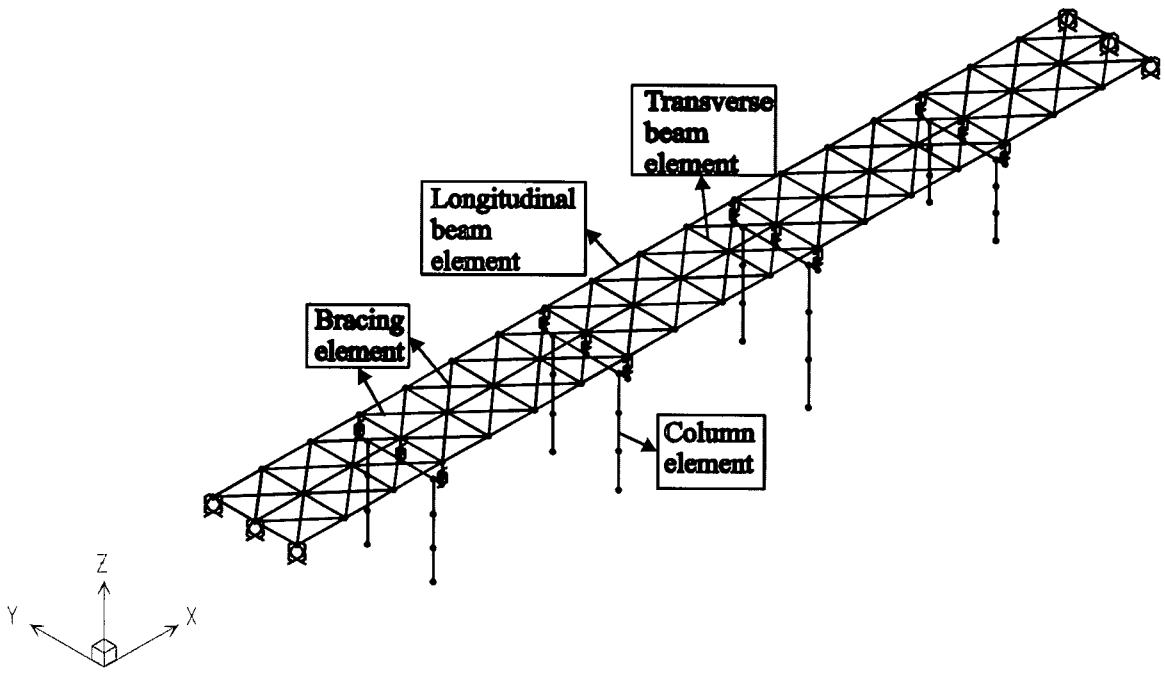

Fig. 4.1 Global analysis model for original bridge

Table 4.1 Section properties of superstructure elements

Section property	Area A (m^2)	Inertia of moment $I_{YY}*10^{-4}$ (m^4)	Inertia of moment $I_{ZZ}*10^{-4}$ (m^4)	Inertia of torsion $J*10^{-4}$ (m^4)	Mass distribution (kg/m)
Longitudinal beam	0.145	165.69	1739.98	4.808	3099
Transverse beam	0.0369	2.9885	50.2009	1.6708	
Bracing element	0.0305	N/A	N/A	N/A	

Note: All properties are transformed into steel sections
Mass value includes all superstructure components

Section properties of these elements are calculated based on the gross sections. Consideration is given for the possible cracking in concrete deck during seismic events. The calculated section property and the superstructure mass distribution are shown in Table 4.1. The followings specific points are considered for the modelling of superstructure:

- Composite steel girder and concrete deck section is considered for the calculation of moment of inertia
- Stiffness and mass contribution from sidewalk and parapet wall are accounted
- Mass of wearing surface is taken into account
- Only translation mass is included in each node point due to the grillage model used; No rotation mass is considered
- Large in-plane stiffness of concrete deck is approximated using bracing elements. This simplification is proven to be appropriate and effective for this study
- A short link element is introduced to represent the offset between the gravitational axis of superstructure and the centreline of cap beam

- Link elements are used to model steel bearings that connect the superstructure with the substructure

4.2.1.3 Substructure

Beam/column elements are used for the modelling of the reinforced concrete bents. Four elements are needed for each cap beam and three elements for each column respectively. Section effective stiffness is computed based on the sectional moment-curvature analysis. The possible cracking of the concrete and the yielding of the longitudinal reinforcement are taken into consideration. A typical moment (M) - curvature (Φ) curve of cap beam and column is shown respectively in Fig. 4.2 and Fig. 4.3. The non-linear sectional analysis program Response – 2000 (Bents & Collins, 1998) is used to compute M – Φ relationship of each section. This program will be described in detail in Section 4.5 for calculating sectional force capacity and deformation capacity.

Fig. 4.2 Moment - curvature curve for original cap beam

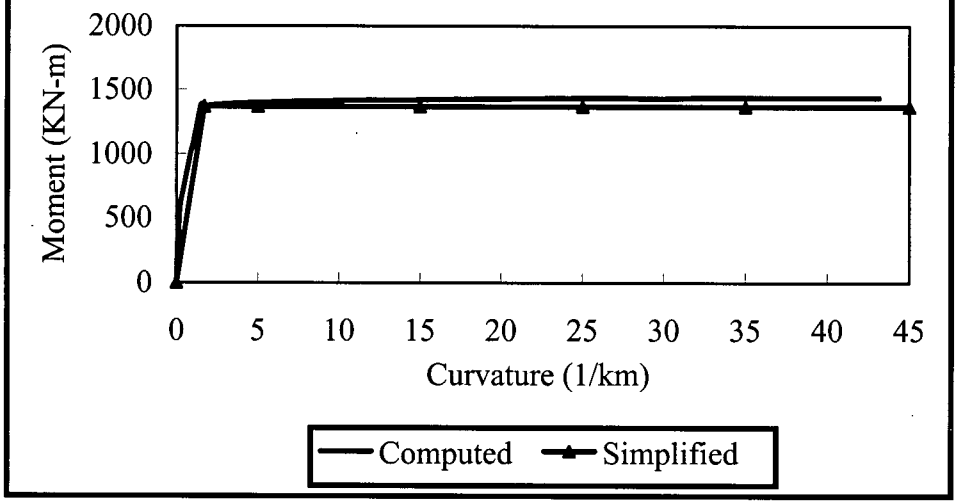

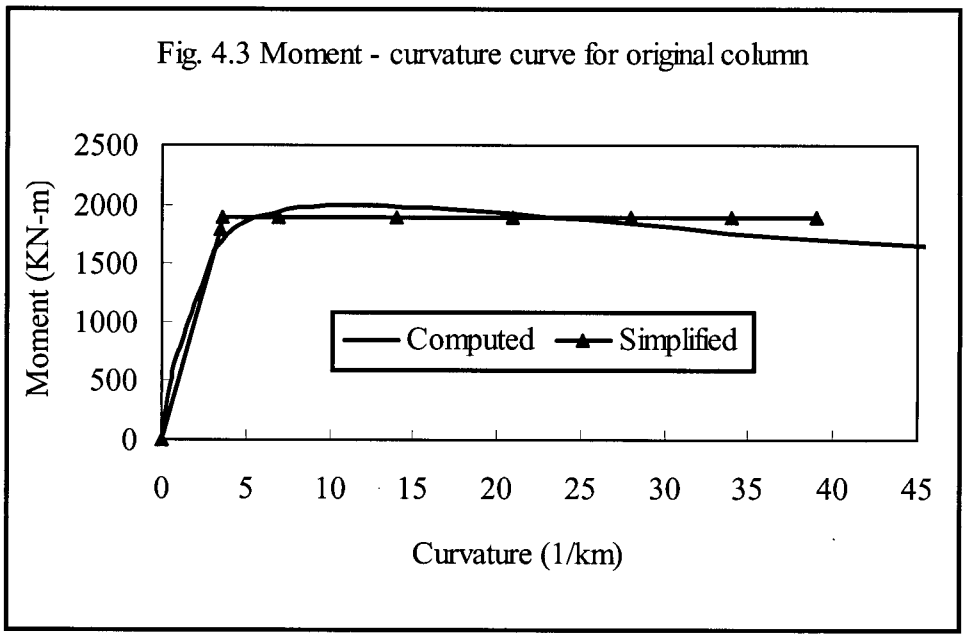

Fig. 4.3 Moment - curvature curve for original column

Sectional effective stiffness obtained from the M - Φ curve is 0.38 and 0.50 times elastic stiffness based on the gross sectional property for the cap beam and the column respectively. These values are similar to the values obtained from other researches.

4.2.1.4 Soil - structure interaction

Bridge foundation modeling has an important role to play in the overall seismic performance of a bridge structure. Recognizing this important fact, many researches insist on the importance of including the foundations in the structural model of the bridge. Modern design codes and manuals including AASHTO – 83 (AASHTO, 1983), ATC – 32 (ATC, 1996) and Caltrans (Caltrans, 1999) suggest the use of a set of single valued discrete springs to represent the effect of foundations in the bridge model. In design practice, the stiffness of soil spring has been usually selected on the basis of simple empirical rules or simplified procedures.

In this study, the uncoupled elastic soil springs are used to model soil - structure interaction. The procedure recommended by FEMA – 273 (FEMA, 1997) is used for the determination of spring stiffness for the spread footing; the spring stiffness of pile foundation is calculated based on FEMA – 273 and ATC – 32.

The computed soil spring stiffness for footing and pile foundation are shown in Table 4.2. The analyses show that the foundation flexibility influences the vibration of the bridge in the transverse direction even under low level of shaking.

Table 4.2 Soil spring stiffness

Spring stiffness	K_V (kN/m)	K_H (kN/m)	K_{YY} (kN-m/rad)	K_{ZZ} (kN-m/rad)	K_T (kN-m /rad)
Spread footing	183300	144400	111700	111700	145200
Pile foundation	1224000	240400	682800	291300	1328000

4.2.1.5 Abutment

For short and moderate length bridge, the abutment has a big effect on the seismic behaviour of the bridge. Many researches have identified the importance of appropriate modeling of the abutment in the global bridge analysis. However, the difficulties existed for the abutment modeling have resulted in the adoption of simplified boundary conditions for bridge models in the past. These simplified boundary conditions assume roller supports or pinned end conditions at bridge boundaries. The effect of abutment on the bridge behaviour is not considered. For vertical vibration or for transverse vibration with a low level of shaking, the simplified boundary condition may be appropriate. But for high level of shaking, the flexibility of the abutment will play an important role in the dynamic behaviour of the bridge. In such cases, the effects of abutment need to be appropriately modeled.

ATC – 18 (Rojahn et al, 1997) report states that the state of knowledge and the ability to accurately model abutments was significantly behind that of columns and foundations. It also states that for many bridges, abutments performance would have significant impact on the overall response of a bridge at different levels of shaking. Detailed analyses of various types of abutments covering all the aspects are beyond the scope of this research.

However, methods are presented herein to model the abutments for shaking in the transverse and longitudinal directions. Again, a simplified model for the abutment is to be sought.

- Wilson and Tan (1990) model

A typical bridge usually includes abutments and approach embankment. The abutment is buried in the embankment soil. Wilson and Tan modeled the abutment embankment soil system as a trapezoidal soil wedge, as shown in Fig. 4.4.

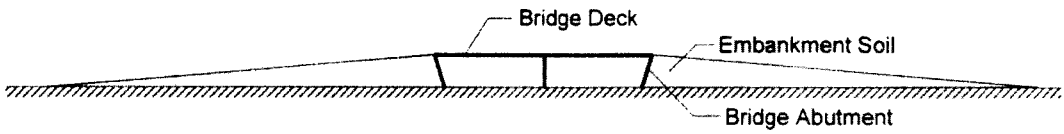

(a) A Typical Two Span Bridge and the Abutment-Embankment Soil System

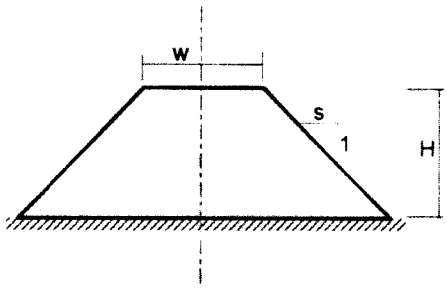

(b) A Typical Abutment - Soil System

Fig. 4.4 Bridge abutment – soil system

Wilson and Tan (1990) developed analytical expressions for the static stiffness of the trapezoidal wedge assuming linear elastic behaviour. The proposed expressions for transverse stiffness k_t per unit length of the abutment is,

$$k_t = \frac{2sG}{\ln(1+2s\frac{H}{w})} \qquad \text{Equation 4.1}$$

in which G is shear modulus of the soil, w is the top width, H is the height and s is the side slope. Wilson and Tan (1990) showed that the stiffness calculated agrees with the stiffness from a plane strain finite element analysis. The difference between the two solutions was less than 20% and the finite element solutions were lower than that from the proposed analytical expression.

- Lam and Martin (1986) model

Maragakis (1986) presented an approach to determine the elastic longitudinal and rotational stiffness of the abutment by assuming the abutment to be rigid wall and so neglecting the deformation due to bending and shear. The effect of backfill was represented by a set of Winkler springs.

Lam and Martin (1986) presented the following simplified expressions for the longitudinal and rotational stiffness of a rigid wall abutment,

$$K_L = 0.425E_S B$$
$$K_R = 0.072E_S BH^2 \qquad \text{Equation 4.2}$$

in which H is the height of the wall, E_s is the Young's modulus of soil and B is the width of the abutment wall.

- CalTrans (1988) model

Based on passive earth pressure tests and the force deflection results from large-scale abutment testing, a linear elastic model is used by CalTrans (Memo 5 - 1, 1988) to determine effect of the abutment on the bridge behaviour. An effective abutment stiffness K_{eff} is adopted in this model. K_{eff} accounts for expansion gaps and incorporates a realistic value for the backfill stiffness.

The maximum effective soil pressure behind the back wall is limited to 370 Kpa. The effective soil pressure is reduced for back wall heights less than 2.5 m as specified as follows,

$$p_{bw} = 370KPa \times \frac{h_{bw}}{2.5m} \qquad \text{Equation 4.3}$$

in which, p_{bw} is the effective soil pressure, h_{bw} is the back wall height.

The effective abutment stiffness is computed as a ratio of the design capacity as obtained from Equation 4.3 and the acceptable deformation in the abutment. Two abutment deformations are normally used for the effective stiffness calculation, i.e., 1.0 inch and 2.4 inch.

Identifying the limitations existed for the three aforementioned models, a refined model is developed by Thavaraj (2000) to determine the stiffness and damping of the abutment at different levels of shaking. In his study, the abutment soil system is modeled as trapezoidal soil wedge using plane strain soil elements and the analysis is carried out in the frequency domain. Much more time and effort are needed for this model compared with other simple models, therefore it's not used here.

The computed abutment stiffness using the three aforementioned models is shown in Table 4.3, and the adopted stiffness values are also shown in the table.

To compare the effect of abutment spring stiffness on the global structural behaviour, three models with different boundary conditions are analyzed. Model 1: with longitudinal and transverse springs at two abutments; Model 2: with transverse springs at two abutments and pin support in longitudinal direction; Model 3: with transverse springs at two abutments and rolled support in longitudinal direction. The computed first three modes and their periods are shown in Table 4.4. From the computed modes, it can be concluded that the abutment spring stiffness has a very big effect on the dynamic properties of bridge in both longitudinal and transverse directions. In the vertical direction, the abutment has least effect.

Table 4.3 Abutment spring stiffness

Abutment spring stiffness	Longitudinal stiffness K_L(KN/M)	Transverse stiffness for E. Abutment K_H(KN/M)	Transverse stiffness for W. Abutment K_H(KN/M)
Wilson & Tan	N/A	75740	116600
Lam & Martin	107900	N/A	N/A
CalTrans	70480	94570	87370
Adopted	70480	75740	116600

Table 4.4 Vibration modes of structure with/without abutment springs

Modes	Springs at both longitudinal and transverse directions		Springs at transverse direction, fixed at longitudinal direction		Springs at transverse direction, free at longitudinal direction	
	Description of Mode Shape	Period (s)	Description of Mode Shape	Period (s)	Description of Mode Shape	Period (s)
1	1st transverse	0.55	1st transverse	0.28	1st longitudinal	1.02
2	1st longitudinal	0.54	1st torsion	0.18	1st transverse	0.42
3	1st torsion	0.23	1st vertical	0.18	1st vertical	0.18
4	1st vertical	0.18	2nd vertical	0.11	2nd vertical	0.13

4.2.1.6 Material property

For the seismic assessment of existing old structures, the capacity of structural members should be based on the most probable material strengths (Priestley et al, 1996). Based on the experience gained from California, Priestley recommended the following multiplication factors to be considered to convert nominal strength to probable strength: a factor of 1.5 for concrete compressive strength, and 1.1 for yielding strength of steel.

The case study bridge was built in the 1950's. According to the as - built drawings (BCMoTH, 1953), the compressive strength of 20Mpa was used for concrete, and the steel reinforcement had a yielding strength of 275Mpa. Material samples were taken from the original structure and lab tests were done in 1992 to evaluate strength of concrete and steel before the formal seismic retrofitting was commenced. From Engineer's report, the most probable material strength is 30Mpa compressive strength for concrete and 300Mpa yielding strength for steel respectively. They are in accordance with the values suggested by Priestley et al (Priestley et al, 1996). Therefore, these two values for material properties are used in the subsequent analyses.

4.2.2 Dynamic property

The global bridge analysis is undertaken using the program SAP – 2000 (Computers and Structures, Inc., 1999). Many programs are available for the structural analysis nowadays. SAP – 2000 is chosen due to powerful graphical interaction, convenient input/output, and proven reliability and effectiveness in structural analysis.

4.2.2.1 Dynamic property at low level of shaking

At low level of shaking, the structure behaves elastically. Therefore elastic stiffness based on the gross section property is used for the analysis. No reduction to the initial shear modulus of soil is considered. During low level shaking, the gap between the bridge deck and the abutment back wall will not be closed and abutment capacity due to the passive soil pressure cannot be mobilized. Therefore the abutment soil springs cannot be used in

the model. The effect of soil – structure interaction and abutment on the structural behaviours are small.

As stated in Chapter 3, the longitudinal movement of the bridge is restrained due to the tilted bolts at both abutments. Even though the longitudinal stiffness due to the abutment cannot be used, the restraints from the bolts need to be correctly modelled (Felber, 1993). The stiffness recommended by Felber (Felber, 1993) is used in the analysis.

The computed dynamic property of the bridge is shown in Table 4.5. To validate the analytical model, the computed dynamic properties are compared with the field ambient vibration test (AVT) made by Felber et al in 1992. The measured modes and corresponding periods are shown and compared in Table 4.5 too.

From the Table 4.5, it can be seen that the analytical model can model the first three modes effectively, the percentage of error for corresponding period is in the range of 3% to 6%. We will see from section 4.3 that, the first three modes will contribute over 90% modal mass to the vibration in the longitudinal and transverse directions. Therefore, the aforementioned analytical model is able to model the structural dynamic behaviours at low level shaking efficiently and it will be used for the subsequent global analysis of the bridge.

Table 4.5 Comparison of computed vibration modes with test

Modes	Description of Mode Shape	Period from Analysis (s)	Period from Test (s)	Percentage of error
1	1st Longitudinal	0.62	0.60	3.0
2	1st Transverse	0.37	0.36	3.0
3	1st Vertical	0.18	0.17	6.0

4.2.2.2 Dynamic property at high level of shaking

At high level of shaking, such as in strong earthquakes, the concrete will be cracking, the steel be yielding, and the structural stiffness will be decreased. At the same time, the shear modulus of soil will be decreased dramatically, so soil spring stiffness will be deteriorated. All these need to be accounted in the analysis model. Previous researches have found that many structures experienced a lengthening of period during seismic shaking.

Contrary to the model used in the low level of shaking, effective stiffness is considered for the structure at high level of shaking. Reduced soil spring stiffness due to decreased shear modulus is used and the abutment spring stiffness capacity is calculated based on the mobilized soil passive pressure.

The calculated dynamic property of the bridge simulating earthquake event is shown in Table 4.6. It can be seen that, the first transverse mode period have been lengthened 62% compared with the structure at elastic stage. This corresponds to a stiffness decreasing of nearly 40% to the previous value. It is also worth noting that the first vertical vibration mode is almost the same.

Table 4.6 Comparison of vibration modes at high level shaking and low level shaking

Modes	Low level of shaking		High level of shaking		Percentage of period change
	Description of Mode Shape	Period from Analysis (s)	Description of Mode Shape	Period from Analysis (s)	
1	1st Longitudinal	0.62	1st Longitudinal	0.55	-11.3
2	1st Transverse	0.37	1st Transverse	0.60	62.2
3	1st Vertical	0.18	1st Vertical	0.19	5.6

4.3 Response spectrum analysis

4.3.1 Outline

Based on the computer model developed in the section 4.2, response spectrum analysis (RSA) is used to calculate global and component seismic demands. The structural components designed in accordance with current design codes will experience inelastic behaviour during high level seismic shaking. Under such circumstances, component forces obtained from RSA are not realistic values. It can be argued that RSA is not appropriate for the cases where concrete cracking and/or steel yielding are going to occur. However, a linear elastic analysis can help understand structural seismic behaviour globally and realize dynamic force distribution among various components, thus the critical load path can be identified. Moreover, the component capacity to demand ratio (C/D) based on RSA can give insight to high vulnerable members and help identify seismic deficiencies in the structure components from the point of a global view.

4.3.2 Response spectrum (RS) used in the analysis

Different response spectra can be input in the RSA. In the past decade, AASHTO bridge design code (AASHTO – 88, 90) was mainly used for the seismic design standard for bridges in British Columbia. RS in AASHTO code is a general spectrum applicable to all areas in United States. Because this study is for a site - specific bridge in Victoria, RS recommended by Geological Survey of Canada (1999) is adopted rather than that from AASHTO code. As described in Section 3.4, Uniform Hazard Spectra (UHS), computed at the both 10% and 2% probabilities of exceedence in 50 years, are presented in the new seismic hazard map of Canadian cities by GSC (1999). The UHS for the city of Victoria is used in this study. Table 4.7 gives spectral acceleration values at different structural periods excerpted from the GSC file and AASHTO code.

Table 4.7 Spectral acceleration values from GSC file and AASHTO code

Period (s)	Spectral acceleration from GSC (% g)		Spectral acceleration from AASHTO (% g)
	10% exceedence in 50 years	2% exceedence in 50 years	
0.1	59	110	87.5
0.15	69	120	87.5
0.2	68	120	87.5
0.3	58	110	87.5
0.4	50	92	87.5
0.5	45	83	87.5
1	20	38	42
2	9.6	19	26.5

Fig 4.5 Design Response Spectrum

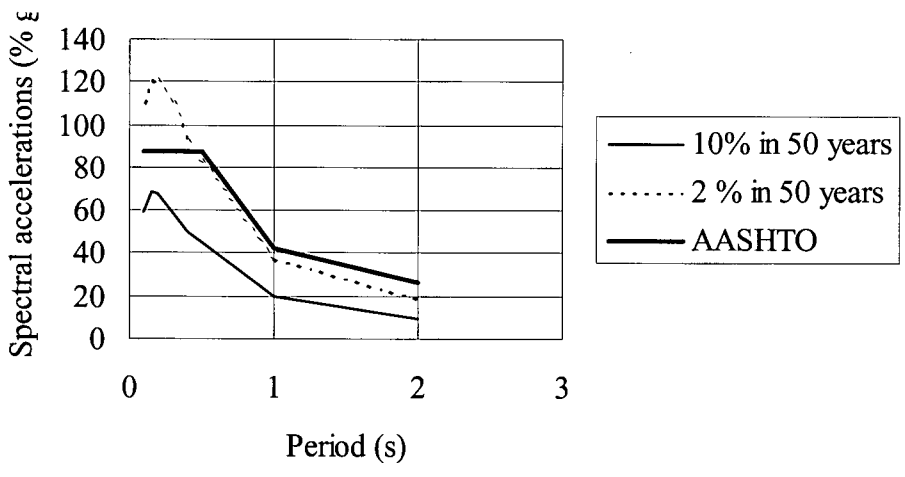

The response spectrum obtained from AASHTO – 92 and GSC (1999) is depicted in Fig. 4.5 respectively. It can be seen that AASHTO spectrum and GSC spectrum based on 2% exceedence in 50 years are quite similar within the period range for the case study bridge. In this study, spectral accelerations based on both 10% exceedence and 2% exceedence of probability in 50 years will be used for the seismic demand analysis.

4.3.3 Component Capacity to Demand ratios (C/D)

4.3.3.1 Outline

The aforementioned global bridge model and response spectrum will be used here to compute component capacity to demand ratios.

4.3.3.2 Seismic force demand

Seismic demands of structural members are calculated through the aforementioned RSA. All calculations are based on the linear, elastic behaviours of the structure. Ten vibration modes are included to ensure a minimum of 90% modal mass is taken into account for the analysis. 5% critical damping is considered for vibration modes. Modal responses are combined using Complete Quadratic Combination (CQC) method. Seismic demands are calculated based on the maximum actions from the following two load cases:

Seismic load case 1: Combine the effects resulting from the longitudinal loading with 40 percent of the corresponding effects from the transverse loading.

Seismic load case 2: Combine the effects resulting from the transverse loading with 40 percent of the corresponding effects from the longitudinal loading.

The computed seismic force demands of components are shown in Table 4.10. From the analysis, the bridge is found to be more vulnerable to seismic excitations in the transverse direction than in the longitudinal direction. As in the latter situation, all bents can behave similarly as an integer part and the abutment will provide greater resistance to the seismic forces after the gap between the bridge deck and abutment wall is closed. Therefore, only the more critical seismic demands in the transverse direction are shown in Table 4.10.

4.3.3.3 Component capacity

Seismic capacities of structural members are computed from the most expected material strength and the new Canadian Bridge Design Code (CAN/CSA-S6-98). The sectional analysis program of RESPONSE – 2000 (Bentz & Collins, 1998) is extensively used for the member capacity calculations. The state-of-practice approach recommended by Priestley (Priestely & Calvi, 1996) is adopted where applicable.

4.3.3.3.1 Flexural capacity

Flexural capacity is calculated directly from RESPONSE – 2000 program (Bentz & Collins, 1998). Stress and strain relationships of concrete and steel are based on the curves recommended by Collins. No strain hardening is considered for the steel reinforcement strength increasing after first yielding. As the cap beam and column are lightly reinforced transversely, confining action for concrete is not taken into account. The material reduction factor is taken as 1.0. The computed flexural capacity of concrete cap beam and column are shown in Table 4.8.

Table 4.8 Component flexural capacity

Component	Location	Flexural capacity (kN-m)
Cap beam	Positive moment	1370
	Negative moment	2700
Column	In push	2020
	In pull	1705

4.3.3.2.1 Shear capacity

Shear capacity of reinforced concrete members is difficult to be accurately estimated. Different approaches are available for this estimation. However, shear capacity calculated from various approaches can have a ratio of difference up to 2. Three methods are used here to compute shear capacity of concrete sections in this study.

- Method 1: Canadian Bridge Design Code (CAN/CSA – S6 – 00)

  The new Canadian Bridge Design Code calculates shear capacity based on the modified compression field theory (Collins & Mitchell, 1987). Shear strength is taken as sum of the shear carried by the concrete and by the shear reinforcement. That is,

  $$V_r = V_c + V_s \qquad \text{Equation 4.4}$$

  The second term is taken as,

  $$V_s = A_v f_y \frac{d_v}{s} \frac{1}{\tan\theta} \qquad \text{Equation 4.5}$$

  where A_v and f_y are the area and yield strength of the shear reinforcement, d_v is the effective depth and s is the stirrup spacing, θ is the principle compressive strain inclination angle.

  The first term is dependent on the inclination angle θ of the principle compressive strain, and the longitudinal strain ε_x at mid – depth of the section. It's calculated as in equation 4.6.

  $$V_c = 2.5\beta f_{cr} b_v d_v \qquad \text{Equation 4.6}$$

  where f_{cr} is the tensile strength of the concrete, b_v is the section width, d_v is the effective depth of the section, and β is determined from table 8.7 in the CAN/CSA – S6 – 00. Several iterations are needed to get a reasonable value of β. Normally it will take 2 to 3 iterations.

- Method 2: Program RESPONSE – 2000 (Bentz & Collins, 1998) using modified compression field theory

  RESPONSE – 2000 is a Windows based program which is designed to predict the load – deformation response of reinforced concrete sections subjected to bending moments, axial loads and shear forces. The analytical procedures in RESPONSE – 2000 are based on traditional engineering beam theory, which assumes that plane sections remain plane and that the distribution of shear stresses across the section is defined by the rate of change of flexural stresses. When relating stresses and strains at various locations across the section, the program uses the modified compression field theory (Collins & Mitchell, 1986).

  RESPONSE – 2000 can perform analysis on various sections and with different material properties. Confining effect on the concrete sections can be modelled through modified stress – strain relationships of concrete. Different initial load conditions can be input for the calculations. The program can output axial (N), shear (V) and bending (M) strength of the section with the interactions between (N – V – M) being considered or not considered. Also load – deformation curves can be computed and output.

  In this study, RESPONSE – 2000 is used for the calculation of sectional capacity of axial load, bending moment and shear force. And it's also used to compute the sectional moment – curvature curves.

- Method 3: Priestley's method (Priestley & Calvi, 1996)

  In this approach, shear strength is taken as the sum of three items, given in equation 4.7,

$$V_r = V_c + V_s + V_p \qquad \text{Equation 4.7}$$

  The second term is the same as in equation 4.5.

The third term is the contribution resulting from axial compression force in the structural member,

$$V_p = P \times \tan\alpha \qquad \text{Equation 4.8}$$

in which P is compressive axial force in the structural member, α is the angle formed between the member axis and the compression strut.

The first term is the contribution from the concrete section. It is given in equation 4.9,

$$V_c = k\sqrt{f_c' A_e} \qquad \text{Equation 4.9}$$

$$A_e = 0.8 \times A_{gross} \qquad \text{Equation 4.10}$$

in which, A is the gross section area, f_c' is the concrete compressive strength, k is a factor, which depends on the member curvature ductility. A relationship between k and curvature ductility is recommended by Priestley and Calvi to calculate the value of k.

The shear capacity of cap beam and columns using the above three approaches are shown in Table 4.9. The adopted shear capacities are also shown in Table 4.9.

Table 4.9 Component shear capacity

Component	CAN/CSA-S6-98 (kN)	RESPONSE - 2000 (kN)	Priestely and Calvi (kN)			Adopted (kN)
			μ_Φ=3.0	μ_Φ=5.0	μ_Φ=8.0	
Cap beam	953	850	1192	912	492	850
Column in push	669	635	1079	858	526	635
Column in pull	570	531	940	729	398	531

4.3.3.3 Component Capacity to Demand ratios

Component Capacity to Demand (C/D) ratios are calculated and shown in Table 4.10 for earthquake level at 10% exceedence in 50 years and Table 4.11 for earthquake level at 2% exceedence in 50 years respectively.

From the tables, the following observations can be made,

- Among the four concrete bents, components in bent 1 have the lowest C/D ratios. Therefore, bent 1 is the most critical bent.
- For each bent, the cap beam shear force has a lower C/D ratio than that of bending moments. Cap beam may subject to premature shear failure.
- At column base in bent 1, the C/D ratio has a low value of 0.64 for bending moment. As reinforcement splicing exists at column base, the cyclic earthquake force may trigger the abrupt strength deterioration, thus leading the column more vulnerable to subsequent seismic excitations.
- At 10% exceedence in 50 years earthquake level, most items have C/D ratios of over 1.0 except for the shear force in bent 1 cap beam.
- At 2% exceedence in 50 years earthquake level, cap beam and column in bent1 have C/D ratios of 0.6 ~ 0.8. In other bents, C/D ratios have values bigger than 1.0, except for the shear force in bent 3 cap beam having a C/D ratio of 0.9.

Therefore, it can be concluded that the high vulnerable component is shear failure of cap beam and possible splicing failure in plastic hinge regions in the column in bent 1. Bent1 is the most critical bent from the point of global structural view. If seismic deficiencies in bent 1 are retrofitted, the whole bridge may be able to survive seismic excitations up to 2% exceedence in 50 years earthquake level. The above observations will be verified through the following non-linear static push over analysis of isolated bents.

Table 4.10 Component C/D ratios at 10% exceedence in 50 years earthquake level

Bent No.			Bent1	Bent2	Bent3	Bent4
Seismic Demand at 10% exceedence probability	Cap Beam	Max. Moment (kN-m)	2147	1504	1499	1256
		Shear (kN)	871	595	653	572
	Column	Moment at top (kN-m)	1472	990	947	756
		Moment at bottom (kN-m)	1445	644	625	468
		Shear (kN)	440	195	187	160
Seismic Capacity	Cap Beam	Max. Moment (kN-m)	2700	2700	2700	2700
		Shear (kN)	850	850	850	850
	Column	Moment at top (kN-m)	1705 ~ 2020	1705 ~ 2020	1705 ~ 2020	1705 ~ 2020
		Moment at bottom (kN-m)	1705 ~ 2020	1705 ~ 2020	1705 ~ 2020	1705 ~ 2020
		Shear (kN)	531 ~ 635	531 ~ 635	531 ~ 635	531 ~ 635
C/D ratio at 10% exceedence in 50 years	Cap Beam	Max. Moment (kN-m)	1.3	1.8	1.8	2.1
		Shear (kN)	0.98	1.43	1.30	1.5
	Column	Moment at top (kN-m)	1.2 ~ 1.4	1.7 ~ 2.0	1.8 ~ 2.1	2.2 ~ 2.7
		Moment at bottom (kN-m)	1.2 ~ 1.4	2.3 ~ 3.1	2.7 ~ 3.2	2.7 ~ 3.4
		Shear (kN)	1.2 ~ 1.4	2.7 ~ 3.3	2.7 ~ 3.4	3.3 ~ 4.0

Table 4.11 Component C/D ratios at 2% exceedence in 50 years earthquake level

Bent No.			Bent1	Bent2	Bent3	Bent4
Seismic Demand at 2% exceedence probability	Cap Beam	Max. Moment (kN-m)	3576	2340	2331	1927
		Shear (kN)	1352	812	919	795
	Column	Moment at top (kN-m)	2722	1830	1751	1397
		Moment at bottom (kN-m)	2673	1191	1157	865
		Shear (kN)	813	360	344	294
Seismic Capacity	Cap Beam	Max. Moment (kN-m)	2700	2700	2700	2700
		Shear (kN)	850	850	850	850
	Column	Moment at top (kN-m)	1705 ~ 2020	1705 ~ 2020	1705 ~ 2020	1705 ~ 2020
		Moment at bottom (kN-m)	1705 ~ 2020	1705 ~ 2020	1705 ~ 2020	1705 ~ 2020
		Shear (kN)	531 ~ 635	531 ~ 635	531 ~ 635	531 ~ 635
C/D ratio at 2% exceedence in 50 years	Cap Beam	Max. Moment (kN-m)	0.8	1.2	1.2	1.4
		Shear (kN)	0.6	1.0	0.9	1.1
	Column	Moment at top (kN-m)	0.62~0.74	0.93~1.10	0.97~1.15	1.22~1.45
		Moment at bottom (kN-m)	0.64~0.76	1.43~1.70	1.47~1.75	1.97~2.34
		Shear (kN)	0.65~0.78	1.48~1.76	1.54~1.85	1.81~2.16

4.4 Non-linear static push over analysis

4.4.1 Outline

As a global response spectrum analysis of the bridge gives insight to the general behaviour of the structure (such as global vibration property, general load path and seismic load distribution between concrete bents and abutments, etc.), the non-linear static push over analysis of an isolated bent can have much information on the inelastic behaviour of components. When appropriately modelled, the push over analysis can realistically represent the structural behaviour from initial elastic stage to complete collapse. The concrete cracking load, first yielding load and the ultimate load capacity can all be obtained from the analysis. And most importantly, push over analysis can be used to determine failure mechanism of structures and identify seismic deficiencies in structural members.

4.4.2 Modelling

Isolated concrete bents are modelled for the non-linear static push over analysis. The purpose of this analysis is to understand inelastic behaviour of single bent subjected to seismic event, determine failure mechanism and identify seismic deficiency in structural members. The structural analysis program — SAP2000 (Computers and Structures, Inc., 2000) is again used for this analysis.

As demonstrated in global response spectrum analysis, the bridge is more vulnerable in transverse direction than in the longitudinal direction. To simplify the problem and focus on the critical structural behaviour, a 2 - D model in the transverse direction of the bridge is built for the analysis.

Beam element located at the centreline of structural member is used for the modelling. The lumped plasticity model (inelastic behaviour is concentrated in the plastic hinge) is used in the SAP – 2000 to represent inelastic behaviour in the component. With this approach, the location and properties of plastic hinge (PH) need to be predetermined

before the push over analysis can be undertaken. Different plastic hinge models are utilized for the flexural hinge and shear hinge in this study. The sectional analysis program — RESPONSE 2000 is used for the calculation of PH properties. Fig. 4.6 shows modelling of bent 1 with the predefined PH locations in structural members being shown in the figure. The PH properties, including yielding moment and yielding curvature, ultimate moment and ultimate curvature, curvature ductility and rotation ductility, etc. are depicted in Table 4.12.

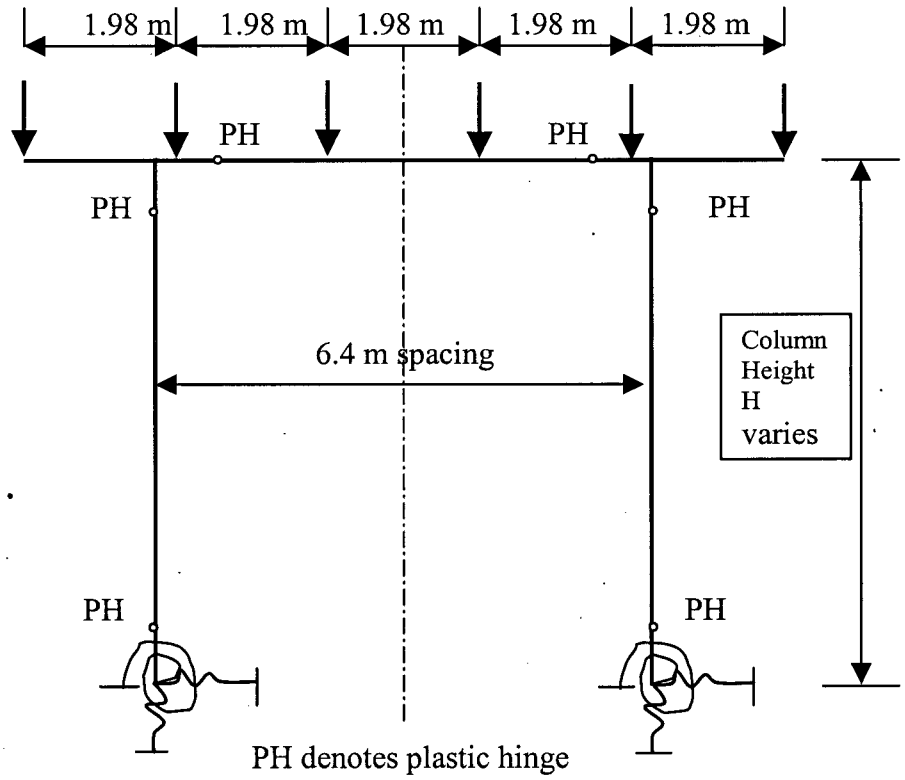

Fig.4.6 Bent model for push over analysis

The foundation flexibility is considered. The same soil springs as for the response spectrum analysis are used here for the push over analysis.

The isolated bent is pushed laterally with a monotonically increasing lateral load. This load is acting at the gravitational axis of superstructure to represent the earthquake force.

The eccentricity between the axis of superstructure and cap beam is modelled in the analysis.

Table 4.12 Plastic hinge properties for bent 1

Plastic hinge property	Cap Beam		Column in push	Column in pull
	"+" Moment	"-" Moment		
Yielding moment (kN-m)	1370	2700	2020	1705
Ultimate moment (kN-m)	1370	2700	2020	1705
Yielding curvature (rad/m)	0.00169	0.00202	0.00388	0.00357
Ultimate curvature (rad/m)	0.0324	0.0370	0.0340	0.0400
Curvature ductility	19.2	18.3	8.8	11.2
Yielding rotation (rad)	0.0027	0.0032	0.00666	0.00612
Ultimate rotation (rad)	0.0159	0.0180	0.0173	0.0200
Rotation ductility	5.9	5.6	2.6	3.3
Plastic hinge length (m)	0.492	0.492	0.510	0.510

4.4.3 Push over analysis

Lateral force control is used for the analysis at the elastic stage. After concrete cracking and steel yielding occur, the bent is pushed using displacement control. At each stage, the

forces and deformations at critical sections can be output and displayed graphically. Push over curves of lateral load against lateral bent top displacement are depicted in Fig. 4.7 for all four bents.

Fig. 4.7 Push over curve for bents

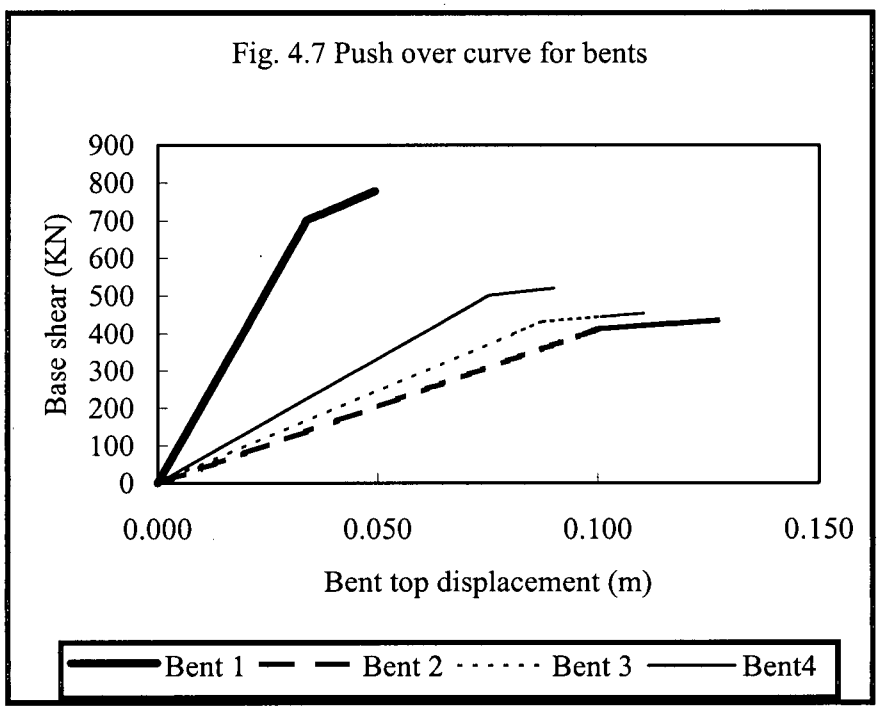

From push over analysis, the following observations can be made:

- Bent 1 has the biggest lateral stiffness among all four bents. Short column length combined with the stiff pile foundation give the bent a stiffness three to five times of that of other bents. The large lateral stiffness in bent 1 has a great effect on the global seismic force distribution and local bent behaviour.

- Bent1 is the most critical bent due to its large stiffness. From the Fig. 4.7, cap beam in bent 1 experiences shear failure at a lateral displacement of only 34 mm, i.e. a drift of 0.5%. But all other three bents have shear failure in cap beam at a drift of about 0.9%. During seismic excitations, the bridge global displacement demand forces all four bents move proportionally with their respective local displacement demands. The inadequate displacement capacity in bent 1 limits this

movement, therefore it will fail firstly and the whole bridge capacity will be limited by failure of bent 1.

- The seismic behaviours in all four bents are non – ductile. The failure mechanism is brittle shear failure in cap beam. The premature shear failure limits lateral load capacity of all bents. This phenomenon is very common in the old bridges built before 1970s. A series of cyclic and shake table tests done in UBC on two column concrete bents indicated that the as – built specimen showed very poor ductile behaviour. During the tests, a large diagonal shear crack formed at a very low displacement level. The crack increased in width with each cycle of loading until the specimen failed (Anderson et al., 1995). The test concluded that the premature cap beam brittle shear failure prevented any serious joint and column damage as the load demand on them was limited by such a failure.

Fig 4.8 Push over curve with cap beam shear retrofitted

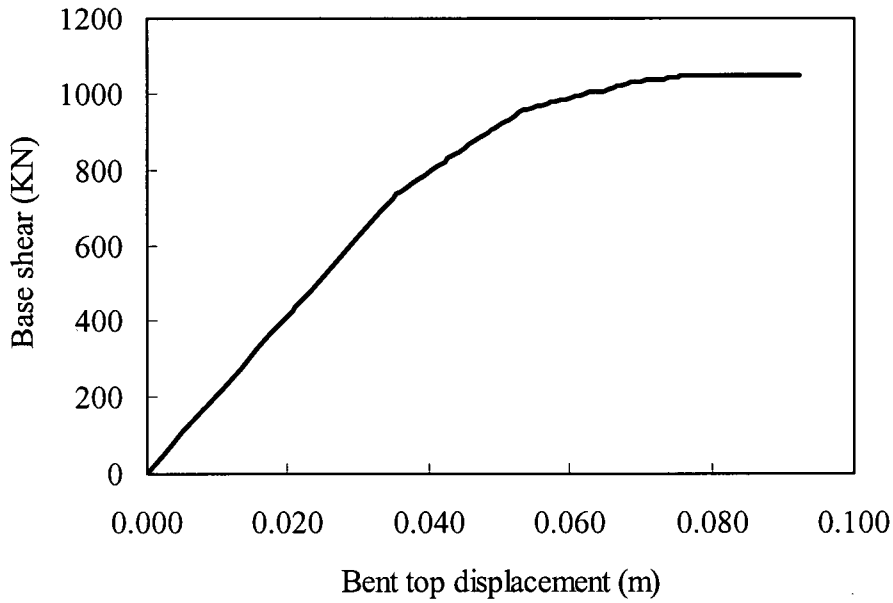

Therefore, both the analysis undertaken in the above and previous lab tests of a similar style of bridge bent show that inadequate shear strength in cap beam is a dominant

seismic deficiency. Also the analysis shows that bent 1 is the most vulnerable one among all four concrete bents for the case study bridge.

In order to identify other seismic deficiencies that may exist in the concrete bents, a separate push over analysis is made on bent 1, assuming the shear strength in the cap beam is retrofitted. The push over curve for this analysis is shown in Fig. 4.8. The plastic hinge sequence and corresponding lateral load and displacement are depicted in Table 4.13.

Table 4.13 Plastic hinge occurring and ultimate load and displacement

Plastic hinge (PH) sequence	Description	Lateral load (KN)	Lateral displacement (mm)
PH 1	Cap beam bottom flexural hinge	742	36
PH 2	Cap beam top flexural hinge	951	53
PH 3	Bottom flexural hinge in the pull column	1027	68
PH 4	Bottom flexural hinge in the push column	1045	76
Bent yielding	Obtained from Fig. 4.8	1045	48
Bent ultimate	Cap beam reaches flexural rotation capacity	1045	92
Ductility	Ultimate/Yielding	1	1.92

The analysis shows an improved seismic behaviour compared to the original bent. The premature shear failure in cap beam is eliminated. The first plastic hinge occurs in the cap beam positive flexural moment at a drift of 0.5%. The bent fails when the cap beam reaches its rotation capacity. The following conclusions can subsequently be made.

- The behaviour is ductile if the lap splicing premature failure in the column bottom is not triggered by the cyclic excitations. A local displacement ductility capacity of 1.9 is attained.
- The column doesn't indicate any brittle shear failure from the analysis.
- The cap beam is still the critical component that controls the lateral load capacity of the bent. The cut – off of bottom positive reinforcement in the cap beam indicates a great seismic deficiency for the structure. The positive flexural capacity in the cap beam is not adequate.
- Deformation capacity in both cap beam and columns are not adequate. That poses a major problem for the bent during a strong earthquake event.
- The lap splicing existed in the column bottom forms a big threat to the seismic resistance of the bent. Previous researches have demonstrated the quick deterioration of lap splicing during cyclic seismic excitations. If cap beam is retrofitted, the lap splicing failure in the potential column plastic hinge regions tends to dominate.

Having identified seismic deficiencies from the seismic behaviour assessment, the following chapter will discuss seismic retrofit design to counteract these deficiencies and upgrade the structure to certain performance levels.

Chapter 5 Seismic Retrofitting Design

5.1 Introduction

Seismic retrofitting design will be undertaken in this chapter to counteract the seismic deficiencies identified in chapter 4. The expected performance levels will firstly be presented. Then two different retrofitting schemes will be developed. The first option is to modify structural dynamic property and change seismic force distributions among structural components. Seismic demands on the vulnerable components will be reduced and the structural components thus are protected. This is a safety level seismic retrofitting. The second option uses capacity design principles to upgrade the structure component capacity to certain performance levels. This is a functional level retrofitting. Finally, bent push over analysis will be performed to explore the effects of retrofitting on the seismic behaviours of the case study bridge.

5.2 Expected performance levels for the seismic retrofitting

The case study bridge is located in Highway #1 at suburb of the city of Victoria. It is designated as in the Emergency Response Route by BCMoTH. Two different seismic retrofit levels in accordance with the Seismic Retrofit Criteria (BCMoTH, 2000) are specified for the seismic retrofit design of the bridge. Structural damage level and performance level of the bridge subjected to various earthquake excitations for these two retrofit designs are depicted in Table 5.1.

Table 5.1 Seismic retrofit levels and bridge performance levels

Retrofit level	Earthquake event	Recurrence interval (Years)	Performance level	Damage state
Safety	Occasional	72	Limited service	Minor
	Rare	475	Collapse prevention	Major
	Very rare	2500	Collapse	Significant
Functional	Occasional	72	Immediate service	Minimal
	Rare	475	Limited service	Minor
	Very rare	2500	Collapse prevention	Major

5.3 Level I retrofitting design - safety level retrofitting

5.3.1 General description

Having identified the concrete bents as more vulnerable in the transverse direction, the level I retrofitting design included adding reinforced concrete shear wall to bent 2 and bent 3 respectively, in which the lateral stiffness was greatly enhanced. With the modified structural configuration, dynamic properties of the bridge were changed and lateral seismic force distributions among the four bents were altered. Seismic demands on bent 1 and bent 4 were reduced, while lateral seismic forces on bent 2 and bent3 were increased, where the concrete shear walls counteract the increased demands. The seismic behaviours of deficient bents were improved through the retrofitting. However, this approach has left bent 1 untouched. The structural behaviour of bent 1 during seismic event is still non-ductile.

5.3.2 Retrofitting design

A new concrete shear wall was added in bent 2 and bent 3 respectively. No retrofitting work was done to bent 1 and bent 4. Fig 5.1 shows the section of added reinforced concrete shear wall with the old bent columns (CWMM, 1994). The new concrete has a compressive strength of 35Mpa and the yielding strength of reinforcement steel is 400Mpa.

This retrofitting design is simple and relatively less expensive than other possible options. The shear walls solve any problems relating to foundations, columns and cap beams. This retrofitting scheme was designed by the structural consultant to upgrade the seismic behaviour of the case study bridge (CWMM, 1994). The final retrofit work was done according to this strategy in 1995 (BCMoTH, 1995).

5.3.3 Effect of retrofitting on the structural behaviour

As part of this study, a global model of the retrofitted bridge is constructed to analysis the modified structural behaviour. This model is based on the original structure global model. The only modification is the added concrete shear walls in bent 2 bent 3, where the increased lateral stiffness is modelled using the bracing elements and the increased mass is directly accounted in the modal mass. Fig. 5.2 shows the modified global bridge model.

The dynamic properties of the retrofitted bridge are calculated and the first four modes are shown in Table 5.2. To compare, the original bridge dynamic properties are also shown in Table 5.2. As expected, the structure is stiffened in transverse direction, with the first mode vibrating in the longitudinal direction and the second mode in the transverse direction. The period of the first transverse mode decreased from 0.6 Hz of original bridge to 0.5 Hz of retrofitted bridge. This period lengthening corresponds to a stiffness increase of about 40% for the structure in the transverse direction.

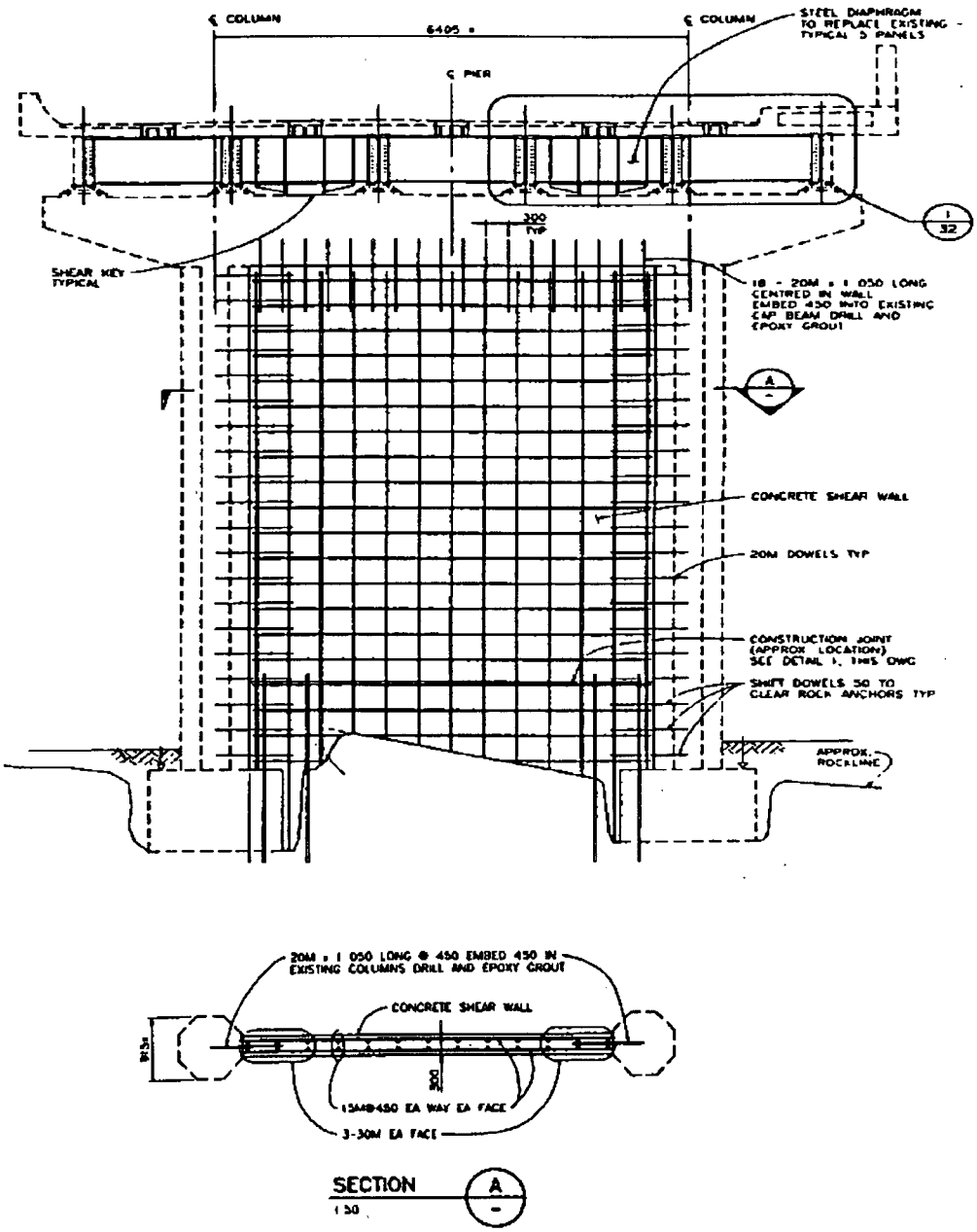

Fig. 5.1 New concrete shear walls to bent 2 and bent 3

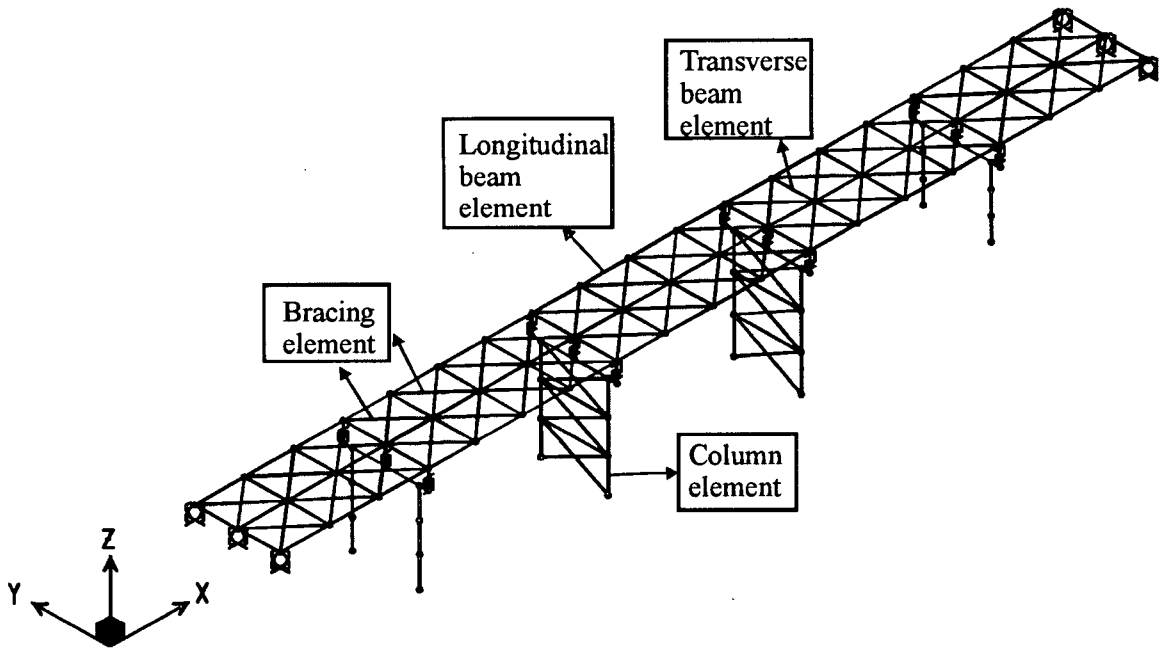

Fig. 5.2 Global analysis model for retrofitted bridge with level I retrofitting

Table 5.2 Comparison of dynamic properties

Mode	Retrofitted structure		Unretrofitted structure	
	Mode description	Period (s)	Mode description	Period (s)
1	1st Longitudinal	0.55	1st Transverse	0.60
2	1st Transverse	0.50	1st Longitudinal	0.55
3	1st Vertical	0.19	1st Vertical	0.19
4	Local bent 2	0.18	1st Torsion	0.18

A linear elastic time history analysis of the retrofitted bridge is also undertaken to calculate the modified lateral force distribution among concrete bents. The Loma Prieta earthquake with a PGA of 0.48g is used. The analysis results for bent base shears are shown in Table 5.3. The base shear distribution of original structure using the same earthquake record is also shown in the Table 5.3 for comparison. After seismic retrofitting, base shear for bent 1 and 4 has reduced by 18% and 7% respectively, while base shear in bent2 and bent 3 has increased by 500% and 288%. It is worth noted that the huge increase of base shear in bent2 and bent 3 is mainly due to the increased concrete mass in those bents. Therefore, seismic demands on bent 1 and bent 4 are reduced because of the modified stiffness ratio of bents. But the effect of this retrofitting scheme on the global structural behaviour is small. A through reliability analysis of the effect of seismic retrofitting design I on the failure probability of the structure during earthquake excitations will be given in the Chapter 6. The decreased structural damage due to this retrofitting will be discussed in detail in Chapter 7.

Table 5.3 Comparison of bent base shear distribution

Bent No.	Base shear (KN)		Percentage of change
	Retrofitted	Unretrofitted	
1	746	912	-18
2	1547	258	500
3	1464	377	288
4	298	322	-7

Although the seismic retrofitting scheme I is able to provide some protections for the most vulnerable bent 1 during certain earthquake excitations, the seismic deficiencies in bent 1 are not tackled. The seismic behaviour of bent 1 is still brittle. During a strong earthquake event, cap beam in bent 1 may still experience premature shear failure.

5.4 Level II retrofitting design - functional level retrofitting

5.4.1 General description

Based on the level I retrofitting design, a hypothetical level II retrofitting is designed in this thesis to upgrade the original bridge to meet functional level requirements during a design earthquake of 10% exceedence in 50 years. Identifying seismic deficiencies existed in bent 1, shear strength and positive moment flexural strength in cap beam will be strengthen through an eternal post tensioning system. Flexural strength in lap splicing at column base and deformation capacity in the column plastic hinge regions will be upgraded using fibre glass jacketing system, QuakeWrap^{TM}. Capacity design principles will be adopted in this retrofitting design.

5.4.2 Design objectives

The retrofit system is to be designed in such a way that the behaviour and the damage mechanism of the bent under the earthquake loading can be predicted, a desirable plastic mechanism in certain regions can be developed to dissipate energy effectively, and undesirable brittle failure can be prevented. The capacity design principle according to Paulay and Priestley (1992) will be adopted in the design. The retrofitted structure will be able to meet performance level specified in section 5.2, i.e. it will maintain structure integrity and stability after experienced an earthquake of 2% exceedence in 50 years.

More specifically, design objectives of seismic retrofitting system for bent 1 will be as follows:

- The cap beam and joints should be provided with adequate shear strength so that the strength in these regions exceeds the demands originating from the over strength of plastic hinges. As the result, the cap beam and joint should remain elastic and no shear failure and other brittle failures should occur, while concrete columns deform plastically.

- Any undesirable mode of inelastic deformation, which might be caused by shear, reinforcing steel buckling, lap splicing failure and others should be prevented in the plastic hinge regions of columns.

- Concrete columns are identified as potential plastic hinge regions, and they should have dependable flexural strength and deformation capacity to ensure the desired plastic mechanism can be developed.

5.4.3 FRP composite wrapping material

The QuakeWrap system is to be used in the retrofitting design. The materials, including the fibreglass wrapping sheets and epoxy, are manufactured by SRC (Structural Rehabilitation Corporation), an Arizona based company.

A unidirectional fabric of E-glass is used in the construction of the composite wraps. The fabrication and the composite are described in the "Repair of Earthquake-Damaged R/C Columns With Prefabricated FRP Wraps (Saadatmanesh et al, 1995). This material is considered to be unidirectional since the majority of the fabric fibres in the wraps are unidirectionally arranged and only a small amount of the fibres are used in the transverse direction to hold the fibres together during the manufacturing.

The fibre volume ratios vary depending on the type of FRP materials, and the tensile strength increases as the fibre ratio increases. In this study, composite wraps with V_r = 50.2% is used, where V_r defines the ratio of the volume of fibres over the total volume of the wrap. The mechanical properties of this material are obtained from tensile test, and are listed in Table 5.4. The fibreglass wrap itself is a brittle material with high tensile strength, and it has a linear stress-strain relation from initial loading to ultimate failure.

Table 5.4 Mechanical properties of FRP

Item	Unit	Value
Tensile strength	MPa	532
Tensile modulus of elasticity	MPa	17,755
Ultimate tensile strain		3%

5.4.4 Wrapping design

The objective of retrofitting design is to ensure that the structure will degrade in a ductile flexural mode and the failure mechanism will be flexural hinge failure in the two columns. To achieve that, shear strength of all structural members, especially shear strength in the cap beam, have to exceed the shear demand required by the forming of this plastic mechanism in the columns. Also the potential lap splicing degradation in the column bottom needs to be addressed.

The wrapping design will generally follow the procedures by Priestley et al (1996). Firstly, the wrapping required by the confinement for concrete in the potential plastic regions of column will be designed. The confinement is determined from the column deformation demand corresponding to the specified structural performance level. Then, the column shear strength will be checked to ensure the shear capacity exceeds shear demand calculated from over strength of column flexural capacity. Last, the protected cap beam will be retrofitted to make sure that it will remain elastic during and after the forming of plastic hinges in the columns.

5.4.4.1 Wrapping for confinement in the plastic regions of columns

(a) Wrapping for inhibition of lap splicing failure in column bottom

In the existing bridge, only # 3 ties with a centre spacing of 12 inches are used for the stirrup. The confinement from the transverse stirrups is very weak, therefore it's neglected in the following design. The wrapping will be designed based on the assumption that the confining stress required for the inhibition of lap splicing failure is provided by fibre glass wrapping only.

Glass fibre volume ratio ρ_{sj} required for the seismic retrofitting is calculated as,

$$\rho_{sj} = 2 \times \frac{[f_l - f_a]}{0.015 E_{sj}} \qquad \text{Equation 5.1}$$

in which f_l is the confining stress for the concrete provided by the glass fibre jacketing, f_a is the active confining stress provided by prestressing the jacket, and E_{sj} is the tensile modulus of elasticity of composite material.

$$f_l = \frac{A_b f_s}{\mu p l_s} \qquad \text{Equation 5.2}$$

in which A_b is area of a lapped bar, f_s is the transfer stress in the bar, which is simply calculated as 1.7 times the nominal strength of the longitudinal reinforcement, μ is the coefficient of friction, which is taken as 1.4, p is the perimeter of the crack surface, and l_s is the lap splice length.

The circular jacket will be used in the design. Then composite material volume ratio can be expressed as the function of fibre thickness t_j and jacket diameter D as in the equation 5.3,

$$\rho_{sj} = \frac{4 \times t_j}{D} \qquad \text{Equation 5.3}$$

If no active pressure is exerted to the jacket, i.e. f_a is zero, the computed glass fibre volume ratio from above equations is 0.013. Therefore, 6 sheets of wrapping fabric are designed, with a total thickness of 5.7 mm, for the confinement of rebar lap splices in the columns.

(b) Wrapping for ductility requirement in columns

As described in 5.4.2, plastic hinges in concrete columns should have adequate flexural strength and deformation capacity to ensure the desired plastic mechanism can be developed. After the plastic mechanism forms, bent displacement capacity depends on the rotation capacity of plastic hinges in the columns. From component push over analysis undertaken in chapter 4, bent 1 has only a displacement ductility of 1.9, and rotation ductility for the column plastic hinge is only 2.6. Therefore, glass fibre wrapping is needed to increase rotation capacity of plastic hinges in columns.

Numerous researches have demonstrated the effectiveness and efficiency of fibre-reinforced polymers (FPR) confining on concrete. Lab tests showed that composite material jacketing could be as effective as steel jacketing in the seismic retrofitting for column ductility. The ultimate strength and strain of concrete confined with FRP are increased greatly. Various equations have been developed to predict the relationship between the maximum confinement pressure f_{lu}, ultimate strain ε_{ju} of the confining member and wrapping fabric thickness t_j. A new analytical model developed by Spoelstra and Monti (1999) is used in this study.

In the research by Spoelstra and Monti (1999), two simplified approximate formulas are derived for the ultimate concrete compressive strain and strength, based on regression analysis of results obtained through the proposed exact models. It is found that the ultimate strength and strain have a direct dependence on the ultimate strain ε_{ju} of the confining composite jacket, the maximum confinement pressure f_{lu}, and the concrete modulus E_c, while they have an inverse dependence on the unconfined concrete strength $f_{co}^{'}$.

Three independent parameters are identified in their article as in equation 5.4,

$$\overline{f_{lu}} = \frac{f_{lu}}{f_{co}^{'}} \qquad \varepsilon_{ju}; \qquad \overline{E_c} = \frac{E_c}{f_{co}^{'}} \qquad \text{Equation 5.4}$$

in which, f_{lu} is calculated as in equation 5.5,

$$f_{lu} = \frac{2t_j f_{ju}}{d_j} \qquad \text{Equation 5.5}$$

where f_{ju} is the ultimate strength of composite material, t_j is the jacket thickness and d_j is jacket diameter.

From the regression analysis, the ultimate strength f'_{cu} and strain ε_{cu} confined with FRP are calculated as follows,

$$f'_{cu} = f'_{co}(0.2 + 3\sqrt{f_{lu}})$$

$$\varepsilon_{cu} = \varepsilon_{co}(2 + 1.25E_c\varepsilon_{ju}\sqrt{f_{lu}}) \qquad \text{Equation 5.6}$$

For the FRP retrofitting of bent 1 in this study, a circular glass fibre jacket is used. Assuming a wrapping fabric thickness of 5.7 mm as that used for the inhibition of lap splicing failure in column bottom, the ultimate strength and strain of the FRP confined concrete are, 46.7 N/mm^2 and 0.035, respectively.

Recalling the compressive strength of unconfined concrete in the case study bridge is 30 N/mm^2, over 50% increase in concrete strength is achieved; while the ultimate strain of confined concrete has been increased substantially. Fig 5.3 shows the stress-strain relationship for both unconfined concrete and FRP confined concrete.

The modified flexural capacity and deformation capacity of concrete columns due to glass fibre wrapping will be re-evaluated in section 5.4.5.

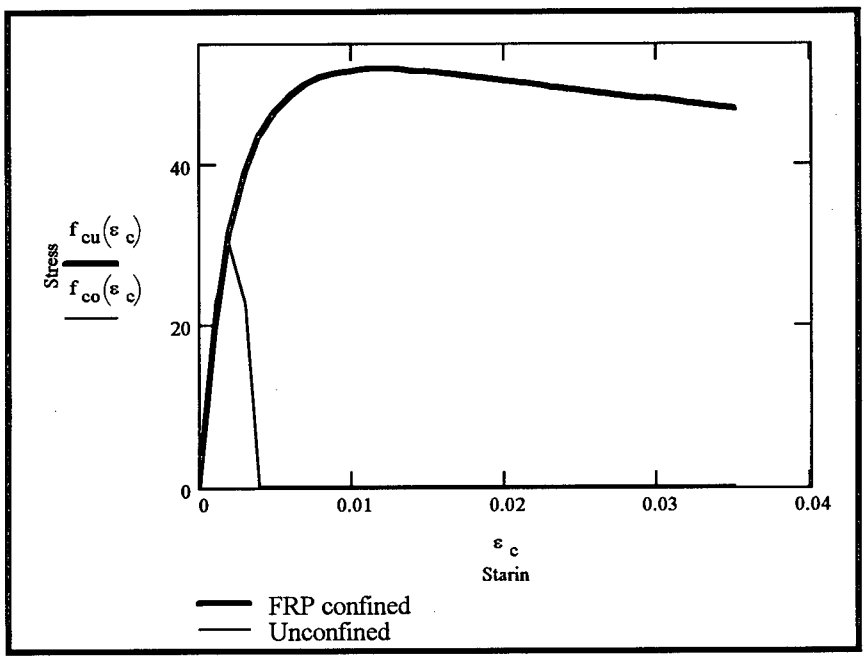

Fig 5.3 Stress-strain relationship for unconfined and FRP confined concrete

5.4.4.2 Wrapping for shear strength enhancement in the column

Shear strength in the column should be checked against the shear demand resulting from the over strength of flexural capacity in the structural member. Assuming a over strength factor of 1.3, shear demand V_{of} corresponding to the available flexural capacity in the column is calculated as in equation 5.7,

$$V_{of} = 1.3 \times \frac{(M_b + M_t)}{H} \qquad \text{Equation 5.7}$$

in which M_b and M_t is the flexural capacity of plastic hinge at column bottom and column top respectively, H is the distance between the top and bottom plastic hinge.

Shear capacity V_r from existing concrete section can be calculated in accordance with procedures in chapter 4. Required shear strength contribution from FRP wrapping, V_{js}, can be computed as in equation 5.8,

$$V_{js} = V_{of} - V_r = V_{of} - (V_c + V_s) \qquad \text{Equation 5.8}$$

Therefore, glass fibre thickness can be obtained from equation 5.9,

$$t_j = \frac{V_{js}}{0.5\pi f_j D_j} \times \frac{1}{\tan\theta} \qquad \text{Equation 5.9}$$

in which f_j is the design stress for the composite material jacket, D_j is the jacket diameter and is θ taken as 35°.

According to the above calculations, a 2.0 mm thickness of glass fibre fabric is needed for the column shear strength enhancement. Practically, three sheets of fabrics will be provided for the column wrapping with a total thickness of 2.85 mm.

5.4.4.3 Post tensioning in the cap beam

As specified in chapter 4, failure of bent 1 is resulted from the brittle shear failure in the cap beam. After the columns have been updated using FRP wrapping, force capacities in cap beam have to be checked using capacity design principles. Adequate flexural and shear capacity should be provided for the cap beam to ensure it will remain in elastic during earthquake events.

Two retrofitting schemes are available for upgrading cap beams, i.e. post tensioning the cap beam and FRP wrapping around the cap beam. The latter is very effective for the ductility enhancement, as demonstrated in the above. But it's not efficient for the flexural capacity enhancement. Shear capacity can be greatly increased through wrapping. As for the seismic retrofitting of the bent in accordance with the capacity design, cap beam is a force-protected member and it will work in the elastic range. So the elastic strength of the cap beam needs to be increased greatly, while confinement and ductility related to the plastic behaviour are not so important here. Also, the execution of post tensioning on site is more convenient compared to FRP wrapping. Therefore, post tensioning will be used in this study to strengthen the cap beam elastic force capacities.

Use VSL prestressing system for the post tensioning. 2 numbers of 19-13mm strands are designed for the cap beam section. Assuming 70% effective stress for the strands, a

compressive stress of 4.4 MPa will be resulted from the post tensioning. The sectional force capacity will thus be increased to the values as in the table 5.5.

Table 5.5 Increased force capacity in cap beam due to post tensioning

Item	Unit	Original member	After post tensioning	Percentage of increase
Positive moment capacity	kN-m	1370	4427	223
Negative moment capacity	kN-m	2700	5244	94
Shear capacity	kN	840	1220	45

From the table 5.5, we can find that post tensioning is very effective to enhance component elastic capacity. As expected, cap beam flexural strength and shear strength have been increased considerably.

5.4.5 Push over analysis

To demonstrate the effectiveness of seismic retrofitting on the seismic behaviour of structural members and ensure that the concrete bent 1 will be able to achieve specified performance levels, push over analysis of retrofitted bent is undertaken. Firstly, the modified component section properties due to retrofitting are computed and summarised in table 5.6. Then, the bent is pushed by a monotonically increasing lateral load till the structure fails. The plastic hinge sequence and yielding loads and displacements will be recorded, and the failure mechanism is to be identified. The analysis results will be compared with that obtained from push over analysis of original bents in Chapter 4.

Table 5.6 Modified component force and deformation capacity of bent 1

Plastic hinge property	Retrofitted structure		Unretrofitted structure		Percentage of change	
	Col in push	Col in pull	Col in push	Col in pull	Col in push	Col in pull
Yielding moment (kN-m)	2214	1893	2020	1705	9.6	11.0
Ultimate moment (kN-m)	2214	1893	2020	1705	9.6	11.0
Yielding curvature (rad/m)	0.00400	0.00397	0.00388	0.00357	3.1	11.2
Ultimate curvature (rad/m)	0.0720	0.0725	0.0340	0.0400	111.8	81.3
Curvature ductility	18.0	18.3	8.8	11.2	104.5	63.4
Yielding rotation (rad)	0.00686	0.00681	0.00666	0.00612	3.0	11.3
Ultimate rotation (rad)	0.0420	0.0430	0.0173	0.0200	142.8	115.0
Rotation ductility	6.2	6.3	2.6	3.3	138.5	90.9

As seen from Table 5.6, the moment capacity in the column due to FRP wrapping is increased by about 10%, while rotation ductility in the plastic hinge regions has been increased to more than one time. It's proved that the FRP wrapping is very effective for the ductility enhancement.

Push over analysis shows that the bent behaviour is ductile after level II retrofitting. Plastic hinge sequence is given in Table 5.7, in which the corresponding lateral load and

displacement are also shown for each hinge sequence. Failure of the bent occurs when lateral displacement capacity is reached. Yielding & ultimate force (displacement) of bent 1 are given in Table 5.7 as well.

Table 5.7 Plastic hinge occurring and ultimate lateral load and displacement

Plastic hinge (PH) sequence	Description	Lateral load (kN)	Lateral displacement (mm)
PH 1	Pull column bottom flexural hinge	1355	66
PH 2	Pull column top flexural hinge	1367	67
PH 3	Push column bottom flexural hinge	1471	78
PH 4	Push column top flexural hinge	1480	81
Bent yielding	Obtained from Fig. 5.6	1480	72
Bent ultimate	Cap beam reaches flexural rotation capacity	1480	305
Ductility	Ultimate/Yielding	1	4.2

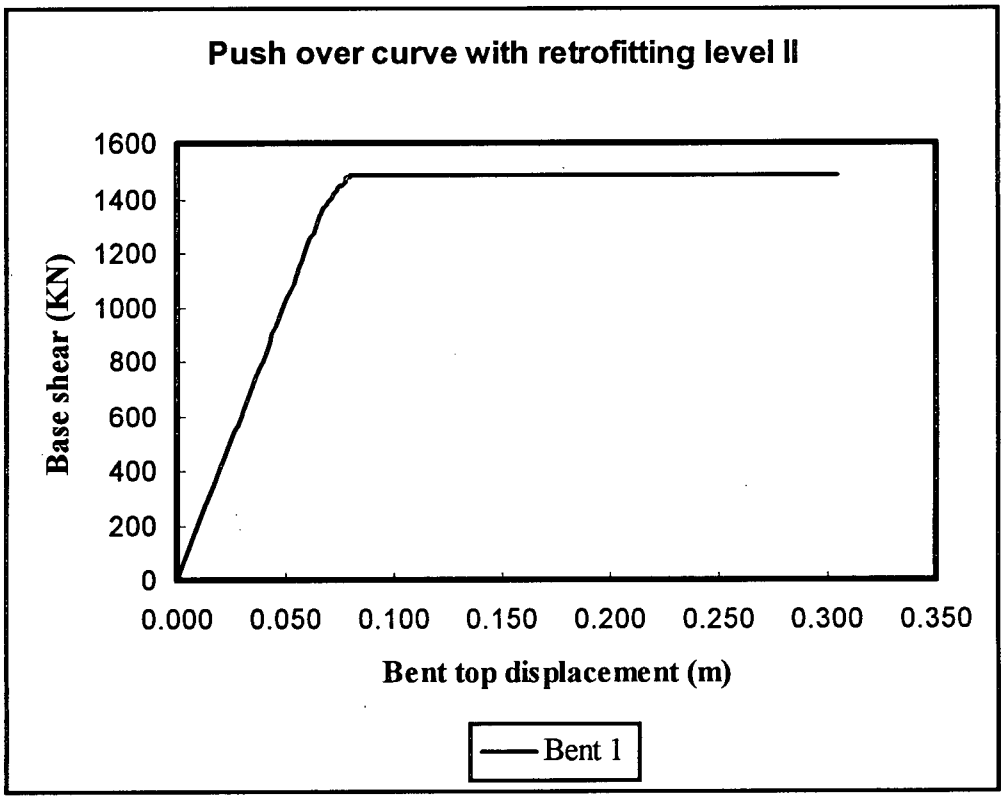

Fig. 5.4 Push over curve of bent 1 after level II seismic retrofitting

Push over curve of bent 1 after level II seismic retrofitting is shown in Fig. 5.4. From Table 5.7 and Fig. 5.4, the following observations can be made:

- Seismic retrofitting is effective in counteract the seismic deficiencies in the original bent.
- The structural behaviour is ductile. No premature shear failure and lap splice bond failure are experienced. Failure mechanism is that the bent reaches its displacement capacity.
- A local displacement ductility of 4.2 is attained after the level II seismic retrofitting, compared with only 1.9 in the original bent.
- The ultimate lateral load capacity is increased from 1045 KN to 1480 KN, with an increase of near 40%. But the bent lateral stiffness is almost the same as that of the original bent.

- Little redundancy is available for the two - column concrete bent of the case study bridge, even after level II seismic retrofitting. The ratio of ultimate load to the first plastic hinge occurring load is 1.09, i.e. only less than 10% strength reserve available after first hinge occurring in the bent.
- The expected performance level can be met when the structure is subjected to design earthquake loadings. It will be verified in detail in Chapter 6 & Chapter 7.

Seismic behaviour assessment of original and retrofitted structure in Chapter 4 and 5 are undertaken deterministically, in which component capacity is given a certain deterministic value and earthquake loading is represented by a two level design earthquake with 2% and 10% exceedence in 50 years respectively. Chapter 6 will evaluate structural behaviours probabilistically, in which structural failure probabilities of both original and retrofitted bridge are to be computed.

Chapter 6 Seismic Reliability Analysis

6.1 Introduction

Seismic reliability analysis will be undertaken in this chapter to compute failure probability of the case study bridge for both original and retrofitted structure during seismic excitations. Failure criterion and performance function will be firstly defined. Then Latin Hypercube Sampling (LHS) technique will be used to generate random variables for the input to calculate seismic demands and seismic capacities. Lastly, failure probability of the case study bridge subjected to earthquake loadings is to be computed based on the fitted probability distribution functions of seismic demands and capacities.

6.2 Development of a performance function

6.2.1 General description

For structural reliability problems under most loadings, e.g. gravity load, traffic load, and/or wind load, reliability calculations are reasonably straightforward using a first – order second – moment (FORM) or second – order second – moment (SORM) approach (Melchers, 1999 and Thoft-Christensen & Baker, 1982). However, for the situations where earthquake loading is the controlling load, the FORM and SORM approach cannot be directly used. The difficulty arises from the fact that an explicit performance function is required for the reliability analysis using FORM and SORM method. But for the structures subject to earthquake loads, such a performance function is usually not readily available. Also the structural behaviour due to earthquake excitations is dynamic and inelastic, it can only be understood in detail by considering complete time history analysis of inelastic response for a series of earthquake motions. Therefore, it is very difficult to assess structural reliability due to earthquake loading.

Some methods have been proposed in the past decades for structural reliability assessment under earthquake load, such as the Monte Carlo simulation approach (Melchers, 1999) and response surface approach (Foschi, 1999). However, both of these

two approaches are very time consuming. Tens of thousands of simulations may be required for the direct Monte Carlo Method to calculate probability of failure to a satisfactory accuracy level. For the Response Surface Method, various response surfaces corresponding to different limit states are required before any reliability analysis can be undertaken. Within the time limit of this study, a less time consuming and simpler approach has to be found. Latin Hypercube Sampling (LHS) (Ayyub & Lai, 1989, and O'Connor & Ellingwood, 1987) is an ideal choice for this purpose. LHS is one of the selective sampling schemes. It can provide a constrained sampling scheme instead of random sampling according to the direct Monte Carlo Method. This method has been successfully employed in other studies [e.g., Dymiotis el al, 1998, and Singhal & Kiremidjian, 1996] and it will be described in detail in the following sections.

6.2.2 Failure criterion

During earthquake excitations, structural failure can happen in many ways. A straightforward failure criterion is not immediately obvious. The situation is simplified by considering only collapse of the structure as a whole. For the case study bridge, where the steel superstructure has sufficient strength to withstand earthquake motions, the vulnerable components are concrete bents. Previous earthquakes have repeatedly proved that bridge piers are very susceptible to the earthquake damages and bridge collapses are mainly due to the collapse of piers (Northridge earthquake, 1994 & Kobe earthquake, 1995). For a continuously supported bridge superstructure with numerous piers, collapse of one pier usually leads to the collapse of the whole bridge. Therefore, failure of concrete bents as a whole can be selected as a failure criterion for the case study bridge.

More specifically, FEMA – 273 (FEMA, 1997) classifies structural behaviours subjected to earthquake excitations into two categories, namely force – controlled actions and deformation – controlled actions. The previous one represents the case where structural behaviours are non – ductile and the structure fails in a brittle way, while the latter is for the case where structural behaviours are ductile and visible deformations can take place. For the case study bridge, the original structure is believed to be seismic deficient and its

structural behaviours are controlled by the premature shear failure of cap beam during earthquake excitations. The retrofitted structure with safety level retrofitting is still brittle, although it is protected somewhat from the earthquake loading. For these two situations, the structure fails when shear force in the cap beam exceeds available shear capacity. In this case, little plastic deformation is experienced by structural component. So they can be categorized as force – controlled actions. The shear force in the cap beam of concrete bent will be selected as failure criterion to compute the failure probability.

After the bridge is upgraded with level II seismic retrofitting, it will behave in ductile mode. Plastic hinges are to occur in the bent columns and the bent will fail when the deformation capacity is exceeded by the deformation demands resulted from the earthquake excitations. Earthquake energy will be dissipated through bent displacements. Therefore, the behaviour of the structure with level II retrofitting can be classified as deformation – controlled action. And the bent lateral displacement can be selected as failure criterion in this case.

With failure criterion selected as in the above, the simple linear elastic response spectrum analysis (RSA) is permitted for the seismic demands computation. In case one, where shear force in cap beam is considered as failure criterion, RSA can be used directly and the results should be similar to the real value because little plastic deformation will be experienced by the structure. In case two, where bent lateral displacement is taken as failure criterion, RSA can still be used to calculate seismic demand. In the latter case, the structure is expected to behave in inelastic mode and much plastic deformation is to occur in columns. While the seismic forces obtained from RSA may not represent the true state of the structure, the seismic displacements calculated from RSA are somewhat comparable to the real displacements that the structure will experience. Also the concept of modification factor as in the FEMA – 273 (FEMA, 1997) can be used here to modify the elastic displacement to the inelastic displacement. Some previous researches have been done to obtain such a modification factor to allow some simple approaches be used for the seismic displacements computation, such as Miranda (1999), Shimazaki and

Sozen (1984), and Whittaker et al (1998), etc. Therefore, the drift at top of the pier can be used as limit state criterion for the reliability analysis.

6.2.3 Performance function

The performance function adopted for the reliability analysis can subsequently be taken as in the follows,

$$G(X) = C - D \qquad \text{Equation 6.1}$$

in which, G(X) is the performance function, X are the random variables, C & D are the cap beam shear capacity & shear demand for the first case, and bent lateral displacement capacity & displacement demand for the second case respectively. The computation of C and D will be given in the section 6.4, in which LHS is used to generate random variables to be input into the analysis programs to calculate seismic demand and capacity.

With performance function defined as in equation 6.1, the simple FORM and/or SORM approach can be used to compute failure probabilities. In this study, a reliability analysis program RELAN (Foschi et al, 2000) will be used to obtain probabilities of failure.

6.3 Random variables

6.3.1 General description

Great uncertainties exist for the estimation of seismic demands and capacities of structures subjected to earthquake excitations. The uncertainty includes actual uncertainty, which is caused by our inability (or unwillingness) to describe the phenomena accurately, as well as randomness, which is caused by variations imposed by nature. Two categories of uncertainties can be classified here: those associated with earthquake loading (ground motion) prediction, and those with assessment of structural properties, i.e., demand computation and capacity evaluation. Ground motion prediction is highly variable and huge uncertainty is expected for earthquake loading estimation. NEHRP – 1994 considered a coefficient of variation of up to 100% for seismic hazard

calculation. Some researches thus consider the earthquake loading as the only random variable in the seismic reliability analysis (Bazzurro, P., & Cornell, C.A., 1994, and Arede, A., & Pinto, A.V., 1996). It argued that the large uncertainty in earthquakes, which alone accounts almost entirely for the overall variability in response and renders the effects of the other uncertainties negligible. Most recent researches have considered both the uncertainties in earthquake loading prediction and structural properties estimation for the reliability analysis (Singhal & Kiremidjian, 1996). In this study, the focus will be on the variability in structural property evaluation while the efficiency of the overall procedure is to be sought. The conditional probability of structural failure conditioned on the earthquake occurrence is to be computed in this Chapter. The seismic hazard will be modelled as a type II extreme distribution function and the occurrence of earthquake loading is to be represented by a Poisson distribution.

6.3.2 Selection of random variables

Random variable selection has an important impact on the efficiency and effectiveness of reliability analysis. The considered random variables should include those that have big effects on the structural seismic behaviour and a balance between precision and computation time is to be sought.

Various structural properties affect structural behaviours during seismic excitations. They can be classified as,

- Structural geometry: total length, span, deck width, pier height, section size, etc.
- Boundary conditions: foundation type, abutment, soil condition, soil – structure interaction, etc.
- Material property: compressive strength of concrete, ultimate concrete strain, yielding strength and strain of steel reinforcement, ultimate strength and strain of steel reinforcement, etc.

- Modeling uncertainty: currently available analysis techniques cannot guarantee the real behaviour of the structure during an earthquake be obtained, many assumptions and simplifications are still necessary. Modeling uncertainty is high.

A review of random variables considered by some previous researches is given in table 6.1.

It can be found that most researches choose material properties as the random variables (R.V.) for the reliability analysis and less than 10 R.V. are normally used. Considering that numerous repeated dynamic analyses are needed for the reliability analysis, the number of R.V. needs to be limited in practical application.

For the case study bridge, seismic behaviour assessment in Chapter 4 have shown that soil springs modeling and effective elastic stiffness of piers have very big effects on the structural dynamic property and inertia force distribution among piers and abutments. Therefore, soil spring stiffness, abutment spring stiffness and effective elastic stiffness of piers will be chosen as random variables for the seismic demand computation. As for seismic shear capacity calculation, basic material properties, such as $f_c^{'}$, f_y and component curvature ductility are considered as random variables to be input directly into reliability analysis. Displacement capacity at bent failure of concrete bent with level II retrofitting is taken as a random variable too. The chosen R.V. in this study are given in Table 6.2. Their probability distribution functions and parameters are also listed in the table 6.2.

Having chosen R.V. to be included in the reliability analysis, random combinations of R.V. need to be input into dynamic analysis program to calculate seismic demands and capacities. Latin Hypercube Sampling (LHS) is used here for this purpose, which is to be introduced in detail in the next section.

Table 6.1 Review of Random Variables (R.V.) considered by other researchers

Researcher	No. of R.V.	Random Variables	Probability Distribution	Mean value	COV
Dymiotis et al (1999)	5	$f_c^{'}$	Lognormal	$f_{ck}^{'} + 8MPa$	18.0%
		f_y	Lognormal	$f_{yk} + 40MPa$	6.0%
		f_u	Lognormal	$1.15 * f_y$	6.0%
		ε_{su}	Lognormal	0.09	9.0%
		ε_m	Lognormal	1.0	39.0%
Song & Ellingwood (1999)	9	β_1	Uniform	0.4	29.0%
		β_5	Uniform	0.95	29.0%
		F_y (Col)	Lognormal	393	12.0%
		F_y (Beam)	Lognormal	290	12.0%
		F_y (Panel)	Uniform	414	9.0%
		E	Uniform	200	6.0%
		G	Uniform	77	9.0%
		Damping 1	Uniform	0.05	29.0%
		Damping 2	Histogram	0.023	62.0%
Sighal & Kiremedjian (1996)	2	$f_c^{'}$	Normal	1.14*Nominal	14.0%
		f_y	Lognormal	1.05*Nominal	11.0%
Seya et al (1993)	2	Damping	3 Values	0.01, 0.02, 0.03	N/A
		Yield strength	Lognormal	1.07*Nominal	15.0%
O'Conner & Ellingwood (1987)	3	Frequency	Lognormal	Norminal	30.0%
		Damping	Lognormal	Norminal	50.0%
		Yield displa.	Lognormal	Norminal	15.0%

Table 6.2 Random Variables for the Reliability Analysis

Item	Random Variables		Probability Distribution	Mean value	COV
Structural Properties that Affect Seismic Demand	Spread Footing Soil Spring Stiffness	K_v (kN/m)	Lognormal	183300	40.0%
		K_h (kN/m)	Lognormal	144400	40.0%
		K_{YY}(kN-m/rad)	Lognormal	111700	40.0%
		Kzz(kN-m/rad)	Lognormal	111700	40.0%
		K_T(kN-m/rad)	Lognormal	145200	40.0%
	Pile Foundation Soil Spring Stiffness	K_v(kN-m)	Lognormal	1224000	40.0%
		K_h (kN/m)	Lognormal	240400	40.0%
		K_{YY}(kN-m/rad)	Lognormal	682800	40.0%
		Kzz(kN-m/rad)	Lognormal	291300	40.0%
		K_T(kN-m/rad)	Lognormal	1328000	40.0%
	Pier Effective Stiffness	EI_{eff}	Lognormal	$0.5*EI_{gross}$	20.0%
Seismic Shear Capacity	Concrete Compressive Strength	$f_c^{'}$	Lognormal	30	18.0%
	Steel Yield Strength	f_y	Lognormal	300	15.0%
	Curvature Ductility	μ_ϕ	Lognormal	4	40.0%
Bent Displacement Capacity at Failure	Lateral Displacement	Δ	Lognormal	0.03*H	40.0%

The meanings of symbols in the table 6.1 and 6.2 are the same as in Chapter 4.

6.3.3 Latin Hypercube Sampling (LHS) technique

LHS is a technique that provides a constrained sampling scheme instead of random sampling according to the direct Monte Carlo Method.

Traditionally, random numbers are generated between 0 and 1 randomly. These random numbers are then used to generate random variables according to the prescribed distribution function for each variable. In LHS, the region between 0 and 1 is uniformly divided into N non – overlapping intervals. The N non – overlapping intervals are selected to be of the same probability of occurrence as illustrated in Fig 6.1. Then, N different values in the N non – overlapping intervals are randomly selected for each random variable, i.e., one value per interval is generated. The random number in the m^{th} interval, U_m can be calculated as follows,

$$U_m = \frac{U}{N} + \frac{m-1}{N} \qquad \text{Equation 6.1}$$

in which m = 1, 2, …, N, U is a random number in the range (0, 1).

U = 0.5 is selected for this study to simplify the process, which means the generated random number will be at the middle of each interval. But in reality, any random number of U in the range of (0,1) can be used.

After the "constrained" random values, U_m's, are obtained, the inverse transformation method can be used to map these numbers through the cumulative distribution function to produce the generated random variables. It is done by the following equation,

$$x_m = F_x^{-1}(U_m) \qquad \text{Equation 6.2}$$

in which x_m is the m^{th} generated random variable for variable X, and F_x^{-1} is the inverse cumulative distribution function for variable X.

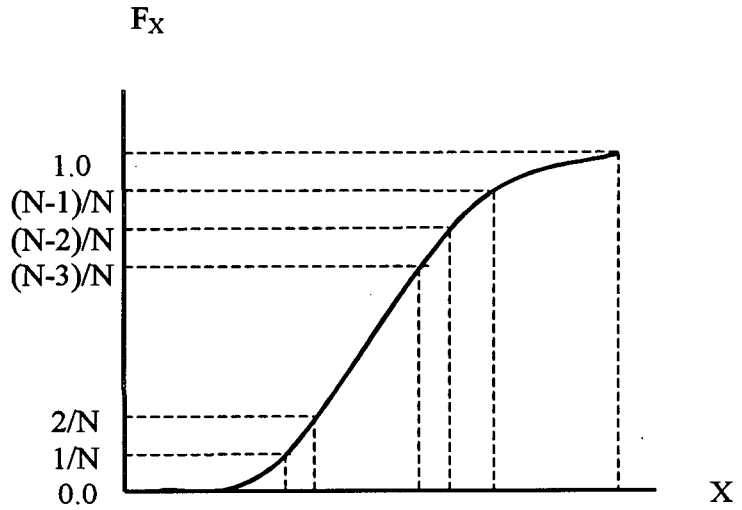

Fig. 6.1 Intervals used with a LHS of size N in terms of the Cumulative Distribution Function

With the N random values for different random variables selected, grouping of these values is required to be input into the analysis program. Random permutation of the N integers corresponding to the N simulation cycles is used here for each variable. The grouping is accomplished by associating those different random permutations in each simulation cycle. For example, variable X and Y are generated for 5 simulation cycles. The random permutation set for variable X is (2, 1, 5, 3, 4), and the random permutation set for variable Y is (4, 3, 1, 2, 5). Then the grouping can be formed as shown in follows,

Processing No.	(X	Y)
1	(X_2	Y_4)
2	(X_1	Y_3)
3	(X_5	Y_1)
4	(X_3	Y_2)
5	(X_4	Y_5)

6.3.4 Generation of input random variables

The aforementioned Latin Hypercube Sampling technique will be used here to generate N sets of random variables to be input into structural analysis program to compute seismic demand and seismic capacity. Accordingly N simulations will be undertaken.

20 simulation cycles are used in this study with 15 random variables, as specified in section 6.3.2. The inverse transformation as in equation 6.2 is done using the commercial program MathCAD 8 (MathSoft Inc., 1998). Random permutation and grouping are made through a statistics program.

6.4 Computation of failure probability

6.4.1 General description

20 different simulations are undertaken with response spectrum analysis to obtain cap beam shear force and bent lateral displacement for seismic demands computation. Then, seismic demands and capacities are fitted to the appropriate probability distribution functions. Finally, after the distribution functions of demand and capacity are defined, probability of failure is calculated using the reliability analysis program - RELAN (Foschi et al, 2000).

6.4.2 Representation of earthquake loading

For the deterministic analysis in previous chapters, earthquake excitation is represented by specified earthquake loadings, i.e. design earthquakes with 10% exceedence in 50 years and 2% exceedence in 50 years respectively. Although it's recognized that there is a high variability in earthquake loading prediction, the adoption of spectral acceleration S_a from the new seismic hazard map by GSC (1999) for structural design is generally accepted by practicing engineers.

For reliability analysis, there is a possibility to consider earthquake loading stochastically to taking account of the high uncertainty in earthquake prediction. But for a site – specific

analysis, as for the case study bridge, where seismic hazard at the site is computed from the new seismic hazard map by GSC (1999) and local soil conditions are generally known, the uncertainty in earthquake loading estimation should be much less than in general situations. Also the focus of this study is the uncertainty in structural behaviour. Therefore the earthquake loading is to be represented by spectral acceleration S_a on site. S_a is computed from a type II extreme probability distribution function, which is discussed in detail in Chapter 3. Table 6.3 gives spectral acceleration ranges at the period T = 0.5s corresponding to different earthquake occurrence rates for the reliability analysis. It is worth to be noted that the computed failure probabilities are conditional structural collapse probabilities given the earthquake occurrence.

Table 6.3 Spectral acceleration ranges for reliability analysis

Probability of exceedence		Return Period (Years)	Spectral acceleration (g)
50 years	Annual occurrence rate		
70%	0.023	43	0.185
50%	0.014	72	0.22
10%	0.0021	475	0.45
5%	0.001	1000	0.59
2%	0.000404	2500	0.83
1%	0.0002	5000	1.075

6.4.3 Fitting probability distribution function

6.4.3.1 Original structure

Seismic demand is computed from a response spectrum analysis with various spectral accelerations using structural analysis program SAP2000. The computed cap beam shear demand is fitted with a Lognormal distribution function, as shown in Figure 6.2, which shows cumulative probability distribution function (CDF) of shear force in cap beam subjected to 10% exceedence earthquake in 50 years. CDF for other earthquake levels are similar but they are not shown here to save space.

Lognormal probability distribution function fits the calculated shear demands reasonably well with an error of 0.029 by F test. The mean value of shear demand is 579 KN and the standard deviation is 96 KN.

Fig. 6.2 Cumulative Probability Distribution of Cap Beam Shear Demand before retrofit

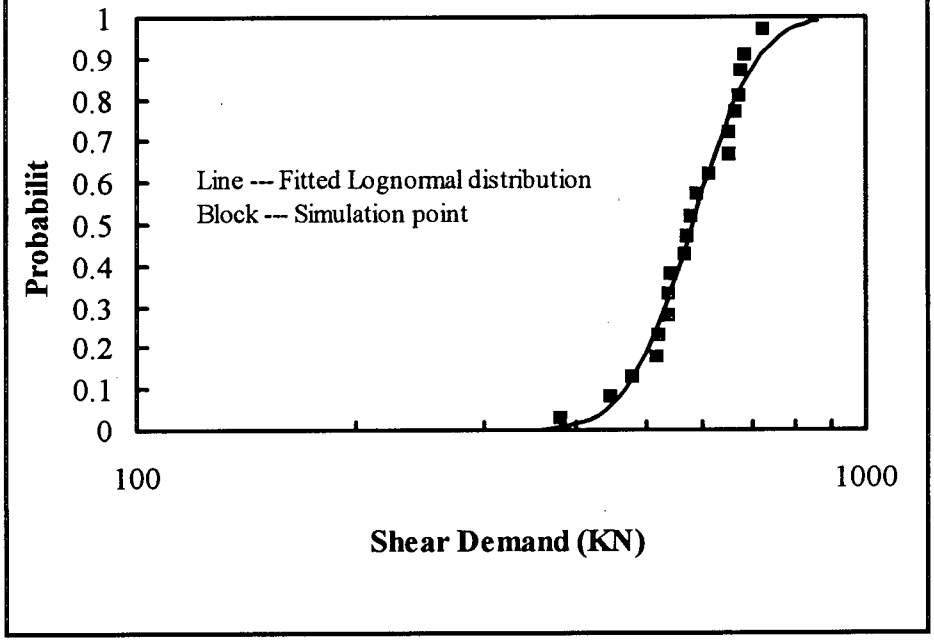

6.4.3.2 Structure with retrofitting level I

Due to the effect of modified structural dynamic property by seismic retrofitting, shear demand is reduced in bent 1. Fig 6.3 shows the fitted cumulative probability distribution function (CDF) for shear demand. Lognormal probability distribution function is used for the fitting. The fitting has an error of 0.029 by F test. The mean value of shear demand is 467 KN and the standard deviation is 91 KN.

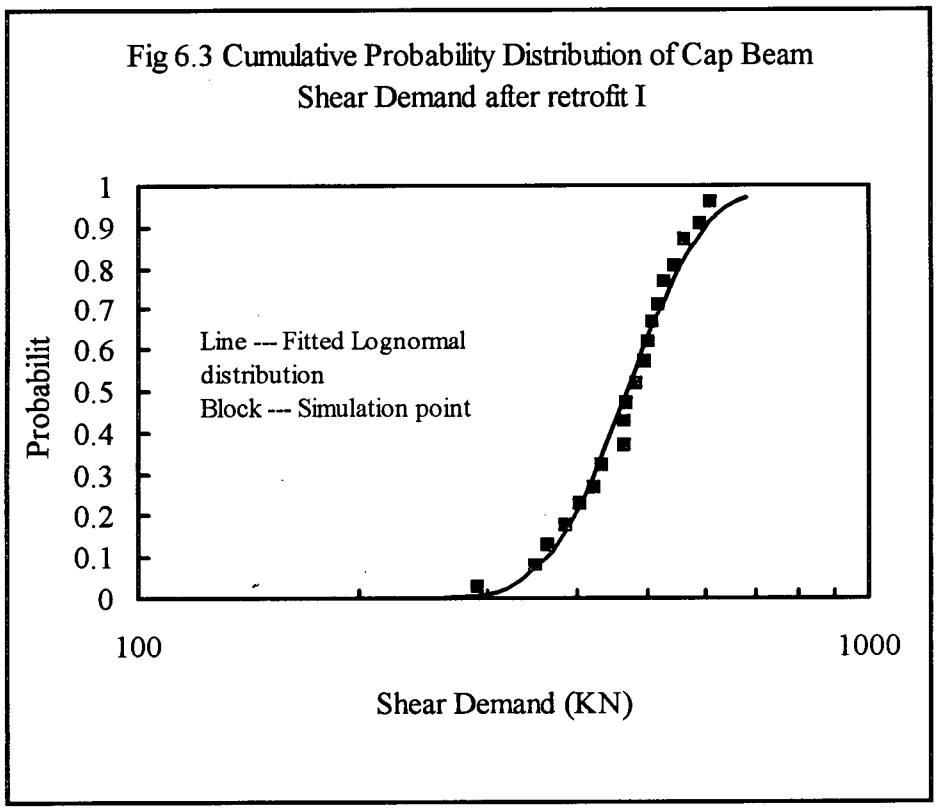

Fig 6.3 Cumulative Probability Distribution of Cap Beam Shear Demand after retrofit I

6.4.3.3 Structure with retrofitting level II

Bent lateral displacement is chosen as failure criterion for the reliability analysis. Fig. 6.4 shows the fitted cumulative probability distribution function (CDF) for lateral displacement at top of the bent. It's fitted with a Lognormal probability distribution function. The fitting has an error of 0.0165 by F test. The mean value of lateral displacement is 39 mm and the standard deviation is 5 mm.

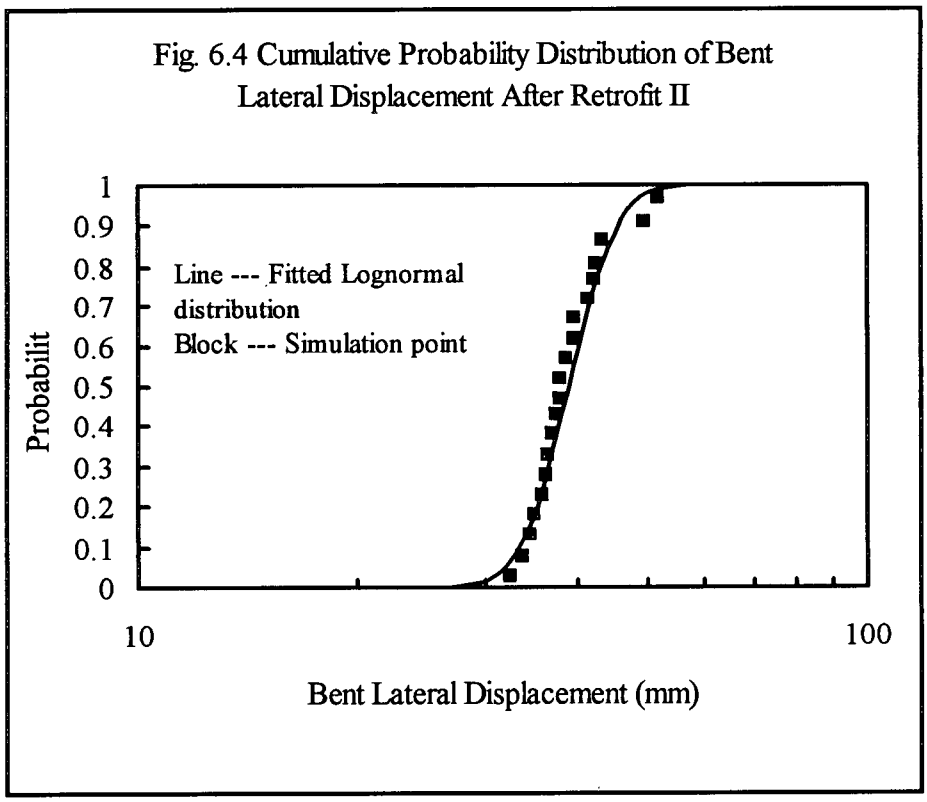

The obtained displacement as in the above is calculated from the linear, elastic response spectrum analysis. As demonstrated in Chapter 5, much plastic deformation is expected for the updated bent with level II retrofitting. Some modifications are necessary to estimate the maximum displacement demand from the elastic displacement. In this study, the modification factor recommended by Miranda is used to modify the elastic displacement to inelastic displacement. Miranda (1999, 1991) analyzed 31,000 SDOF systems using 124 different ground motions, 50 periods, and five levels of displacement ductility to generate and statistically study constant ductility spectra. This computational endeavour produced relations between elastic and inelastic displacement. An inelastic displacement ratio β defined as the ratio of the maximum inelastic displacement to the maximum elastic displacement is calculated as follows,

$$\beta = \left[1 + (\frac{1}{\mu} - 1)\exp(-12T\mu^{-0.8})\right]^{-1} \qquad \text{Equation 6.4}$$

in which T is vibration period of the structure, and μ is the displacement ductility ratio.

Fig. 6.5 shows the ratio β varies with vibration period T at different displacement ductility. For the case study bridge, the upgraded structure with level II seismic retrofitting has a period T = 0.5s in the first transverse vibration mode. The retrofitted bent can sustain a displacement ductility of $\mu = 4.0$. Substitute T and μ into equation 6.4, the inelastic displacement ratio β is 1.10.

Fig. 6.5 Ratio of inelastic diaplacement to elastic displacement

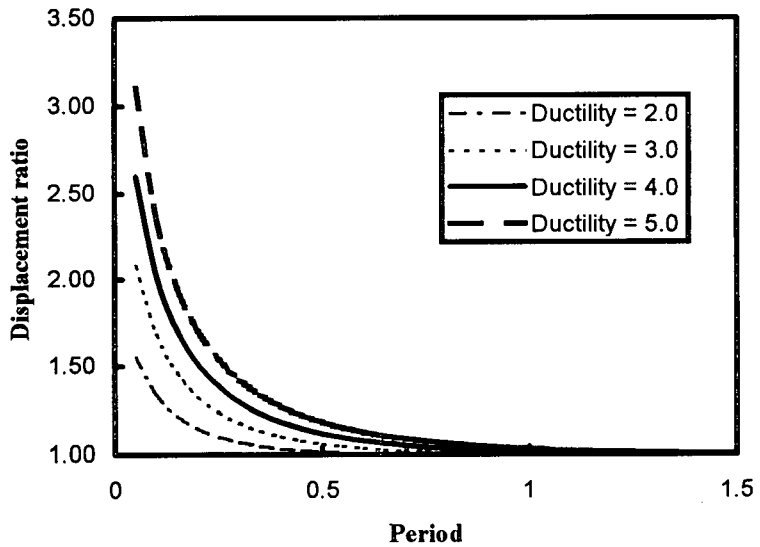

6.4.4 Probability of failure

6.4.4.1 General description

Probability of failure is evaluated using the reliability analysis program RELAN (Foschi, Yao and Li, 2000). RELAN is a general reliability analysis program to calculate the probability of non – performance in specified performance criteria. It is developed in the Civil Engineering Department, the University of British Columbia. In RELAN, each performance criteria is written in the form of performance function G, such that non –

performance corresponds to $G < 0$. Probability of failure can be calculated based on the simple FORM/SORM approach, Direct Monte Carlo Simulation or Importance Sampling. In this study, FORM/SORM approach will be used to compute structural failure probabilities.

6.4.4.2 Original structure

Seismic demand D, which is designated as shear force in cap beam, is simulated and fitted with Lognormal probability distribution function as in section 6.4.3. Seismic capacity C, which is designated as shear capacity in cap beam, is calculated by Priestley's approach. The computed probabilities of failure of the structure subjected to various earthquake excitations are depicted in Fig. 6.6.

6.4.4.3 Structure with retrofitting level I

The same computation procedure as in the section 6.4.4.2 is undertaken for the structure with level I retrofitting. To compare the effect of retrofitting on the probability of failure, the computed failure probabilities of the structure with level I retrofitting are also given in Fig. 6.6.

6.4.4.4 Structure with retrofitting level II

Various damage states will be experienced by the updated structure with level II retrofitting before it fails finally due to the excessive deformation. To simplify the analysis, only the complete collapse state will be discussed here. The failure probability corresponding to complete collapse is computed as follows.

Bent lateral displacement demand D is simulated and fitted with Lognormal probability distribution function as in section 6.4.3. Bent displacement capacity C at complete collapse is highly variable with different geometry and reinforcement arrangement for bridges. Determination of an appropriate displacement capacity is in controversy. A series of lab tests were undertaken in the University of California at San Diego on the

behaviour of concrete bents subjected to earthquake loadings. The test results showed that a drift ratio of 3% to 5% is attained at complete collapse of the structure. For the reliability analysis in this study, a Lognormal probability distribution function is assumed for the bent displacement capacity with a mean drift ratio of 3.5% and COV of 40%.

The computed failure probabilities with different earthquake excitation levels are shown in Fig. 6.6. As expected, the probability of structural collapse has reduced sharply due to the level II seismic retrofitting.

Fig. 6.6 Probability of failure at collapse

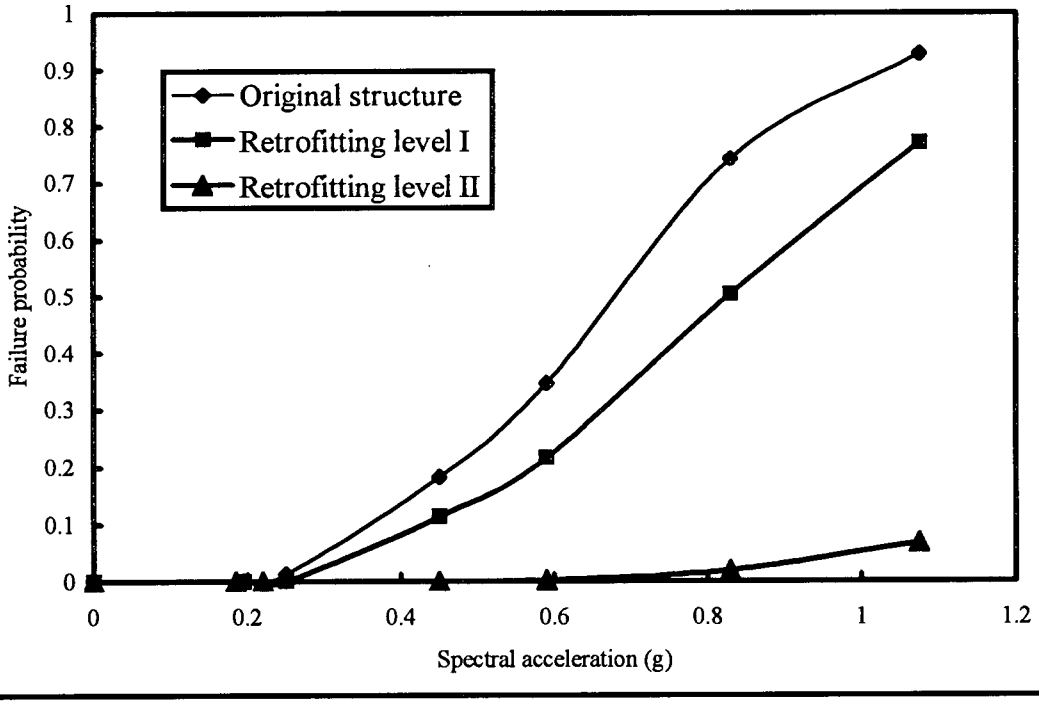

6.4.5 Failure probability comparison and discussion

The computed failure probabilities against a range of spectral accelerations from section 6.4.4 are listed in detail in Table 6.4.

Table 6.4 Comparison of failure probabilities

Earthquake return period (years)	Spectral acceleration (g)	Probability of failure at collapse		
		Original structure	Structure with level I retrofitting	Structure with level II retrofitting
43	0.185	3.42E-04	0	0
72	0.22	0.0128	5.58E-04	0
475	0.45	0.183	0.114	2.40E-04
1000	0.59	0.347	0.217	2.00E-03
2500	0.83	0.743	0.504	0.019
5000	1.075	0.928	0.771	0.068

The following observations can be made from Table 6.4and Fig. 6.6,

- The original structure has a very high probability of failure at collapse due to earthquake loadings. Table 6.4 shows that the structure is at 18% probability of collapse during an earthquake with a 10% exceedence in 50 years (Earthquake I). The failure probability is increased to 74% during a 2% exceedence in 50 years earthquake (Earthquake II).
- The updated structure with level I retrofitting has a reduced probability of failure at collapse of 11% and 50% for Earthquake I and Earthquake II respectively. But the effect of retrofitting on the failure probability is small.
- With level II retrofitting, the probability of failure at collapse is reduced to 0.024% for Earthquake I and 1.9% for Earthquake II respectively. Therefore, the structure is protected from any integrity loss. The effect of retrofitting is obvious and failure probability is decreased two to three magnitude from unretrofitted structure.

It is worth to note that probabilities of failure obtained here are conditional probabilities given specific earthquake spectral acceleration occurrences. The structural failure probability subjected to earthquake loadings will be discussed in Chapter 8. The next chapter will give the seismic physical damage estimation and mapping of financial damages in dollars based on the physical damages.

Chapter 7 Seismic damage analysis and direct financial damage estimation

7.1 Introduction

Seismic damage analysis will be undertaken in this chapter to compute damage index of the case study bridge subjected to real earthquake records. The purpose of seismic damage analysis is, firstly to obtain damage status of the case study bridge during real earthquake events and testify the effectiveness of the seismic retrofitting, secondly to quantify the seismic damages by damage index. The nonlinear, inelastic dynamic analysis program CANNY – E (Li, 1996) will be used for the analysis. The earthquake records will be first chosen and the structure is to be modelled with CANNY – E. Both the original and retrofitted bent will be analyzed and the damage index against a range of peak earthquake accelerations will be tabled. Then, the direct financial damages in dollars will be mapped out based on the relationship between damage index and damage in dollars. Empirical data on the relationship between physical damage and damage index from laboratory tests will be utilized in this study.

7.2 Modelling for the seismic damage analysis

7.2.1 General description

As demonstrated in the seismic behaviour assessment in Chapter 4 and Chapter 5, the inelastic and nonlinear behaviour of the case study bridge will concentrate in concrete bents. The steel superstructure is assumed to be mainly in elastic range. It also shows that bent 1 is the most vulnerable substructure subjected to earthquake loadings. Moreover, a time history analysis of the whole bridge is time consuming and not acceptable for the time allowance for this study. Therefore, the seismic damage analysis is to be done for the isolated bent 1 only. However, the tributary mass assigned to bent 1 is obtained from the global structure elastic analysis to get an appropriate mass distribution among substructures.

Modelling of the bent 1 will generally follow the procedures set out in ATC – 32 (ATC, 1996) and specification and manual of program CANNY – E (Li, 1996).

7.2.2 Analysis program CANNY – E

7.2.2.1 General description

CANNY – E (Li, 1996) is developed for the nonlinear static and dynamic analysis of reinforced concrete frame and/or shear wall structures. It was initially developed by Mr. Kang Ning Li at the University of Tokyo, Japan where he was studying for his PhD. The first version was written in FORTRAN. Many revisions were made later for the initial version and the newest version now is CANNY – E, which is re-written in C – language.

The main features of this program that set it apart from other analysis programs are its modelling of the triaxial interaction among axial load and bi-directional bending moments through a multi-spring model and a hysteresis library where a number of realistic, easy-to-use hysteresis models are available. CANNY – E also has a post – processor that calculates damage index at each element and then combines all the indices to give an overall damage index for the structure being analyzed.

7.2.2.2 Hysteresis model

The program includes a number of hysteresis models representing nonlinear force – displacement relationships. Some are used for one-component models to simulate the inelastic behaviour of uniaxial bending, shear and axial deformation. Others are used for multiple axial spring models (MS model) to represent the behaviour of biaxial – bending and axial force interaction. Only one – component models will be introduced here.

A total of 22 one – component models are available to be used in the analysis. They include the simple Degrading Bilinear/Trilinear Model, Bilinear Slip Model, and the more complicated CANNY Simple/Sophisticated Model. The versatile hysteresis models make the program capable of modelling very large types of structural behaviours, especially for the seismic behaviours, where strength loss, stiffness degradation and

pinching behaviour can all happen together. CANNY sophisticated model, which is used in the analysis for the case study bridge, is discussed in detail as follows. The other hysteresis models can be found in the program's manual.

CANNY sophisticated model (CA7) is meticulously designed to represent the stiffness degradation, strength deterioration and pinching behaviour by a series of control parameters, θ, β_e, β_d, δ, $\lambda 3$, ε and λs. The meaning and likely values of hysteresis parameters are given in Table 7.1. The hysteresis models are schematically shown in Fig. 7.1.

Table 7.1 Values of CANNY hysteresis parameters

Parameter	Physical meaning	Range of values
θ	Stiffness degradation	Any positive number 0.0 = very severe stiffness degradation ≥ 10.0 =virtually no stiffness degradation values between 1.5 and 3.0 suitable for most concrete structures
β_e	Energy-related strength loss	0.0 to1.0 0.0 = no strength deterioration 1.0 = very severe deterioration
β_d	Ductility-related strength loss	0.0 to1.0 0.0 = no strength deterioration 1.0 = very severe deterioration
δ	Unloading control axis UU'	0 to 0.05
λ_3	Softening yielding stiffness	0 to 1.0
ε	Pinching effect	0 to 1.0
λ_s	Pinching effect	0 to 1.0

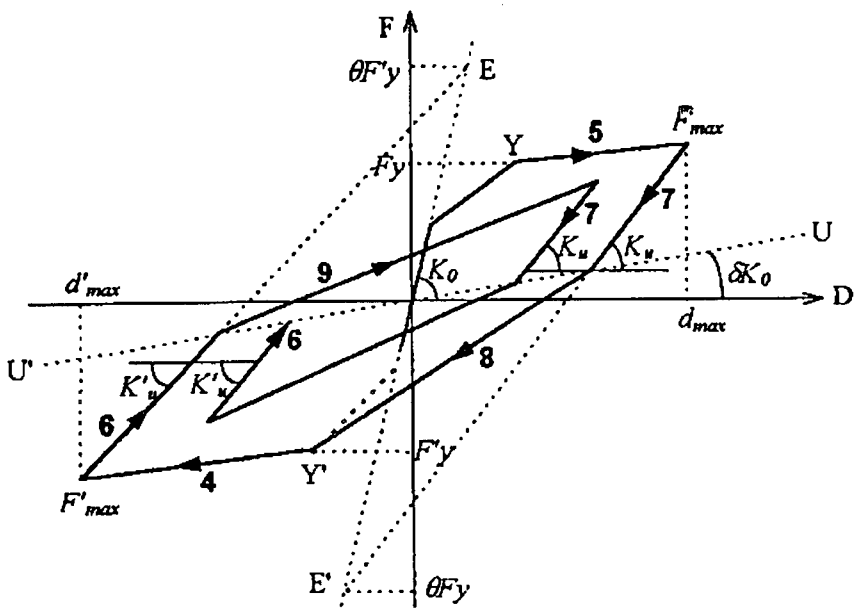

(a) Unloading Stiffness Degradation

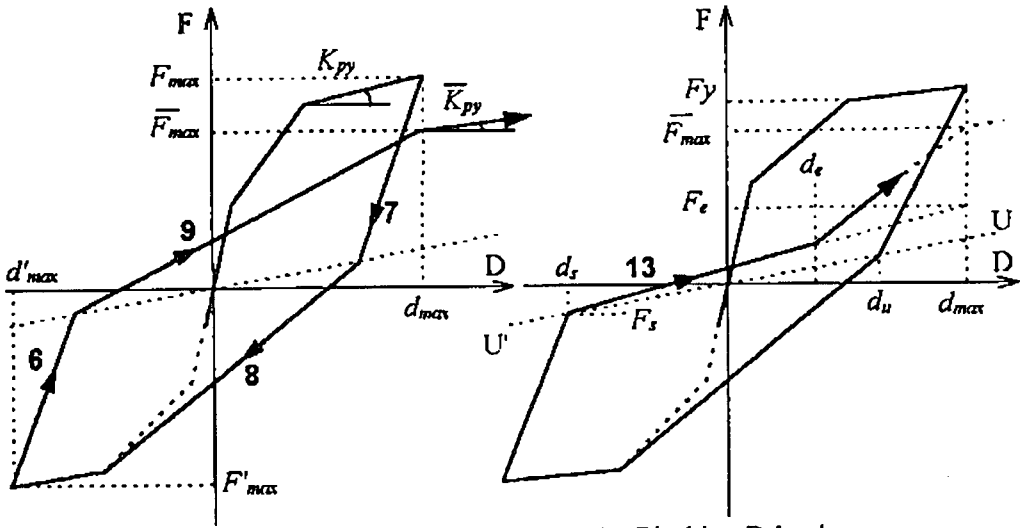

(b) Strength Deterioration

(c) Pinching Behavior

Fig. 7.1 CANNY sophisticated hysteresis model, HN = CA7

7.2.2.3 Damage index

In the case of concrete structures, damage indices have been developed to provide a way to quantify numerically the seismic damage sustained by individual elements or complete structures. Indices may be based on the results of a nonlinear dynamic analysis, on the measured response of a structure during an earthquake, or on a comparison of a structure's physical properties before and after an earthquake (Williams & Sexsmith, 1994). Various damages indices are available for the damage computation. The damage index D_i built into CANNY – E is based on the combined index proposed by Park and Ang (1985), and is defined as

$$D_i = \frac{\delta_m}{\mu\delta_y} + \beta_e \frac{E_i}{F_y \mu\delta_y} \qquad \text{Equation 7.1}$$

The first term is the ratio of the maximum displacement δ_m achieved to the displacement at failure (here defined as ductility μ times yield displacement δ_y), and is referred as the deformation damage. The second term, known as the strength damage, is a normalized form of the energy E_i absorbed in the hysteresis loops, scaled by the user – input hysteresis parameter β_e. This parameter is chosen to represent the level of strength degradation of the concrete when loaded beyond yield and can take any value between 0.0 and 1.0. This implies that, for well reinforced and confined concrete (low β_e) the damage is dependent solely on the ductility level achieved, whereas for poor quality concrete (high β_e) the number of cycles of loading at a given level becomes increasingly important. The choice of β_e is likely to be rather subjective unless test data are available against which the hysteresis parameters can be tuned, making it difficult to apply the index to a wide range of different structural types. A default value of $\beta_e = 0.1$ is assumed in the CANNY – E program.

Overall damage indices D_s for storeys and complete structures are found by taking a weighted average of the local indices found from Equation 7.1, in which the weighting

factors are proportional to the energy absorption at a given location. D_s is given as in the Equation 7.2,

$$D_s = \frac{\sum E_i D_i}{\sum E_i} \qquad \text{Equation 7.2}$$

Thus, if damage is concentrated at a single location, then the index at the location will dominate the overall index, whereas if damage is evenly distributed, then the overall damage index will be closer to the mean of the local indices.

7.2.2.4 Elements and analysis options

CANNY – E is applicable to the structures that can be idealized by rigid nodes and linear elements and spring elements. It can be used for analysis of most buildings structures, towers, trusses, and also some bridge structures. It accepts the structures in irregular shape and with complicated geometrical configuration.

Two sets of numbering system are used in the program for the numbering of nodes and elements. One is frame – floor number system and the other is sequential number system. The frame – floor number system uses the name of floor level and frame, and is available for frame building structure. It makes input data and output results in simple form and readable. The sequential number system is generally applicable to all types of structures. This makes the program very flexible for the input of data.

There is a rich element library available for the program. The following elements are included in the element library,

- Beam element:

A beam element is limited to have uniaxial bending and shear in the vertical plane formed by the Z – axis and the beam axial line, and may have axial deformations. The inelastic flexural deformation of the beam element is assumed to be concentrated at its ends, and represented by the rotation of two nonlinear bending springs. The shear and

the axial deformations of beam, are approximated by independent shear and axial spring placed at its midspan. Such beam models does not include the interactions among the bending, shear and axial deformation.

- Column element

A column element may be idealized by any one of three types of analysis model: one – component model for uniaxial bending column element, biaxial bending model, and multi – spring model. User can choose the models according to the analysis assumptions and load types. Multiple spring models (MS model and biaxial shear model) are used to present the interactions among the biaxial lateral loads and the varying axial load in column element.

The shear deformation of the column is optional as with the beam. It is represented by a uniaxial shear spring for the column under uniaxial bending, and by the multiple shear spring model.

The axial deformation of the column element is always included when using MS model to simulate the axial load – bending moment interaction.

- Shear panel element

Shear panel is assumed to have bending, shear and axial deformations in the panel plane, and have no resistance against the deformation of out – panel plane. The shear panel is idealized as a line element located at the panel central line. The bending, shear and axial springs are simple one – component springs without interaction between them. Plane section assumption is applied to determine the rotation at the panel base and top sections from the vertical translations of the nodes at the panel four corners. The plane section assumption means that there is rigid beam at the panel base and top.

- Truss – type link element

Any line element connecting two nodes and subjected to tension/compression with no bending can be treated as truss – type link element. Truss – type element has its axial direction pointing from the initial – end to the terminal – end. Truss – type element has its force and displacement presented in positive value for compression and negative value for tension.

- Spring – type link element

A link element can be a single translational spring that resists the relative displacement between two nodes in the global X (or Y or Z) direction only. Spring – type link elements are identified by notations as follows,

TX	X – translational link element	$d_x = D_{x1} - D_{x2}$
TY	Y – translational link element	$d_Y = D_{Y1} - D_{Y2}$
TZ	Z – translational link element	$d_Z = D_{Z1} - D_{Z2}$

The direction of the spring – type link elements is not an essential issue. User can input the initial – end node and terminal – end node arbitrarily.

- Cable element

Cable element has a start node and a terminal node, and may have some middle nodes that cause the cable change its direction in the space. The cable element can resist tension only. The tension force and elongation are presented in negative value.

- Support element

Support element is one – component spring element. It is used to confine any one of the six displacement components at nodes. The element displacement is equal to the corresponding displacement component at the supported node. Therefore, the direction of the positive force and displacement in support element is identical with that at the node.

The rich element library combined with the numerous hysteresis models makes CANNY – E very powerful in the seismic analysis of various types of structures. The program can

be used effectively to model some complicated hysteresis behaviours, in which the old existing structures with seismic deficiencies tend to display during seismic excitations.

Several analysis options are available, such as Mode shape analysis; Design load analysis: Static push - over analysis; Static cyclic/reversal load analysis; Pseudo-dynamic analysis; and Dynamic analysis.

7.2.3 Modelling of an isolated bent

7.2.3.1 General description

Attempts will be made to model both original and retrofitted bent subjected to real earthquake records. Numerous seismic deficiencies are identified in Chapter 4 for the existing concrete bent, such as: bar cut off and inadequate shear capacity in the cap beam, inadequate confining for concrete at potential plastic regions in the columns, bar splice in the columns bottom, etc. These deficient details make the modelling very difficult and complicated with CANNY – E. Aiming to the balance between precision and computation effort, some assumptions and approximations are made in this study to simplify the modelling and analysis.

7.2.3.2 Modelling

- General aspects of the CANNY – E model

The 2 – D model will be used for the modelling of isolated concrete bents. The layout and overall dimension of the bent model are shown in Fig. 7.2. Sufficient nodes and elements are assigned to the model to capture potential inelastic behaviours. The node locations in the cap beam are chosen so as to coincide approximately with the major change in longitudinal reinforcement, and to allow accurate positioning of the vertical point loads from the superstructure, so that the correct bending moments and shear forces will be generated in the structure.

Beam elements with shear deformation and axial deformation are to be used for the modelling of cap beam. Columns are modelled with column elements. The one –

component spring model is to be used for the modelling. The axial load and bending moment interaction is modelled approximately. Column properties corresponding to the most probable axial force experienced by the column in the earthquake event are input into the analysis program. Several trial runs are undertaken before the properties are determined.

The same elastic soil springs as in the Chapter 4 are used here to model the structure – soil interactions. No attempt is made to model the inelastic behaviours of soil springs.

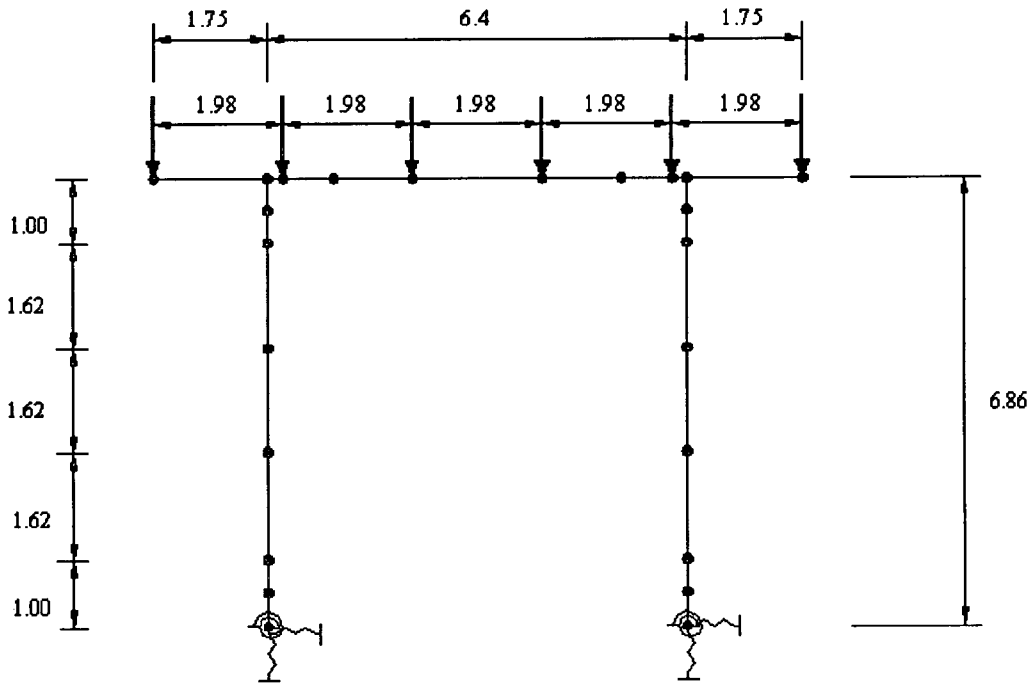

Note: 1.Dot represents the location of element nodal points,
2.The dimension is in meters.

Fig. 7.2 General layout of bent model for CANNY

- Component load – deformation characteristics

The inelastic dynamic analysis is based on the component load – deformation characteristics, which are computed by the nonlinear sectional analysis program Response 2000 (Bentz & Collins, 1998). The details of this program and moment –

curvature calculation are described in Chapter 4. Fig. 7.3 shows the moment (M) – curvature (Φ) relationship for cap beam and columns in original structure. The M - Φ relationship for components in strengthened structure with level II retrofitting is given in Fig. 7.4.

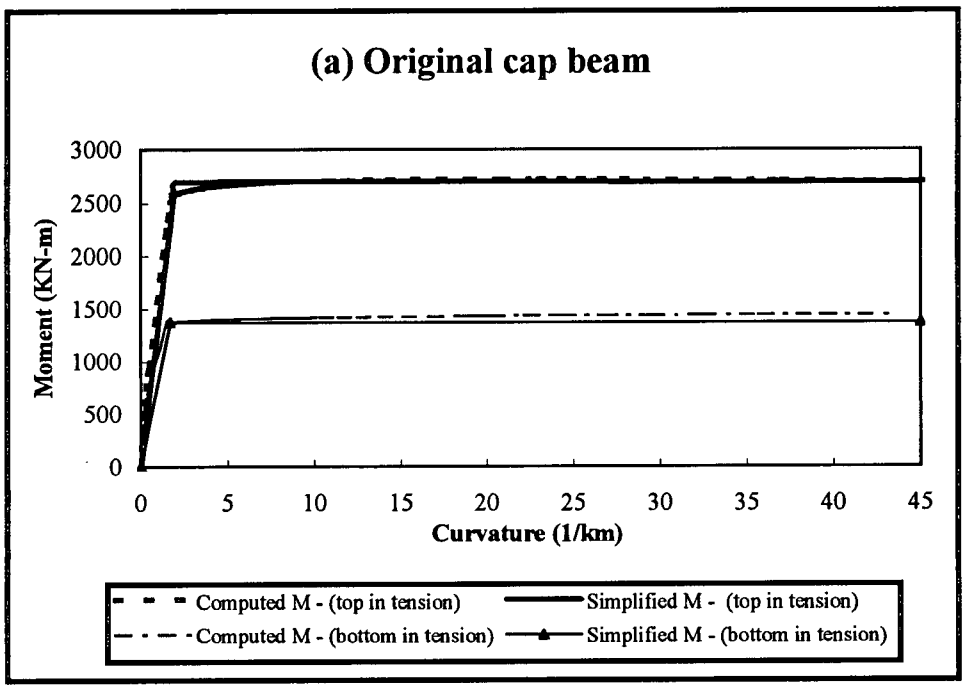

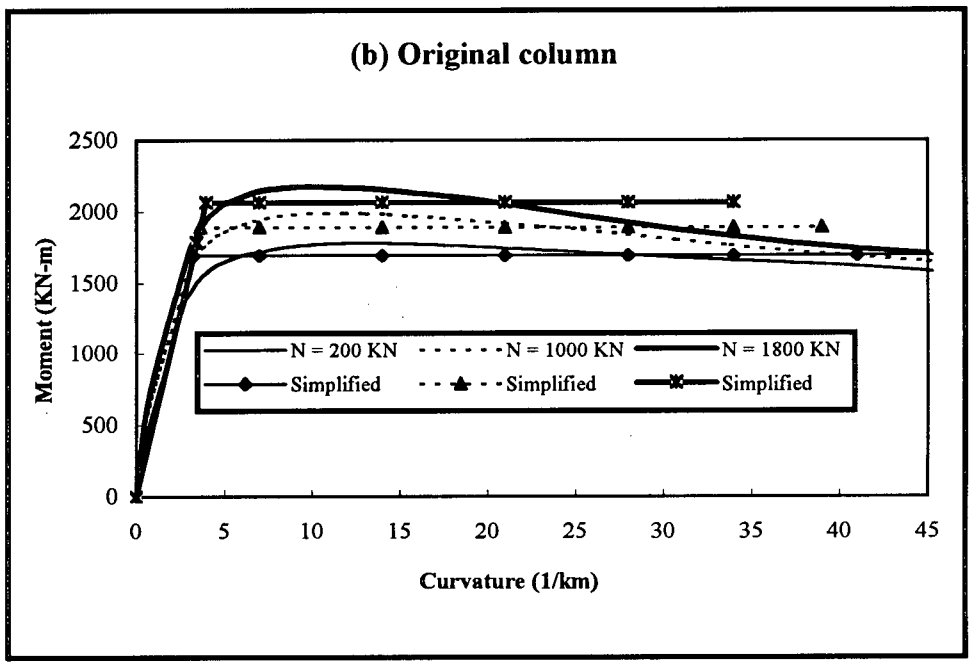

Fig. 7.3 Moment – curvature relationship for original structure

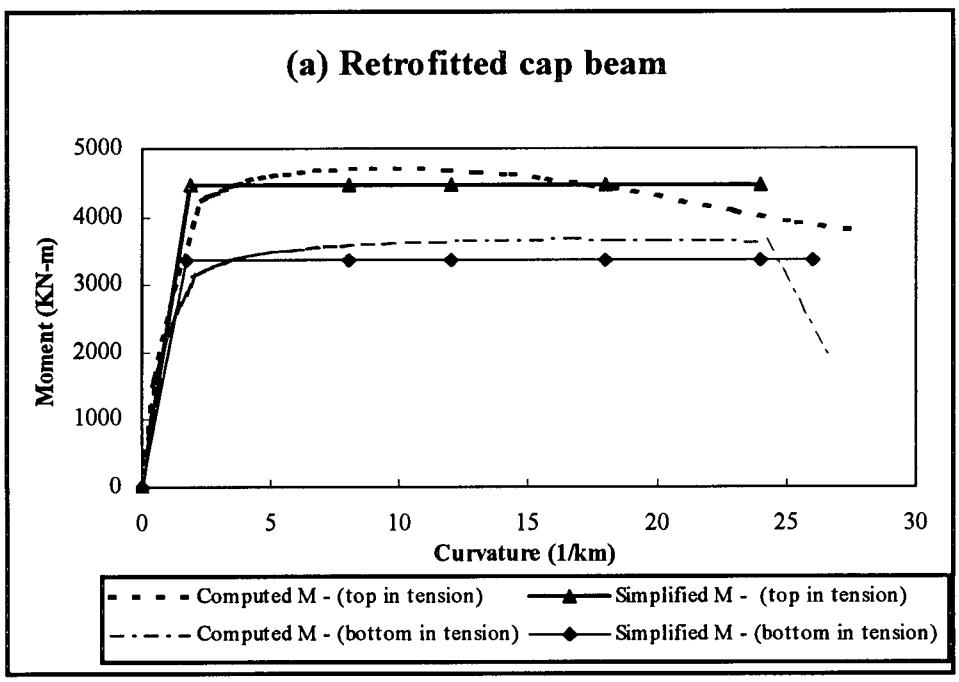

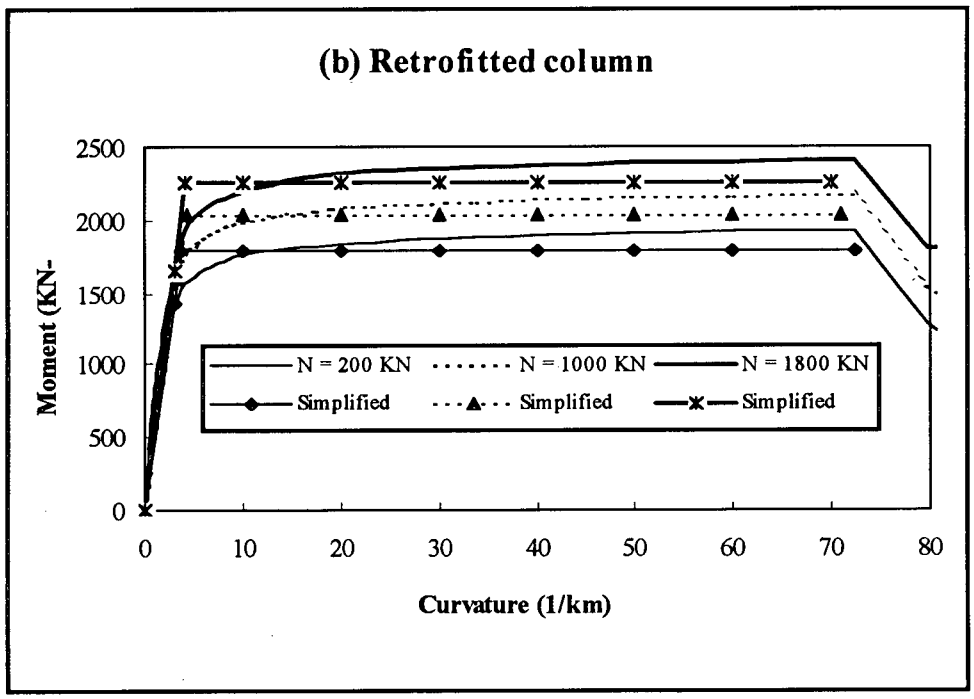

Fig. 7.4 Moment – curvature relationship for retrofitted structure

As demonstrated in Chapter 4, shear failure in cap beam is the controlling failure mechanism for the unretrofitted structure. Since the inelastic shear damage cannot be modelled directly using CANNY, the approach taken is to modify the flexural properties to account for the likelihood that shear failure will occur before flexural yielding. This is done by reducing the yield moment in the beam elements to the moment that will exist simultaneously with the limiting shear force under elastic conditions.

Since the one – component spring is used for the element modelling, the interactions between axial load and bending moment in columns can not be modelled directly by CANNY. As seen from time history analysis subjected to earthquake records, the axial loads in the columns vary substantially during earthquakes. Accordingly, the flexural capacity is changing greatly with different axial forces in the columns. To obtain an appropriate flexural property of columns, several trial runs are undertaken before a reasonable axial load is chosen to be input into Response 2000 to compute column flexural property.

- Hysteresis model and hysteresis parameters

CANNY sophisticated model is used to model the hysteresis behaviours of components. A detail description of this model is given in section 7.2.2. The hysteresis parameters are however difficult to determine. While it is possible to make rough estimates of appropriate hysteresis parameters for a given concrete quality and structural type, an accurate model of hysteretic behaviour can only be achieved by tuning the parameters against experimental data (Williams, 1994).

Williams (Williams, 1994) made a series of trial runs and sensitive studies to determine the relative sensitivity of the model to the various hysteresis parameters. With the experimental data obtained from lab cyclic tests on Oak Street and Queensborough bridge bents made in UBC (Anderson et al, 1995), Williams tuned in the parameters in his analysis model and compared analysis results with the tests. Numerous of calculations and modifications were undertaken. Finally, the optimum set of hysteresis parameters was determined as follows,

$$\theta = 2.0 \qquad \beta_e = 0.25 \qquad \beta_d = 0.025 \qquad \lambda_s = 0.2$$

The physical meanings of these parameters are given in Table 7.1. Recognizing the similarity between Oak Street & Queensborough bridge bents and the concrete bents in the case study bridge, the aforementioned parameters are slightly modified and subsequently used in the seismic damage analysis of this study. The other parameters defined in Table 7.1 are given values by trial runs of analysis programs. The adopted values of hysteresis parameters for both original and retrofitted bent are shown in Table 7.2.

Table 7.2 Adopted hysteresis parameters for analysis

Parameter	Original bent	Retrofitted bent
θ	2.0	5.0
β_e	0.25	0.05
β_d	0.025	0.0
δ	0	0
λ_3	0	0
ε	0.7	0.9
λ_s	0.7	0.9

7.3 Earthquake records

7.3.1 General description

In the inelastic dynamic analysis of structures, the nonlinear response varies significantly with the input ground motion time history. Ideally, a large number of actual earthquake records that are judged to likely occur at the specified site should be used. For a site specific assessment, only records corresponding to the hazard scenarios for the site have to be considered, in which case the variability in the response is not as high as otherwise, particularly when scaling of the records corresponding to a given range of magnitudes and distances from the source is made (Shome et al, 1998). In the recent published NEHRP documents (FEMA 273, 1997) and ATC – 32 (ATC, 1996) it is recommended that the maximum response data from time history analyses with a minimum of three real input motions may be used for design, whereas the mean response parameters may be adopted if seven or more motions are used. In this study, three real earthquake records, which are scaled to spectral accelerations of the structure at the bridge site, are used in this study. Spectral accelerations are computed from the seismic hazard obtained from the new GSC document (GSC, 1999), which is introduced in detail in Chapter 3. A range of

spectral accelerations is used for each earthquake event to compute seismic behaviours probabilistically.

7.3.2 Selection and scaling of earthquake records

The basis of selecting the earthquake records is to ensure that a wide range of periods is covered by the envelope of the spectra for different vibration periods. For the earthquake records chosen for this study, appropriate causative mechanisms and soil characteristics at the recording station are taken into consideration and care is given in the choice of inputs to ensure appropriate energy and frequency content in the earthquake records. But in any way, the choice of suitable earthquake records is an art and a great amount of consideration is necessary. The details for this complicated process will not be tackled here due to the limited space and time. The chosen three earthquake records for this study are given in the Table 7.3. Fig 7.5 shows time history of these three records.

Table 7.3 Input earthquake motions

Earthquake record	Date	Station and Component	Distance (km)	Magnitude	Peak Acceleration (g)	A/V
San Fernando	Feb.9, 1971	8244 Orion Blvd. N00W	20	6.4	0.255	0.856
Imperial Valley	Oct.15, 1979	USGS 5028 S40E	27	6.6	0.338	0.664
Loma Prieta	Oct.17, 1989	USGS 57007 S00E	18	7.1	0.63	1.141

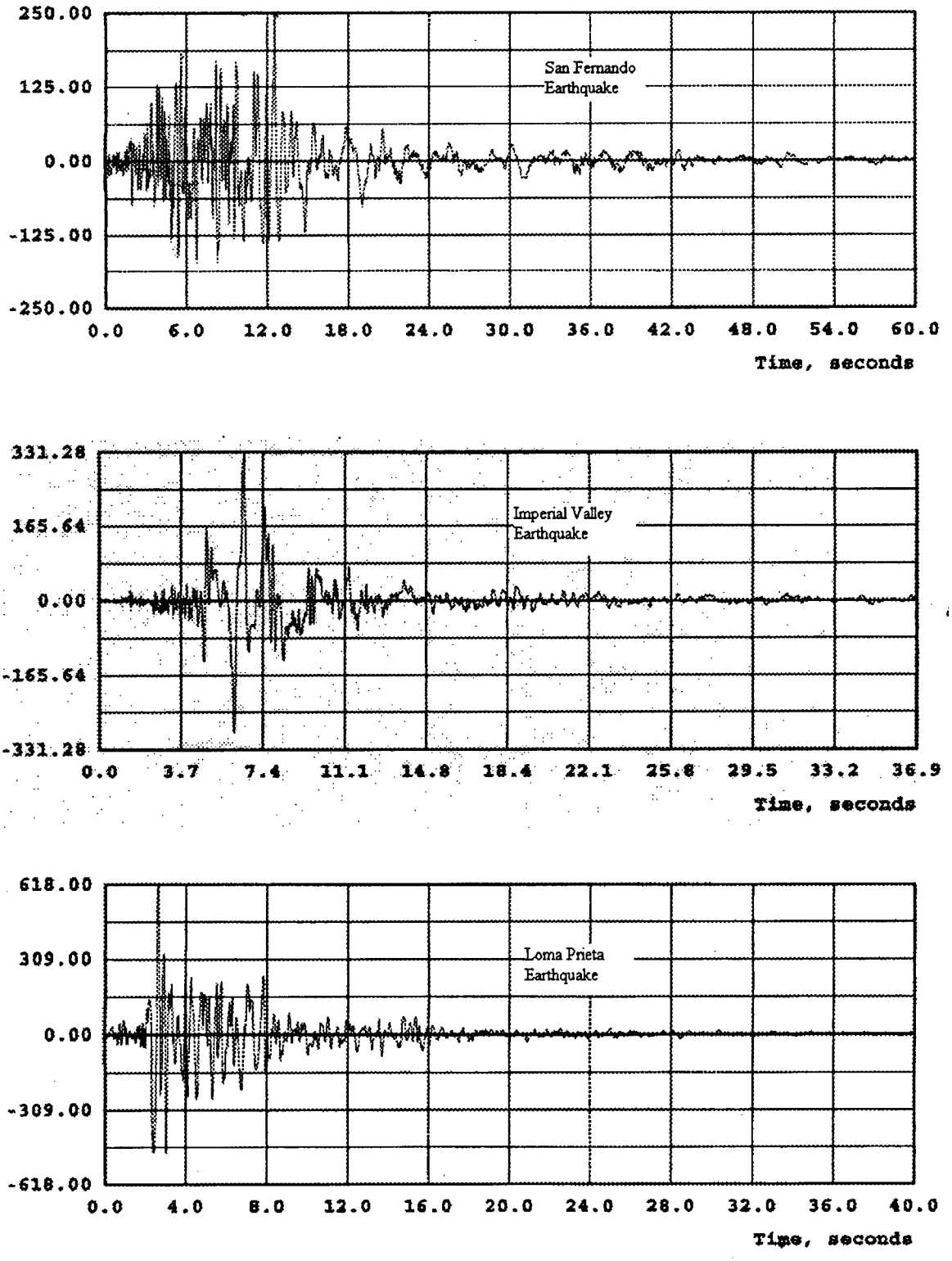

Fig 7.5 Earthquake records time history

To use the recorded earthquake records in this analysis, they are scaled in the way proposed by Shome (Shome et al, 1998) to the spectral accelerations at the bridge site. That is, all records will be multiplied a scale factor F_i, which is defined as,

$$F_i = \frac{S_{ai}}{a_g} \qquad \text{Equation 7.3}$$

in which, S_{ai} is the spectral acceleration at different occurrence rates, a_g is the peak acceleration of each earthquake record.

It was demonstrated by Shome et al that (Shome et al, 1998) the inelastic analysis using the earthquake records scaled as in the above could reduce the number of records required to estimate the median response and the variability could be reduced too.

7.4 Seismic damage analysis

7.4.1 General description

The deterministic analysis will be undertaken for seismic damage analysis using the aforementioned analysis model and earthquake records. Median values of structural properties are to be used for the modelling. Each earthquake record will be scaled to six different spectral accelerations to be input into the analysis. Both original and retrofitted bent are to be analyzed. There are total 54 runs of the program CANNY – E.

The analysis results will be presented and discussed in this section. Firstly, bent top displacement time history will be shown and the failure mechanism will be discussed. Then the evolution of damage through the earthquake time history will be presented in the figures. Finally, the damage indices against various spectral accelerations are to be tabulated.

7.4.2 Bent top displacement time history

Fig. 7.6 shows time histories of bent top displacement for original bent, updated bent with level I retrofitting and level II retrofitting respectively. The displacements obtained from

all three earthquake records are given in the figure. The results shown in here are computed based on the same earthquake level of design earthquake 1, i.e., all records are scaled to the spectral acceleration of 10% exceedence in 50 years.

The following observations can be made from the figure,

- The original bent will experience brittle shear failure in cap beam when the bent is subjected to all of three earthquake motions. The failure occurs at the time when the earthquake motion has its first large impulse. The analyses show that the unretrofitted bent cannot survive design earthquake 1.
- For the updated bent with level I retrofitting, although the seismic demand, such as shear forces in cap beam and bent top displacement, is reduced due to modified dynamic properties, the bent will still experience sudden shear failure at the almost the same time as that for original bent.
- The updated bent with level II retrofitting will not experience brittle shear failure subjected to all of three earthquake motions. The seismic behaviour is more ductile with small plastic deformations remaining at the end of earthquake excitations. It is to be noted that the bent will have a much larger displacement demand subjected to San Fernando EQ than the other two earthquake events. This peak displacement demand occurs at the time of about 13 seconds when the earthquake attains its peak accelerations. The larger bent top displacement is due to the reduced bent stiffness after a series of large cyclic excitations. But for the other two earthquake records, the input accelerations experience their peak accelerations at the first 5 to 6 seconds and only one to two large impulses are existed for the input motions.

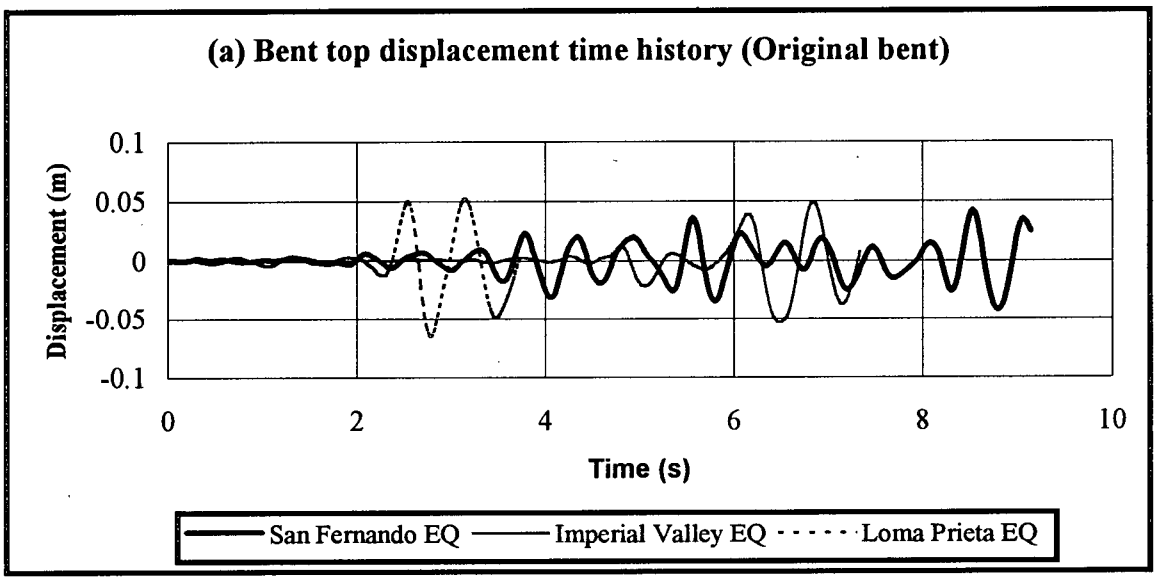
(a) Bent top displacement time history (Original bent)
Displacement (m)
0.1
0.05
0
-0.05
-0.1
0
2
4
6
8
10
Time (s)
San Fernando EQ
Imperial Valley EQ
Loma Prieta EQ

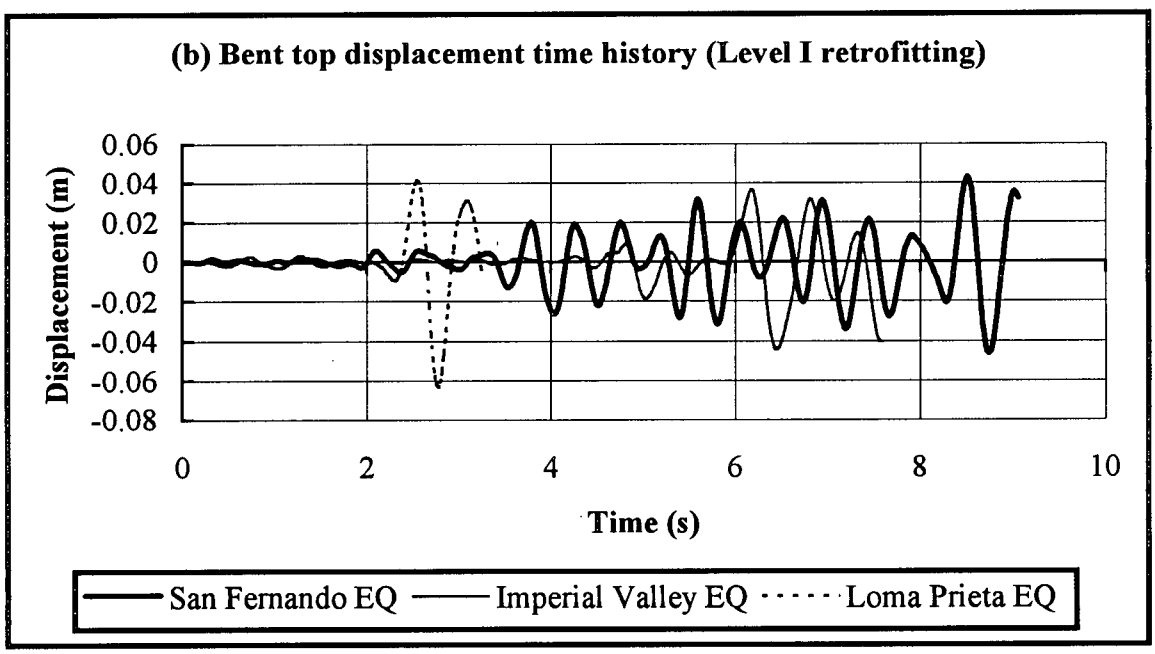
(b) Bent top displacement time history (Level I retrofitting)
Displacement (m)
0.06
0.04
0.02
0
-0.02
-0.04
-0.06
-0.08
0
2
4
6
8
10
Time (s)
San Fernando EQ
Imperial Valley EQ
Loma Prieta EQ

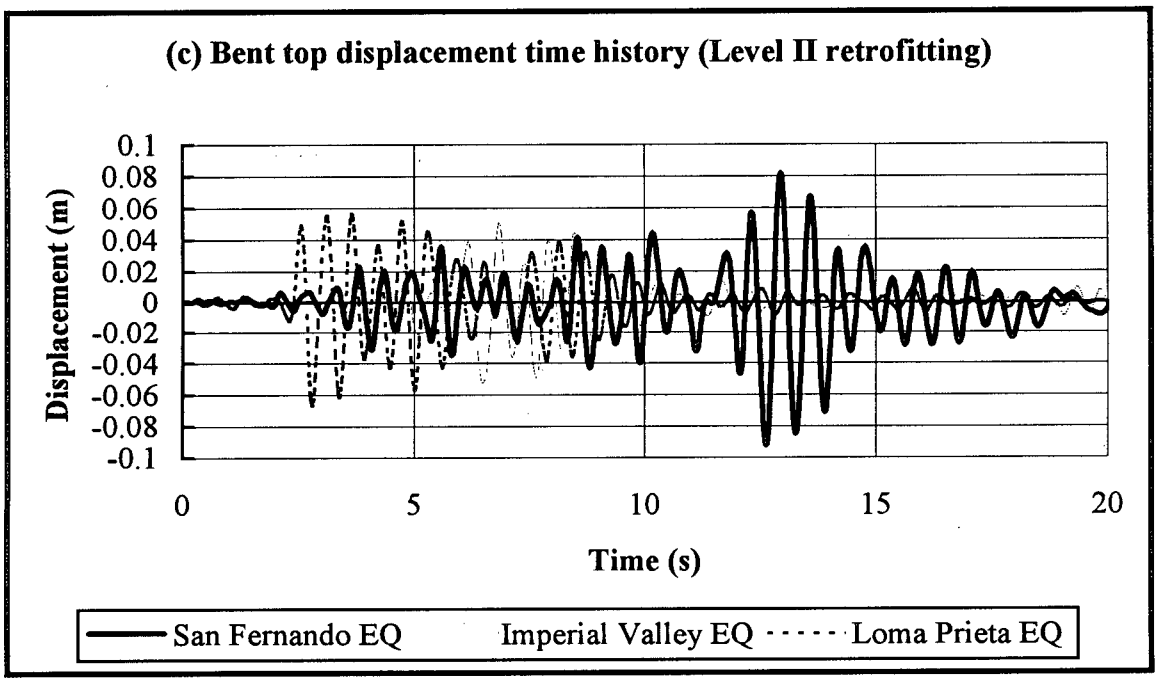

Fig 7.6 Bent top displacement time history

7.4.3 Damage indices

To illustrate the progress of seismic damages in both original and retrofitted bent, time history of damage indices are presented in Fig. 7.7. The results obtained from three earthquake motions are given in the figure in order to show the effect of different earthquake motions on the damages. To save spaces, as in the above, all records are scaled to the spectral acceleration of 10% exceedence in 50 years.

The variation of damage index with spectral acceleration for the worst earthquake motion among the chosen three earthquake records is shown in Fig. 7.8. The damage index values against a range of spectral accelerations are also tabulated in the Table 7.3.

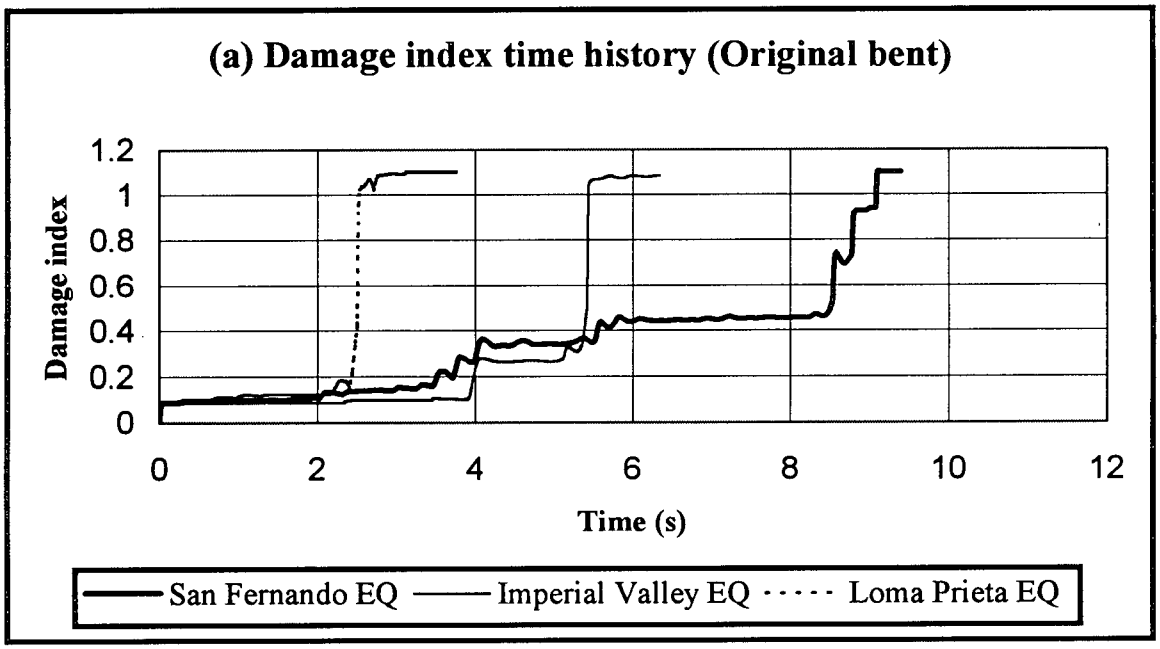
(a) Damage index time history (Original bent)
Damage index
1.2
1
0.8
0.6
0.4
0.2
0
0
2
4
6
8
10
12
Time (s)
San Fernando EQ
Imperial Valley EQ
Loma Prieta EQ

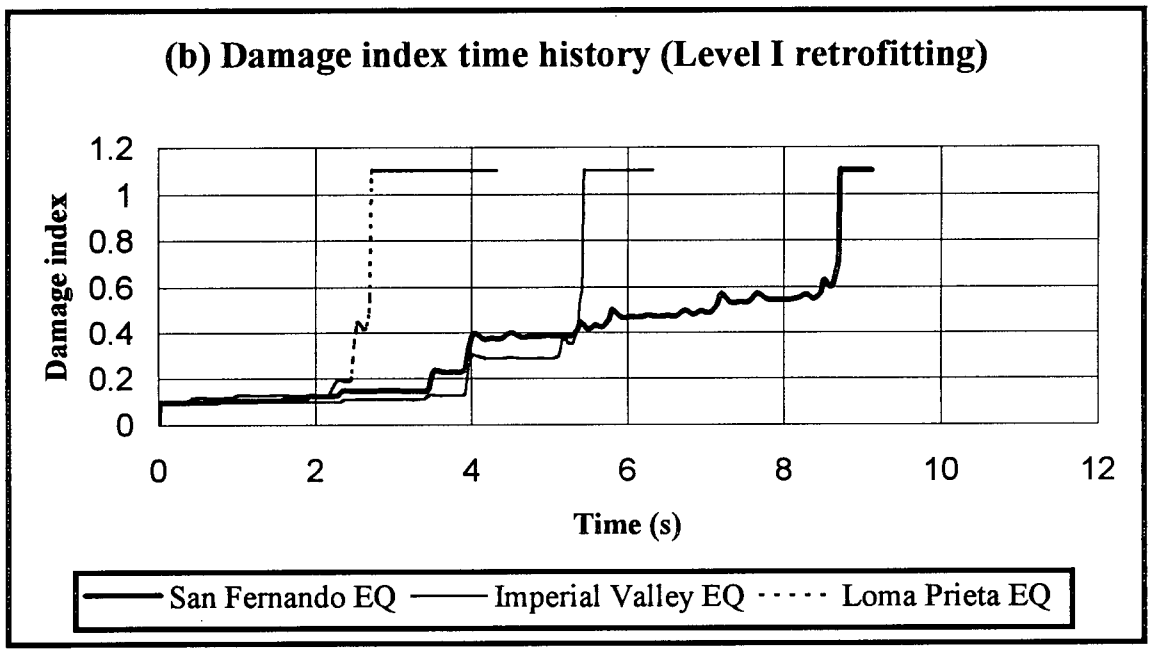
(b) Damage index time history (Level I retrofitting)
Damage index
1.2
1
0.8
0.6
0.4
0.2
0
0
2
4
6
8
10
12
Time (s)
San Fernando EQ
Imperial Valley EQ
Loma Prieta EQ

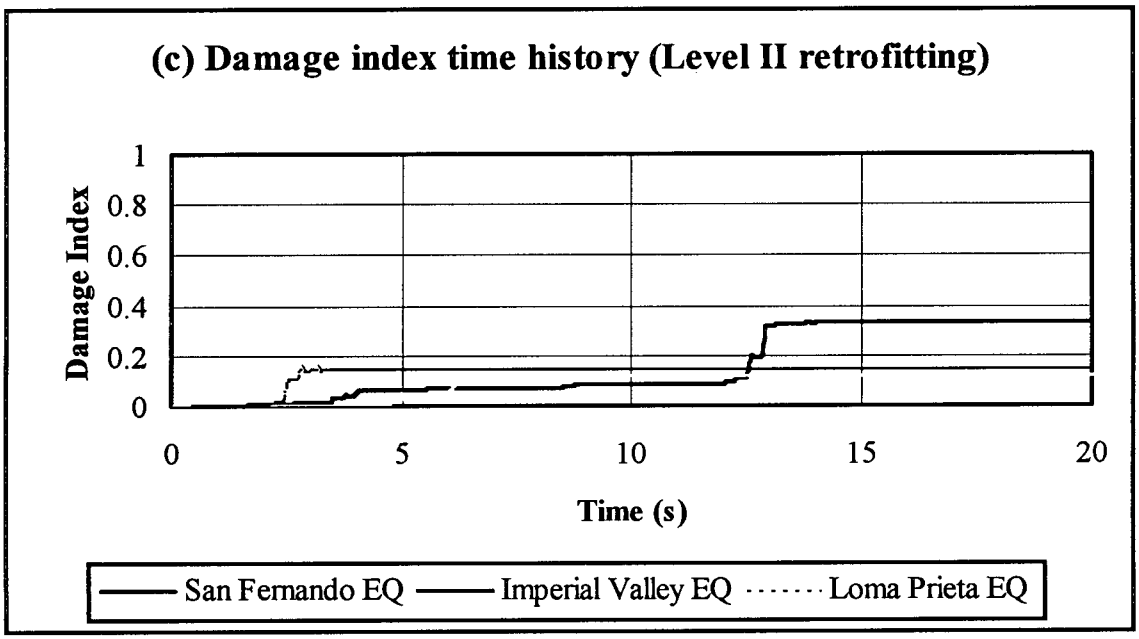

Fig 7.7 Time history of seismic damage indices

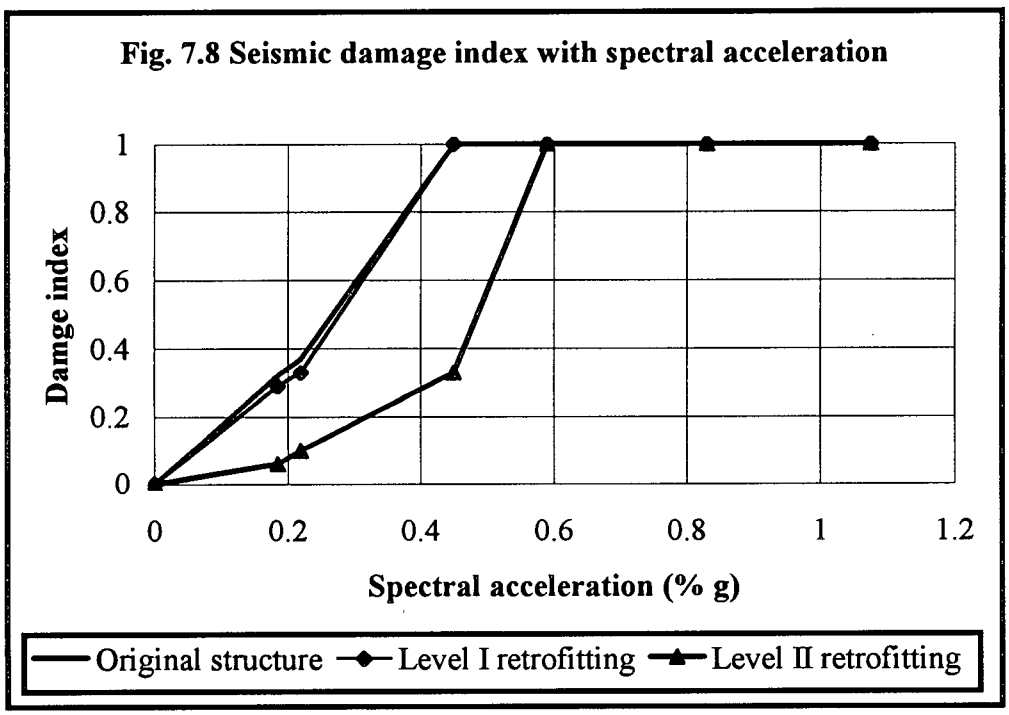

Table 7.4 Seismic damage indices with spectral accelerations

Earthquake occurrence rate (years)	Spectral acceleration (% g)	Damage index		
		Original structure	Level I retrofitting	Level II retrofitting
43	0.185	0.32	0.29	0.06
72	0.22	0.37	0.33	0.10
475	0.45	1.00	1.00	0.33
1000	0.59	1.00	1.00	1.00
2500	0.83	1.00	1.00	1.00
5000	1.075	1.00	1.00	1.00

Fig. 7.7 shows that for the original structure subjected to earthquake 1, the large acceleration impulse for the three earthquake records causes sudden failure of cap beam. Damage index jumps abruptly from less than 0.4 to 1.0. The updated structure with level I retrofitting has reduced damage index slightly before the large acceleration impulse hits the structure. But the structure cannot survive the large acceleration impulse and the sudden failure will still occur in the cap beam. For the updated structure with level II retrofitting subjected to earthquake 1, the structure will experience moderate damage with a damage index around 0.3. The bridge can still maintain limited traffic after this level earthquake event. Effect of retrofitting on the reduction of seismic damages is obvious.

From Fig. 7.8 and Table 7.4, we can see that the damage index varies with the spectral acceleration linearly when the spectral acceleration is below certain level. But as soon as the spectral acceleration reaches certain value, damage index jumps abruptly to 1.0 and the sudden failure occurs. As shown in Fig. 7.8 (c) for the retrofitted bent with level II retrofitting, damage index jumps from 0.33 at S_a = 0.45 to 1.0 at S_a = 0.59. As demonstrated in Chapter 5, the level II retrofitting increases structural resistance to earthquake motions. The damaging peak earthquake acceleration has increased from

0.26g for original structure to 0.50g for the retrofitted one. However the structure has little redundancy, poor post – yield behaviour is observed for the retrofitted bent. Once the acceleration amplitude is increased sufficiently to cause the first yielding in the bent columns, failure mechanism forms very quickly and sudden failure occurs. Little strength enhancement is available for the structure after yielding. This is demonstrated by the push over analysis in Chapter 5, in which there is only about 10% lateral load increase from the first yielding to the ultimate state. This phenomenon has also been observed and discussed in Williams's analysis (Williams, 1994).

7.5 Financial damage estimation

7.5.1 General description

Financial or monetary damage estimation is necessary for the decision analysis. Ideally, the estimation should be based on the damage data obtained from previous earthquake events and the relationship between the observed physical damage to structures and the monetary damage estimated. A direct mapping out from the computed seismic damages (here quantified as damage index) to the financial damage is desirable. However, such information is very scarce and not readily available. Fortunately, some laboratory tests were undertaken to correlate damage index with seismic physical damage. Therefore, a two - step procedure will be utilized in this study to estimate seismic financial damages. Firstly, the damage index calculated in section 7.4 will be correlated with the physical damage states based on the data from laboratory tests. Then, the relationship between damage index and financial damages (represented by percent of replacement cost) will be mapped out.

It is worth to be noted that seismic financial damages will be represented by the ratio to structural replacement cost and only the direct physical damages will be discussed in this chapter. The indirect economic damages and the actual replacement cost in dollars will be given in Chapter 8, in which a thorough description of cost and damage will be presented.

7.5.2 Relationship between damage index and financial damage

7.5.2.1 Correlation between damage index and observed physical damage

Based on the extensive monotonic and cyclic test data of reinforced concrete beams and columns reported in the U.S. and Japan, a systematic regression analysis was undertaken by Park, Ang and Wen (1985) to correlate the proposed damage index (as in Equation 7.1) and physical damage degrees. The following damage classification was suggested by Park, Ang and Wen (1985),

Damage index	Physical damage state
$D < 0.1$	No damage or localized minor cracking
$0.1 \leq D < 0.25$	Minor damage – light cracking throughout
$0.25 \leq D < 0.4$	Moderate damage – severe cracking, localized spalling
$0.4 \leq D < 1.0$	Severe damage – concrete crushing, reinforcement exposed
$D \geq 1.0$	Collapse

Using the method described in the above, the damage index was calibrated to the nine reinforced concrete buildings that were damaged during the 1971 San Fernando earthquake and the 1978 Miyagiken – Oki earthquake in Japan. The calibration was relatively good. $D = 0.4$ was recommended by the same authors as a threshold value between repairable and irrepairable damage.

By examining the statistical distribution of calculated Park and Ang damage indices from laboratory tests of 82 spiral reinforced bridge piers, threshold damage indices for the yield, ultimate and failure damage states were estimated by Stone and Taylor (1993). They used tenth percentile threshold damage indices for the three damage states from the observed histogram. The threshold damage indices for the three damage states are shown in Table 7.5.

Table 7.5 Threshold damage indices

Damage state	Threshold damage indices	Standard error	90% confidence interval
Yield	0.11	0.03	(0.08, 0.17)
Ultimate	0.40	0.03	(0.32, 0.43)
Failure	0.77	0.05	(0.71, 0.86)

Four damage conditions that might exist in a bridge column following an earthquake were classified by Stone and Taylor (1993) as follows,

Damage index	Physical damage state
$D < 0.11$	No damage – the column has not yielded, the serviceability of the structure is not compromised
$0.11 \leq D < 0.4$	Repairable damage – the column has yielded but has not reached ultimate load. Economics will likely indicate that the structure should be repaired rather than replaced.
$0.4 \leq D < 0.77$	Demolish – the column has been loaded beyond ultimate load but remains standing. The column and possibly the entire bridge structure must be replaced.
$D \geq 0.77$	Collapse – the column has completely failed

A new damage model was proposed recently by Hindi and Sexsmith (2001) to quantify seismic damages of reinforced concrete columns subjected to earthquake loadings. They defined damage index as in Equation 7.4,

$$D_n = \frac{(A_n - A_0)}{A_0} \qquad \text{Equation 7.4}$$

in which A_0 is the energy under a monotonic load – displacement curve up to failure, A_n is the total energy under a monotonic load – displacement starting from the end of last cycle n (zero force point) to failure after the actual load history up to point n.

This damage model is accumulative, and it is capable of combining energy, ductility, and low cycle fatigue. The damage index computed from the new model is compared and calibrated to the observed damage of laboratory tests of 12 reinforced concrete column specimens. The following correlation between the computed damage index and the observed physical damage is suggested by Hindi and Sexsmith (2001),

Damage index	Physical damage state
$D < 0.1$	No damage
$0.1 \leq D < 0.2$	Minor damage – light cracking – very easy to repair
$0.2 \leq D < 0.4$	Moderate damage – severe cracking, cover spalling - repairable
$0.4 \leq D < 0.6$	Severe damage – extensive cracking, reinforcement exposed – repairable with difficulties
$0.6 \leq D < 1.0$	Severe damage – concrete crushing, reinforcement buckling – irrepairable
$D \geq 1.0$	Collapse

It is found that the correlations between computed damage index and observed physical damage proposed by three different researches are quite similar, especially for the first and third one. As damage index is calculated in accordance with Park & Ang (1985) in this study, the correlation recommended by Park, Ang and Wen (1985) will be used here to estimate seismic financial damages. The only modification is to classify in detail the damage state when the damage index is in the range of $0.4 \leq D < 1.0$ as that proposed by Hindi and Sexsmith (2001).

7.5.2.2 Mapping out the relationship between damage index and financial damage

Financial damage will be represented as the ratio of damages to replacement cost of the structure in this Chapter. Based on the correlation between damage index D and observed physical damage described in the above, financial damage corresponding to certain physical damage states can be mapped out. When D is less than 0.1, the damage can be neglected for calculating monetary loss. So replacement cost can be considered as 0 at $D \leq 0.1$. When $D \geq 0.6$, the structure will experience severe damages and the damage is irrepairable economically even though the structural integrity is maintained. Therefore, replacement cost is 100% at $D \geq 0.6$. When $0.1 < D < 0.6$, some level of damages will occur to the structure and the damages can be repaired economically. A linear relationship is assumed here for the replacement cost estimation at $0.1 < D < 0.6$. The mapped out relationship between damage index and replacement cost is shown in Fig. 7.9.

Fig. 7.9 Mapping out financial damages

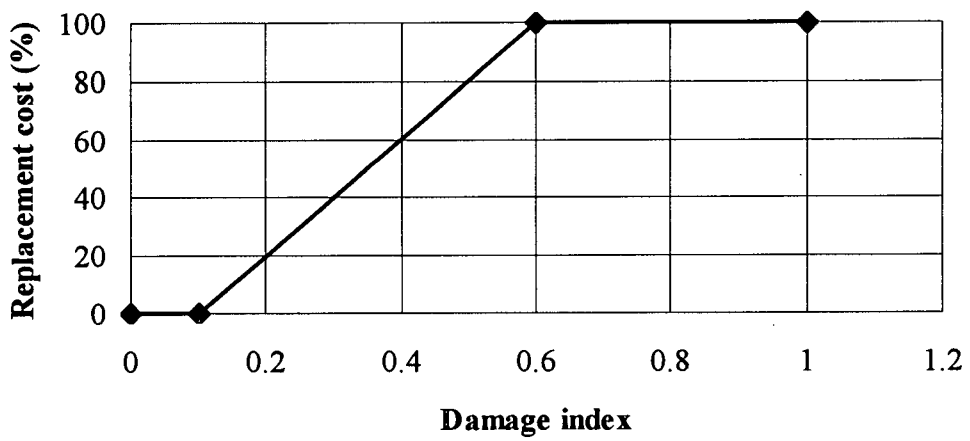

7.5.3 Computation of seismic financial damage

Seismic financial damages, expressed as the ratio to structural replacement cost, will be computed here for both original and retrofitted structure subjected to earthquakes with a range of peak spectral accelerations. The calculation results are given in Table 7.6.

Table 7.6 Seismic financial damage estimation

Earthquake return period (years)	Original structure		Level I retrofitting		Level II retrofitting	
	D	C (%)	D	C (%)	D	C (%)
43	0.32	44.00	0.29	38.00	0.06	0.00
72	0.37	54.00	0.33	46.00	0.10	0.00
475	1.00	100.00	1.00	100.00	0.33	46.00
1000	1.00	100.00	1.00	100.00	1.00	100.00
2500	1.00	100.00	1.00	100.00	1.00	100.00
5000	1.00	100.00	1.00	100.00	1.00	100.00

Note: D is the computed damage index, and C is the percent of replacement cost.

The present value decision model will be constructed in Chapter 8, in which the present value of total cost will be computed and the optimal retrofitting level is to be found based on the benefit – cost analysis.

Chapter 8 Performance – based Present Value Decision Model and Sensitivity Analysis

8.1 Introduction

Based on the failure probabilities and seismic damages obtained in the previous chapters, the performance – based present value decision model will be constructed in this chapter following the procedures set out in Chapter 2. This model is to be used for the determination of optimal seismic retrofitting level for the case study bridge. The direct economic cost, including initial retrofitting cost and repair, and replacement cost, will be firstly calculated based on the retrofit design and seismic damage analysis. Then, the indirect economic cost is estimated. Thirdly, the total economic costs for different retrofitting options will be obtained and the costs are discounted to the same calculating year. Thus, the present value decision model is constructed and a benefit/cost analysis can be undertaken. The optimal seismic retrofitting level is found corresponding to the maximum benefit/cost ratio. Finally, a sensitivity analysis is undertaken to analyze the effects of various variables on the outcome of decisions.

8.2 Economic cost calculation

8.2.1 General description

Total economic cost includes initial seismic retrofitting cost and seismic damages occurring in the future years, which is represented in this study by monetary loss in dollars. The retrofitting cost can be relatively accurately calculated based on the data from seismic retrofitting design. The direct economic loss, which is given in the ratio to replacement cost, is computed from the mapping out relationship between damage index and monetary damages and presented in Chapter 7. But the indirect economic loss is difficult to estimate and some subjective judgements are used here to obtain values of indirect loss.

8.2.2 Initial retrofitting cost

Two seismic retrofitting schemes are designed in this study. The detailed designs can be found in Chapter 5, where scheme I represents a safety level retrofitting, i.e. the structure will not collapse during an earthquake of 10% exceedence in 50 years; scheme II is a functional level retrofitting, i.e. normal or limited traffic will be maintained immediately after the same earthquake event.

More specifically, scheme I includes superstructure retrofitting and substructure retrofitting respectively. The first is to strengthen superstructure integrity to efficiently transfer horizontal earthquake loads from bridge deck to the substructure. A direct and efficient load path is identified and corresponding structural components are strengthened. The construction work consists of adding new shear keys and replacing & adding new steel diaphragms at concrete bent locations & abutments. The substructure retrofitting is to add shear walls to bent 2 and bent 3. More details about retrofitting scheme I can be found in Chapter 5. The construction cost for this retrofitting is obtained from Consultant's seismic retrofit report for the case study bridge (CWMM, 1994) and is reproduced in Table 8.1. Noted that the cost is calculated in the year of 1994.

Superstructure retrofitting in scheme II is the same as in the scheme I, but a different approach is adopted for the substructure retrofitting. Identifying bent 1 is the most critical component for earthquake loading, bent 1 is firstly strengthened and updated to certain performance levels. The retrofitting work includes post – tensioning to cap beam and composite material wrapping to the columns. The detailed retrofit design can be found in Chapter 5. In order to ensure the structure will not collapse during a 2% exceedence in 50 years earthquake, other bents (bent 2 to 4) may need to be strengthened too. Therefore, retrofitting costs for all four bents will be included in the calculation to get a practical estimate of the initial retrofitting cost for the case study bridge.

After columns are strengthened using capacity design principle, higher flexural strength will be required for the footings to ensure plastic hinges occurring in columns. The detail design for footing retrofitting will not be presented here. Only construction cost

corresponding to seismic retrofitting will be discussed and given in this study. The unit cost data for scheme II retrofitting is based on the information from one of similar bridge seismic retrofit project (Klohn – Crippen CBA Consultants Ltd. 1999). The construction cost for scheme II is also given in Table 8.1 and the cost data is valid in 1999.

Table 8.1 Construction cost for retrofitting

Category		Item	Unit	Quantity	Unit Price	Cost
Retrofit I	Superstructure	Add new diaphragms and shear keys	L.S.	1	$94,000	$94,000
	Substructure	Add new concrete shear walls	L.S.	1	$85,000	$85,000
	Total					$179,000
Retrofit II	Superstructure	Add new diaphragms and shear keys	L.S.	1	$94,000	$94,000
	Substructure Concrete Bent	Post - tensioning	kg	816	$7	$5,712
		Concrete coring	m	39.6	$600	$23,760
		Composite material wrapping	m^2	258.9	$200	$51,732
	Footing Overlays	Excavation	m^3	220	$10	$2,200
		Concrete	m^3	16	$250	$4,000
		Reinforcing	kg	2512	$1.5	$3,768
		Cleaning & Roughening Concrete	m^2	42	$50	$2,120
		Concrete Formwork	m^2	72	$100	$7,200
	Total					$194,492

8.2.3 Direct loss estimation

8.2.3.1 General methodology

Direct loss due to an earthquake event usually includes two parts of losses. The first part is facility damage/repair cost incurred from the direct physical damages to structures. The second part is deaths and injuries resulted from the structural damage or collapse. In the case of bridges, the latter one has negligible effect on the outcome of decisions due to the very small probabilities of people get injured or killed during an earthquake while using the bridge. Therefore, only the first part will be discussed and included in the decision model.

The damage/repair cost is evaluated in this study as a function of mean damage index which is computed in Chapter 7. The mapped out relationship between damage index and monetary loss and Table 7.5 will be used in this chapter to calculate the direct economic loss.

8.2.3.2 Replacement cost

In British Columbia, the bridges have not been tested to large earthquakes recently and earthquake damage/repair cost and replacement cost is not readily available. But in California, earthquakes in recent years, such as San Fernando earthquake in 1971, Loma Prieta earthquake in 1989 and Northridge earthquake in 1994, have brought extensive damages to some bridges. Some cost information is available from Caltrans regarding the structural replacement cost of bridges immediately after an earthquake. Although the bridges in California are mostly concrete box girder bridges and they are generally larger and more complicated than the ones in British Columbia, the replacement cost data can be still used as a reference for real replacement cost estimation in BC.

Table 8.2 gives the average replacement costs for various types of bridges as reported by Caltrans (Caltrans, 1995). An average replacement cost of $\$1028USD/m^2$ of deck is obtained for the total of 112 bridges. A removal cost of 20% of replacement cost, i.e. $\$205USD/m^2$ of deck is estimated by Caltrans (Caltrans, 1995).

The direct use of these cost data to the bridges in BC may overestimate the real costs that will be incurred here. In order to obtain a realistic replacement cost that can be used in BC, the numbers in Table 8.2 are compared with the cost data of new bridge construction from MoTH, BC. An in-house computer program SQ_METER (BCMoTH, 1980) is available for the calculation of new bridge cost in the ministry. Cost data of hundreds of different types of bridges are stored in the program. The cost is based on the contractor's tendering data when the bridge is being tendered. Nine criterions can be input into the program to search for the specified type of bridge. Running this program for several times, a construction cost of $\$1055/m^2$ deck (Canadian dollars. The following costs will all be in Canadian dollars except specified.) is found for the type of case study bridge. This number is similar to the replacement cost of $\$1028USD/m^2$ of deck (similar number, but different currencies) in California. Therefore, the replacement cost of $1055 per square meter deck and removal cost of $210 per square meter deck are used in this study to compute the direct economic loss.

Table 8.2 Bridge replacement cost from Caltrans (1995)

Type of bridge	Total # of bridges	Amount (USD)	Deck area (m^2)	Average cost (USD/m^2)
RC Slab	17	$6,466,177	7478	$864.71
RC Box Girder	10	$14,774,702	16141	$915.35
CIP/PS Slab	5	$5,260,219	44902	$117.15
CIP/PS Box Gdr	70	$211,691,470	215357	$982.98
PC/PS I Gdr	2	$1,862,557	1346	$1,383.69
PC/PS Slab	2	$750,502	648	$1,157.31
Steel Girder	6	$74,064,563	41754	$1,773.84
Totals	112	$314,870,190	327627	$1,027.86

8.2.3.3 Direct economic loss

Direct economic losses of the case study bridge subjected to earthquake events are computed based on damage/repair cost (which is represented as the ratio to replacement cost, see Table 7.5 in Chapter 7) and replacement cost. The values are presented in Table 8.3.

Table 8.3 Direct economic loss

Earthquake return period (years)	Original structure		Level I retrofitting		Level II retrofitting	
	Ratio to replacement cost	Direct economic loss	Ratio to replacement cost	Direct economic loss	Ratio to replacement cost	Direct economic loss
43	0.44	$547,023	0.38	$472,429	0.00	$0
72	0.54	$671,346	0.46	$571,887	0.00	$0
475	1.00	$1,243,234	1.00	$1,243,234	0.46	$571,887
1000	1.00	$1,243,234	1.00	$1,243,234	1.00	$1,243,234
2500	1.00	$1,243,234	1.00	$1,243,234	1.00	$1,243,234
5000	1.00	$1,243,234	1.00	$1,243,234	1.00	$1,243,234

8.2.4 Indirect loss estimation

8.2.4.1 General methodology

Indirect loss generally includes Economic impacts (such as Business interruption) and Social impacts (such as Individual pain and loss, disruption to the community, etc). Both impacts are ambiguous and difficult to quantify. No readily available data is available for indirect loss estimation and a complete economic evaluation is not possible for this study. Therefore, some subjective judgements and assumptions are undertaken here for the purpose of illustration of indirect loss estimation of the case study bridge due to earthquake damages.

Transportation network plays an important role in the economy and community. A bridge is an indispensable component in the whole transportation network. A bridge is more susceptible to earthquake damage and it is usually difficult to find an alternative route for the damaged bridges. Keeping the bridge open to normal or limited traffic is vital for the emergency response and early recovery activities. Bridge closure will bring out tremendous disruptions to the community and local economy. Previous earthquakes in California, Japan and Taiwan have demonstrated the significance of keeping the normal traffic flow immediately after an earthquake.

For the extensively damaged or collapsed bridge, it usually needs to take several months to restore the normal traffic to public. The restoration time of damaged bridges following an earthquake event is somewhat difficult to determine. It depends on the damage status, bridge scales and available resources for the restoration work. A bridge restoration curve, which describes the fraction or percentage of the bridge that is expected to be open or operational as a function of time following the earthquake, is presented in the HAZUS99 document (FEMA, 1999). These curves are developed based on a best fit to ATC – 13 (ATC, 1985) data for the social function classification interest consistent with the following five damage states: No damage (ds1), Slight/Minor damage (ds2), Moderate damage (ds3), Extensive damage (ds4), and Complete damage (ds5). It is found that the damage states described in the above are similar to the definitions given by Park et al (1985) and Hindi & Sexsmith (2000), which are described in detail in Chapter 7.

The restoration functions for highway bridges given in the HAZUS99 (FEMA, 1999) are reproduced here in Table 8.4(a) and 8.4(b). The former table gives means and standard deviations for each restoration curve that fits ATC – 13 data, while the second table gives approximate discrete functions for the restoration curves developed. For example, for an extensive damaged bridge, Table 8.4(a) shows that the bridge will be restored to full operation after a mean time of 75 days with a standard deviation of 42 days. Table 8.4(b) gives that after 90 days, the bridge is restored to a functional level of 65% full operation. Note that the values given here are based on the statistical calculation. The values presented in Table 8.4 are used in this study to estimate the closure time of the case study

bridge subjected to various levels of earthquakes, which is subsequently used for the indirect loss estimation. Table 8.5 presents the bridge closure time for the case study bridge based on the damage state obtained from seismic damage analysis in Chapter 7 and bridge restoration function in Table 8.4. It is worth noted that the bridges considered for the development of bridge restoration curve in ATC – 13 are generally larger in size and more complicated than the case study bridge, more repair time is therefore needed for those bridges in California. Considering the relatively simple structural type and easy accessibility to the bridge site, the bridge closure time for the completely collapsed state adopted for the case study bridge is about half of that given in Table 8.4.

Table 8.4 (a) Continuous restoration functions for bridges (after ATC – 13, 1985)

Damage state	Mean (Days)	σ (Days)
Slight/Minor	0.6	0.6
Moderate	2.5	2.7
Extensive	75.0	42.0
Complete	230.0	110.0

Table 8.4 (b) Discrete restoration functions for bridges

Restoration period	Functional percentage			
	Slight	Moderate	Extensive	Complete
1 day	70	30	2	0
3 days	100	60	5	2
7 days	100	95	6	2
30 days	100	100	15	4
90 days	100	100	65	10

Obviously, the longer the bridge is closed to traffic, the larger the indirect loss will be. When the bridge is kept closed, commuters need to detour or find alternate route to get to work and traffic time is increased. It is assumed that the commuters are willing to pay a certain amount of fares to use the bridge to save traffic time. Average Daily Traffic (ADT) across the bridge can be obtained. Then the indirect loss can be estimated as the product of ADT and fares and the bridge restoration time (closure time).

Table 8.5 Bridge closure time

Earthquake occurrence rate (years)	Original structure		Level I retrofitting		Level II retrofitting	
	Damage state	Bridge Closure Time (Days)	Damage state	Bridge Closure Time (Days)	Damage state	Bridge Closure Time (Days)
43	Moderate	3	Moderate	3	No damage	0
72	Moderate	7	Moderate	7	Minor	1
475	Extensive	100	Extensive	100	Moderate	3
1000	Collapse	150	Collapse	150	Extensive	100
2500	Collapse	150	Collapse	150	Extensive	100
5000	Collapse	150	Collapse	150	Collapse	150

8.2.4.2 Indirect economic loss

ADT across the case study bridge obtained from the ministry is 50,000 per day (BCMoTH, 2001). Assuming each commuter is willing to pay $1.00 for single trip, indirect economic loss can be estimated based on the methodology given in the section 8.2.4.1. The computed values corresponding to various earthquake levels for original and retrofitted structure are summarized in Table 8.6.

Table 8.6 Indirect economic loss

Earthquake occurrence rate (years)	Original structure		Level I retrofitting		Level II retrofitting	
	Bridge closure time (Days)	Indirect economic loss	Bridge closure time (Days)	Indirect economic loss	Bridge closure time (Days)	Indirect economic loss
43	3	$150,000	3	$150,000	0	$0
72	7	$350,000	7	$350,000	1	$50,000
475	100	$5,000,000	100	$5,000,000	3	$150,000
1000	150	$7,500,000	150	$7,500,000	100	$5,000,000
2500	150	$7,500,000	150	$7,500,000	100	$5,000,000
5000	150	$7,500,000	150	$7,500,000	150	$7,500,000

8.3 Present value of total cost

8.3.1 General description

The total costs of different retrofitting schemes, namely, No retrofitting, Retrofitting level I and Retrofitting level II, are determined as the present expected value of initial retrofitting cost, direct economic loss and indirect economic loss. Retrofitting cost calculated in section 8.2.2 can be used directly for the total cost computation. But for direct and indirect economic loss, the values obtained in section 8.2.3 and 8.2.4 need to be combined with annual earthquake occurrence rate to get the annual economic loss.

In order to compare effects of different retrofitting schemes, all costs need to be discounted to the same year, which is defined as present time. Generally, the present time can be defined as the time when the retrofitting is carried out. For this study, it can be set in the year of 1994. Then all other losses occur in the future years due to earthquake events need to be discounted to the year of 1994. Economic principle can be applied to

discount the losses in the future years to the present time. To do that, planning period and discount rate have to be defined firstly.

8.3.2 Planning period T

For seismic retrofitting of existing old bridges, the considered structural design life (Planning period T) represents remaining service life of the bridge. Usually, the old bridges, which are in the need for seismic retrofit, have already been in service for over 30 years or even more than 50 years. How to select the planning period for the retrofit design is not so obvious in this case. For the new bridge design, the code specifies a structural design life of T = 75 years (CSA, 1990), in which the expected traffic load is calculated based on this design life.

Planning period T has effects on present value of total costs through the discounting factor λ, which is to be discussed in the section 8.3.3. For this study, a planning period T = 100 years is assumed for the present value calculation. To analyze the influence of T on the decision outcome, sensitivity study will be presented in the following sections.

8.3.3 Discount rate and discount factor

Costs can be discounted to present values (PV) using equation 8.1,

$$PV = C\lambda$$
$$\lambda = \frac{1}{(1+i)^t} \qquad \text{Equation 8.1}$$

in which, C is the cost occurs in a future year at time t, λ is the discount factor, i is the discount rate, which is equal to the actual interest rate minus the inflation rate.

Discount rate has a very important effect on the present value of costs that occur in the future. Fig. 8.1 shows the change of discount factor λ with various discount rates i at different structural planning periods (design lives) T. It can be seen that increasing i

lowers the present value of future benefits; conversely, decreasing i raises the present value of future benefits.

Fig. 8.1 Discount factor with discount rate and design life

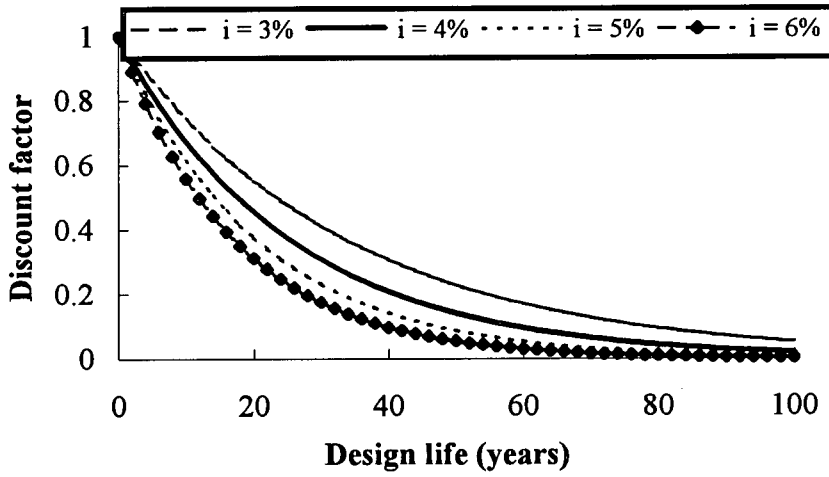

However the choice of an appropriate discount rate is not an easy task. FEMA 227 (FEMA, 1992) recommends the range of 3% to 6% for the discount rate to be used in the benefit – cost analysis of seismic rehabilitation of buildings. It also suggests that for public sector considerations, a discount rate of 3 or 4% is reasonable; for private sector considerations, slightly higher rates of 4 or 6% are reasonable. For this study, a 4% discount rate will be used for the present value calculation.

8.3.4 Calculation of present values of total costs

Based on the methodology presented in Chapter 2, the total expected cost function can be expressed as follows,

$$E[C_T] = C_0 + E[C_D^0] \qquad \text{Equation 8.2}$$

in which, C_0 is the initial construction cost for seismic retrofitting, and C_D^0 is the cumulative damage cost, in present value, which includes the direct economic loss and indirect economic loss under all earthquakes that are likely to occur over the design life of the structure.

Assuming that the occurrences of earthquakes with a specified minimum intensity constitute a Poisson process, that the occurrences and intensities of earthquakes are statically independent, and that the structure is repaired every time a significant earthquake occurs, the expected present value of the cumulative damage cost from future earthquakes over the planning period T is computed as in equation 8.3 (Lee et al, 1998),

$$E[C_D^0] = \int_0^T E[C_D](\frac{1}{1+i})^t \cdot dt \qquad \text{Equation 8.3}$$

The above equation can be transformed as equation 8.4 through integer,

$$E[C_D^0] = E[C_D] \cdot \frac{1-\exp(-\alpha T)}{\alpha} \qquad \text{Equation 8.4}$$

in which,

$\alpha = \ln(1+i)$, i is the actual interest rate,

T is the planning period,

$E[C_D]$ is the expected current damage cost due to earthquakes which occur in future years, in terms of current dollar values.

The expected damage cost can be estimated as follows,

$$E[C_D] = \sum_i C_i P_i \qquad \text{Equation 8.5}$$

where, C_i is the total damage cost (Direct loss & Indirect loss) due to level i earthquake, which is calculated and given as in the above, P_i is the failure probability of the structure due to the same earthquake, which is presented in Chapter 6.

It is noted that the failure probabilities computed in Chapter 6 are conditional probabilities, which are conditioned on the earthquake occurrence of 50% to 1% probability of exceedence in 50 years. In order to use the equation 8.4 to calculate annual damage cost, annual failure probability due to an earthquake event needs to be computed. Since the earthquake occurrences are modeled as a Poisson process with an occurrence rate of ν per year, the annual failure probability can be obtained as follows,

$$P(Annual) = 1 - \exp(-\nu P(Conditional)t) \qquad \text{Equation 8.6}$$

in which,

ν is the earthquake occurrence rate per year,

t = 1 year for annual probability calculation,

P(Conditional) is the conditional failure probability computed in Chapter 6.

The subsequently computed annual failure probabilities for the structure subjected to various levels of earthquakes are given in Table 8.7.

Table 8.7 Annual failure probability

Earthquake return period (years)	Original structure		Level I retrofitting		Level II retrofitting	
	Conditional Failure Probability	Annual Failure Probability	Conditional Failure Probability	Annual Failure Probability	Conditional Failure Probability	Annual Failure Probability
43	3.42E-04	7.95E-06	0	0.00E+00	0	0.00E+00
72	0.0128	1.78E-04	5.58E-04	7.75E-06	0	0.00E+00
475	0.183	3.85E-04	0.114	2.40E-04	2.40E-04	5.05E-07
1000	0.347	3.47E-04	0.217	2.17E-04	2.00E-03	2.00E-06
2500	0.743	2.97E-04	0.504	2.02E-04	0.019	7.60E-06
5000	0.928	1.86E-04	0.771	1.54E-04	0.068	1.36E-05

Table 8.8 (a) Present value of total cost for original structure

Earthquake return period (years)	Original structure				
	Direct & Indirect Loss C_i	$E(C_D)$	Present value of $E(C_D)$	Construction cost for retrofitting	Present value of total cost $E(C_T)$
43	$697,023	$6	$134		
72	$1,021,346	$182	$4,385		
475	$6,243,234	$2,405	$58,079		
1000	$8,743,234	$3,033	$73,259		
2500	$8,743,234	$2,598	$62,747		
5000	$8,743,234	$1,623	$39,187		
Total			$237,790	$0	**$237,790**

Table 8.8 (b) Present value of total cost for level I retrofitting

Earthquake return period (years)	Level I retrofitting				
	Total economic loss	$E(C_D)$	Present value of $E(C_D)$	Construction cost for retrofitting	Present value of total cost $E(C_T)$
43	$622,429	$0	$0		
72	$921,887	$7	$173		
475	$6,243,234	$1,498	$36,183		
1000	$8,743,234	$1,897	$45,816		
2500	$8,743,234	$1,762	$42,565		
5000	$8,743,234	$1,348	$32,558		
Total			$157,294	$179,000	**$336,294**

Table 8.8 (c) Present value of total cost for level II retrofitting

Earthquake return period (years)	Level II retrofitting				
	Total economic loss	$E(C_D)$	Present value of $E(C_D)$	Construction cost for retrofitting	Present value of total cost $E(C_T)$
43	$0	$0	$0		
72	$50,000	$0	$0		
475	$721,887	$0	$9		
1000	$6,243,234	$12	$302		
2500	$6,243,234	$47	$1,146		
5000	$8,743,234	$119	$2,872		
Total			$4,328	$194,492	**$198,820**

The calculated expected damage cost $E[C_D]$ from Equation 8.5 and present value of the expected damage cost $E[C_D^0]$ are presented in Table 8.8 as in the above. Present value of total expected cost $E[C_T]$ including initial construction cost for retrofitting is also shown in the table 8.8.

8.4 Optimal seismic retrofitting level

8.4.1 General description

Based on the calculated present values of total costs for different seismic retrofitting schemes, a benefit/cost analysis can be undertaken following the procedures given in FEMA 227 (FEMA, 1992). According to FEMA 227, the central economic question about rehabilitating earthquake – hazardous structures is whether the benefits which accrue from rehabilitation are sufficiently valuable to warrant the expense. Benefit/cost analysis is a widely – used economic tool for helping to make decisions, especially in the public sector.

Benefits arising from seismic retrofitting include the value of future losses avoided which could result from expected earthquake damages to unretrofitted bridges. Costs include the engineering, construction, and other costs required to retrofit bridges. Retrofitting existing bridges may be economically justified when the expected benefits exceed costs (i.e., benefit/cost ratio greater than one). Retrofitting existing bridges may not be economically justified when the expected benefits are less than the retrofitting costs (i.e., benefit/cost ratio less than one). Therefore, benefit/cost analysis can be used to determine the optimal seismic retrofitting level for bridges.

8.4.2 Determination of optimal retrofitting level

Using the definitions given in section 8.4.1, the computed benefits and costs for each seismic retrofitting scheme are shown in Table 8.9 based on the numbers from Table 8.8.

Table 8.9 Benefit/Cost ratios

Retrofitting scheme	Present value of total cost (1)	Economic loss (2)	Retrofitting cost (3)	Benefit (4)	B/C Ratio (5)=(4)/(3)	Ranking (6)
No Retrofitting	$237,790	$237,790	$0	$0	N/A	2
Retrofitting Level I	$336,294	$157,294	$179,000	$80,496	0.4	3
Retrofitting Level II	$198,820	$4,328	$194,492	$233,462	1.2	1

From Table 8.9, level II retrofitting has the highest benefit/cost ratio of 1.2, compared with the ratio of 0.4 for level I retrofitting. If no retrofitting is to be made and leave the bridge as it is, no benefit will be obtained and huge economic loss will be incurred due to earthquake damages. It also can be seen from column (1) in Table 8.9 that, level II retrofitting has the minimum present value of total cost of $198, 820. Therefore, for the case study bridge with the analysis undertaken in the previous chapters and assumptions made aforementioned, the optimal seismic retrofitting level is the level II retrofitting.

8.5 Sensitivity analysis

8.5.1 General description

Many variables are important in the decision-making process about whether or not to retrofit existing earthquake – hazardous bridges. Some of those variables included in the present value decision model and in the benefit/cost analysis are uncertain and hard to evaluate for a deterministic analysis. To demonstrate the sensitivity of decision outcome on the input variables, a sensitivity analysis will be made as in the following. The influence of indirect economic loss, planning period for structural retrofitting and discount rate will be discussed in detail.

8.5.2 Indirect economic loss

As discussed in the aforementioned, indirect economic loss due to earthquake damages are difficult to evaluate. An approximate method is used in this study to calculate indirect loss based on the assumption that the loss is proportional to bridge closure time immediately after an earthquake and ADT across the bridge. However, bridge closure time $t_{closure}$ is hard to determine. To show its effect on the decision outcome, benefit/cost ratios are calculated by increasing $t_{closure}$ +50% and decreasing $t_{closure}$ –50% respectively. The computed results are shown in Table 8.10.

Table 8.10 Influence of indirect economic loss

Retrofitting scheme	Benefit			Benefit/Cost Ratio		
	-50%	0%	50%	-50%	0%	50%
No Retrofitting	$0	$0	$0	N/A	N/A	N/A
Retrofitting Level I	$47,725	$80,496	$113,266	0.3	0.4	0.6
Retrofitting Level II	$136,111	$233,462	$330,813	0.7	1.2	1.7

With a 50% change of indirect economic loss, benefit/cost ratio varies 40%. When indirect loss is reduced, benefit/cost ratio is decreased too. With a 50% decrease of indirect loss, both retrofitting schemes have a benefit/cost ratio less than 1.0, i.e. retrofitting cost cannot be justified economically. This leaves no retrofitting the optimal retrofitting scheme. However, when the indirect loss is increased, benefit/cost ratios for both retrofitting schemes are also increased. Therefore, the bigger of the economic loss, the more easily will the seismic retrofitting be economically justified.

8.5.3 Planning period T

Two different other planning periods of T = 50 and 100 years are assumed here for the computation of benefit/cost ratios for different retrofitting schemes. The obtained results are given in Table 8.11.

Table 8.11 Influence of planning period T

Retrofitting scheme	Benefit			Benefit/Cost Ratio		
	T = 50 yrs	T = 75 yrs	T = 100yrs.	T = 50yrs	T = 75 yrs	T = 100yrs.
No Retrofitting	$0	$0	$0	N/A	N/A	N/A
Retrofitting Level I	$73,023	$80,496	$83,298	0.4	0.4	0.5
Retrofitting Level II	$211,790	$233,462	$241,591	1.1	1.2	1.2

When T = 50 years, benefit/cost ratio for level I retrofitting is not changed; while for level II retrofitting, the ratio has been slightly decreased to 1.1. At T = 100 years, the ratios for both retrofitting schemes are similar to the ones at T = 75 years and T = 50 years. Therefore, the effect of planning period on the retrofit decision is only significant when T is less than 50 years. When planning period is shorter (less than 30 years), the retrofitting expense is very hard to be justified for this bridge.

8.5.4 Discount rate

Table 8.12 shows the benefit/cost ratios with discount rate i = 3% and 5% respectively. The ratios at i = 4% are also given in the table for comparison.

Table 8.12 Influence of discount rate i

Retrofitting scheme	Benefit			Benefit/Cost Ratio		
	i = 3%	i = 4%	i = 5%	i = 3%	i = 4%	i = 5%
No Retrofitting	$0	$0	$0	N/A	N/A	N/A
Retrofitting Level I	$100,474	$80,496	$66,554	0.6	0.4	0.4
Retrofitting Level II	$291,407	$233,462	$193,028	1.5	1.2	1.0

When the discount rate i is reduced from 4% to 3%, the benefits from both retrofitting schemes are increased; and benefit/cost ratio is increased from 1.2 to 1.5 for level II retrofitting. When i is increased from 4% to 5%, the retrofitting benefits are reduced; and benefit/cost ratio is decreased from 1.2 to 1.0 for level II retrofitting. The higher of the discount rate i, the lower of the benefits obtained from retrofitting and the retrofitting expense is less likely to be justified. For this study, however, with planning period T = 75 years, level II retrofitting is always the optimal retrofitting scheme for the discount rate range from 3% to 5%.

Based on the data from BC, both the benefit/cost analysis and sensitivity analysis show that the optimal seismic retrofitting level for the case study bridge is level II retrofitting, which aims to keep a limited or normal traffic flow immediately after an earthquake of 10% exceedence in 50 years. And it can also conclude that seismic retrofitting is economically justified. In all cases except the situation where planning period is less than 30 years and a very low indirect loss is assumed, the decision outcome keeps unchanged.

The robust result may partly result from the relatively easy and unexpensive retrofitting work for this bridge, where a retrofitting cost close to 20% of replacement cost is obtained.

Chapter 9 Summary, conclusions and discussions

The object of this research is to demonstrate the use of reliability – based risk decision model in the seismic retrofit of bridges. A benefit – cost analysis based on constructed decision model is undertaken to determine the optimal seismic retrofitting level for bridges in British Columbia (BC). A case study bridge with multi – span steel girders and reinforced concrete bents, which is commonly seen in BC, is introduced in order to demonstrate the methodology and procedures involved in the decision analysis.

This study is mainly focused on the decision problem of seismic retrofitting of a particular bridge, in which extensive and in – depth seismic analysis of the structure is undertaken and local data, including seismicity, soil, and cost data, is used. It deviates from the general methodology which is used for the determination of retrofitting of classes of or groups of structures, such as FEMA – 227 (FEMA, 1992) and HAZUS99 (FEMA, 1999). The refined structural analysis and focused effort are deemed to bring more confidence in the outcome of the decision model.

After a brief introduction to the case study bridge, global and local seismic behaviour are assessed. The linear, elastic response spectrum analysis is undertaken to calculate component capacity/demand ratios, on the basis of which the critical structural components are identified. Then, local inelastic push over analysis is made to the deficient isolated concrete bents. Seismic deficiencies are clearly identified and failure mechanism is evaluated.

Two level seismic retrofitting schemes are designed to counteract those deficiencies. Level I is a safety level retrofitting, which aims to save the structure from collapse during a design earthquake of 10% exceedence probability in 50 years; Level II uses capacity design principle to upgrade the structure to certain predetermined performance levels. It's a functional level retrofitting. Detailed designs of both schemes are given. The effects of retrofitting on the structural seismic behaviours are evaluated as well.

Both the failure probability of the case study bridge before seismic retrofitting and after seismic upgrading are computed. Failure criteria is taken as the cap beam shear demand exceeding shear capacity for the original bridge and the upgraded bridge with level I retrofitting; for the bridge after level II retrofitting, lateral displacement capacity of isolated bent is considered as failure criteria. Latin Hypercube Sampling (LHS) is used to generate random variables to be input in the analysis programs to obtain seismic demand and seismic capacity. Then, the computed seismic demand and capacity are fitted into Lognormal probability distribution functions and the conditional probability of failure of the case study bridge during future earthquakes is calculated using FORM/SORM method. It can be found that the original bridge has a probability of failure at collapse of 18% during an earthquake level of 10% exceedence in 50 years. With an earthquake level of 2% exceedence in 50 years, the collapse probability is increased to 74%. After the structure is retrofitted with level II retrofitting, the collapse probability has been reduced to nearly 0 and 2% respectively for the aforementioned two earthquake levels.

Seismic financial damages in dollars are calculated based on the mapping out relationship between physical damage (quantified as damage index) and damage in dollars. Over years, various damage indices have been developed to provide an effective way to quantify numerically the seismic damages sustained by individual elements or complete structures. Damage indices are computed in this research for the original and retrofitted bridge using recorded earthquake records that are scaled to various earthquake levels. The damage indices are then related to predefined damage categories which, in turn, are associated with damage costs. Both direct and indirect economic losses are estimated. An expected value of the future earthquake damage costs are then calculated and discounted to the present year. Present values of the total costs for all retrofitting schemes are calculated. A benefit – cost analysis is undertaken to determine the optimal upgrading option.

The benefit – cost analysis shows that level II retrofitting has the highest benefit/cost ratio of 1.2, compared with the ratio of 0.4 for level I retrofitting. Therefore, level II retrofitting is economically justified. It concludes that for the bridge in this case study,

the optimal seismic retrofitting level would be level II retrofitting, which aims to keep normal or a limited traffic flow immediately after an earthquake with a 10% exceedence probability in 50 years.

Sensitivity analysis indicates that the indirect cost has major effect on the decision outcome, while planning period and discount rate have small effects. When the indirect cost is reduced -50%, "No Retrofitting" becomes the optimal option, which means that the initial retrofitting cost cannot be economically justified for the future losses. With the planning period T equal to or greater than 50 years, change of planning period has negligible effect on the benefit – cost ratio. The planning period has large effect on the decision outcome only when T is less than 30 years. Discount rate influences level II retrofitting more than level I retrofitting. However, for the bridge considered in this research, variation of discount rate from 3% to 5% does not change the decision outcome. Level II retrofitting is always the optimal scheme with the planning period T at 75 years.

Based on the extensive analysis in this research and local data from British Columbia (BC), it concludes that the initial cost spent on the seismic retrofitting of bridges, which are generally structural simple and easily accessible, can relatively easily be justified. The robust outcome both from the benefit – cost analysis and sensitivity analysis may result from the relatively easy and unexpensive retrofitting work for those bridges, where an initial retrofitting cost close to 20% of replacement cost is obtained.

The reliability – based risk decision analysis methodology and procedures are successfully demonstrated through the case study bridge. In the case of complicated seismic retrofitting decision problem with many uncertainties involved, decision analysis can provide an effective tool to search the optimal solution among numerous feasible upgrading options. With more refined analysis and reliable local cost data input into the decision model, more confidence can be found from the decision outcome. However, many things still need to be done for the decision analysis to be widely used in the seismic retrofitting decision of bridges.

An efficient reliability analysis scheme is to be developed for the failure probability evaluation of the whole bridge system during future earthquakes. One of the most important and difficult aspect for the construction of decision model is to compute the structural failure probability. In this research, the simple FORM/SORM method is used with many simplifications and assumptions. Obviously, it needs to be refined in a future research. Another important and controversial aspect of the decision model is the estimation of future seismic damages. The difficulty comes from not only the assessment and category of physical damages to the structures, but also the financial damages (or economic losses) estimation. Although damage indices can be used to quantify numerically the physical damages, the inelastic and non-linear modelling of concrete structures and selection of earthquake motions to be input into the analysis program are in high uncertainty. Moreover, the reliability of the damage index to quantify seismic damages of real structure with many seismic deficiencies to the future earthquakes is still to be explored. The financial damage cost calculation from computed damage indices is based on the empirical relationship from laboratory test. More data from the past or future real earthquake damages are in need to provide more reliable and direct economic loss estimation.

Despite the limitations and simplifications, it is still possible to make rational decision using the available information and data. Valuable information can be obtained from a consistent and rational decision analysis. A promising future can be expected for the decision analysis in the complicated seismic retrofitting of bridges with more earthquake damage data available and more refined analysis undertaken.

REFERENCES

American Association of State Highway and Transportation Officials (AASHTO), 1996, 1992, 1990, 1988, Standard specification for highway bridges, Washington, D.C.

Anderson, D.L., Sexsmith, R.G., English D.S., Kennedy, D.W., & Jennings D.B., 1995, Oak Street & Queensborough bridges two column bent tests, Technical Report 95 – 02, Department of Civil Engineering, University of British Columbia.

Applied Technology Council (ATC), 1996, Improved seismic design criteria for California bridges: provisional recommendations, ATC – 32, Redwood City, California.

Applied Technology Council (ATC), 1988, Rapid screening of buildings for potential seismic hazards: a handbook, ATC – 21, Redwood City, California.

Applied Technology Council (ATC), 1985, Earthquake damage evaluation data for California, ATC – 13, Redwood City, California.

Arede, A., & Pinto, A.V., 1996, Performance of R/C buildings designed for different ductility classes, Proceedings of 11th World Conference on Earthquake Engineering, Pergamon, Tarrytown, N.Y.

Ayyub, B.M., & Lai, K.L., 1989, Structural reliability assessment using Latin Hypercube Sampling, ICOSSAR'89, 5th International Conference on Structural Safety and Reliability, 1177 – 1184.

Basoz, N., & Kiremidjian, A.S., Prioritization of bridges for seismic retrofitting, 1995, Report No. 114, The John A. Blume Earthquake Engineering Center, Stanford University.

Bazzurro, P., & Cornell, C.A., 1994, Seismic hazard analysis of nonlinear structures, I: Methodology, Journal of Structural Engineering, 120(11), 3320 – 3344.

BCMoTH, 2001, Average Daily Traffic across Colquitz River Bridge, BC Ministry of Transportation and Highways, Victoria, BC.

BCMoTH, 2000a, Seismic retrofit design criteria, BC Ministry of Transportation and Highways, Victoria, BC.

BCMoTH, 2000b, Bridge seismic retrofit program, BC Ministry of Transportation & Highways, Victoria, BC.

BCMoTH, 1995, Colquitz river bridge seismic safety retrofit, BC Ministry of Transportation and Highways, Victoria, BC.

BCMoTH, 1994, Geotechnical report for the Colquitz river bridge, BC Ministry of Transportation & Highways, Victoria, BC.

BCMoTH, 1986, Bridge construction cost estimation program, BC Ministry of Transportation & Highways, Victoria, BC.

BCMoTH, 1976, Geotechnical report for the Colquitz river south bridge, BC Ministry of Transportation & Highways, Victoria, BC.

BCMoTH, 1953a, Design drawings of Colquitz River North Bridge, BC Ministry of Transportation & Highways, Victoria, BC.

BCMoTH, 1953b, Geotechnical report for the Colquitz river bridge, BC Ministry of Transportation & Highways, Victoria, BC.

Bentz, E.C., & Collins M.P., 1998, Response – 2000, Reinforced concrete sectional analysis using the modified compression field theory, Version 0.7.5, Department of Civil Engineering, University of Toronto.

Caltrans, 1999, Bridge seismic design criteria, California Department of Transportation, Sacramento, California.

Caltrans, 1995, Bridge replacement cost, California Department of Transportation, Sacramento, California.

Caltrans, 1994, The Northridge earthquake: post earthquake investigation report, Sacramento, California.

Caltrans, 1988, Memo to designers 5 – 1, California Department of Transportation, Division of Structures, Sacramento, CA.

Canadian Standard Association, 2000, New Canadian bridge design code, CAN/CSA – S6 – 00.

Canadian Standard Association, 1990, Canadian bridge design code, CAN/CSA-S6-90.

Colangelo, F., Giannini, R., & Pinto, P.E., 1996, Seismic reliability of reinforced concrete structures with stochastic properties, Structural Safety, 18(2/3), 151 – 168.

Collins, M.P., & Mitchell D., 1987, Prestressed concrete basics, Canadian Prestressed Concrete Institute.

Computers and Structures, Inc., 2000, SAP 2000 Educational version 7.40, Static and Dynamic Finite Element Analysis of Structures, California.

Computers and Structures, Inc., 1999, SAP 2000 Nonlinear version 6.99, Static and Dynamic Finite Element Analysis of Structures, California.

Cornell, C.A., 1968, Engineering seismic risk analysis, Bulletin of Seismological Society of America, 58(5), 1583 – 1606.

CWMM Ltd., 1994, Retrofit strategy report for Colquitz river bridges, Kelowna, BC.

Dymiotis, C., Kappos, A.J., & Chryssanthopoulos, M.K., 1999, Seismic reliability of RC frames with uncertain drift and member capacity, Journal of Structural Engineering, 125(9), 1038 – 1047.

Federal Emergency Management Association (FEMA), 1999, HAZUS99: Economic loss estimation of hazards in U.S.

Federal Emergency Management Association (FEMA), 1997a, Commentary to the seismic rehabilitation recommendations for buildings, FEMA – 273.

Federal Emergency Management Association (FEMA), 1997b, Seismic rehabilitation recommendations for buildings, FEMA – 273.

Federal Emergency Management Association (FEMA), 1992, A benefit – cost model for the seismic rehabilitation of buildings, FEMA – 227.

Felber, A.J., 1993, Development of a hybrid bridge evaluation system, PhD thesis, Department of Civil Engineering, University of British Columbia.

Floren, A., & Mohammadi, J., 2001, Performance – based design approach in seismic analysis of bridges, Journal of Bridge Engineering, 6(1), 37 – 45.

Foschi, R., Yao, F., & Li, H., 2000, Structural reliability analysis program RELAN, Department of Civil Engineering, University of British Columbia.

Foschi, R., 1999, Structural safety and reliability course notes, Department of Civil Engineering, University of British Columbia.

Geological Survey of Canada, 1999, Open File 3724, Trial seismic hazard maps of Canada – 1999: 2%/50 year values for selected Canadian cities.

Hambly, E.C., 1991, Bridge deck behaviour, 2nd Edition, E & FN SPON.

Hindi, R.A., & Sexsmith, R.G., 2001, A proposed damage model for R/C bridge columns under cyclic loading, to be published in Earthquake Spectra, Department of Civil Engineering, University of British Columbia.

Hwang, H., Jernigan, J.B., & Lin, Y.W., 2000, Evaluation of seismic damage to Memphis bridge and highway systems, Journal of Bridge Engineering, 5(4), 322 – 330.

Iman, R.L., Conover, W.J., 1980, Small sample sensitivity analysis techniques for computer models, with an application to risk assessment, Communications in Statistics, A9(17), 1749 – 1842.

Nishimura, K., 1997, Risk-based decision model for bridges, MASc thesis, University of British Columbia, Vancouver, Canada.

King, S.A., & Kiremidjian, A.S., 1994, Regional seismic hazard and risk analysis through geographic information system, Technical Report No. 111, John A. Blume Earthquake Engineering Center, Stanford University, Stanford, California.

Klohn – Crippen CBA Consultants Ltd., 1999, Seismic Retrofit Strategy Report of Tsawwassen Overhead No. 2452..

Lam, I., & Martin, G.R., 1986, Seismic design of highway bridge foundations, Vol. II, Design procedures and guidelines, Report No. FHWA/RD – 86/102, Federal Highway Administration, Virginia.

Lee, J.C., Pires, J.A., & Ang, A.H.-S., 1998, Optimal target reliability and development of cost – effective seismic design criteria for a class of R.C. shear – wall structures, Structural Safety & Reliability, Shiraishi, Shinozuka & Wen (Eds), 1091 – 1098, Balkema, Rotterdam.

Li, K.L., 1996, CANNY – E, Three dimensional nonlinear dynamic structural analysis program, Singapore.

Maffei, J., & Park, R., 1994, Management and prioritization of bridge seismic upgrading, Seismic Design and Retrofitting of Reinforced Concrete Bridges, Proceedings of the Second International Workshop, Queenstown, New Zealand, August, 1994, 515 – 534.

MathSoft, Inc., 1998, MathCAD Professional version 8.

Melchers, R.E., 1999, Structural reliability analysis and prediction, John Wiley & Son Ltd

Miranda, E., 1999, Approximate seismic lateral deformation demands in multistory buildings, Journal of Structural Engineering, 125(4), 417 – 425.

Miranda, E., 1991, Seismic upgrading and evaluation of existing buildings, PhD thesis, Department of Civil Engineering, University of California, Berkeley, California.

O'Connor, J.M., & Ellingwood, B.R., 1987, Reliability of nonlinear structures with seismic loading, Journal of Structural Engineering, 113(5), 1011 – 1028.

Park, Y.J., Ang, A.H-S., 1985, Mechanistic seismic damage model for reinforced concrete, Journal of Structural Engineering, 111(4), 722 – 739.

Park, Y.J., Ang, A.H-S., & Wen, Y.K., 1985, Seismic damage analysis of reinforced concrete buildings, Journal of Structural Engineering, 111(4), 740 – 757.

Paulay, T., & Priestley, M.J.N., 1992, Seismic design of reinforced concrete and masonry buildings, Wiley, New York.

Priestley, M.J.N., Seible, F., & Calvi, G.M., 1996, Seismic design and retrofit of bridges, John Wiley & Sons, Inc.

Roberts, J.E., 1990, Recent advances in seismic design and retrofit of bridges, Proceedings of Fourth U.S. National Conference on Earthquake Engineering, 75 – 82.

Rojahn, C., Mayes, R., Anderson, D.G., etc., 1997, Seismic design criteria for bridges and other highway structures, ATC – 18, Technical report NCEER – 97 – 0002, National Center for Earthquake Engineering Research, Buffalo, NY.

Saadatmanesh, H., Ehsani, M.R., & Jin.,L., 1995, Repair of earthquake damaged R/C columns with prefabricated FRP wraps, ACI Structural Journal, MS No. 8847, June, American Concrete Institute, Detroit.

Sexsmith, R.G., 1994. Seismic risk management for existing structures, Canadian Journal of Civil Engineering, 21(2), 180 - 185.

Seya, H., Talbott, M.E., & Hwang, H., 1993, Probabilistic seismic analysis of a steel frame structure, Probabilistic Engineering Mechanics, 4(4), 127 – 136.

Shimazaki, K., & Sozen, M.A., 1984, Seismic drift of reinforced concrete structures, Research Report, Hazama-Gumi, Ltd., Tokyo, Japan.

Shome N., Cornell C.A., Bazzurro, P., & Carballo, J.E., 1998, Earthquakes, records, and nonlinear responses, Earthquake Spectra, 14(3), 469 – 500.

Singhal, A., & Kiremidjian, A.S., 1996, Method for probabilistic evaluation of seismic structural damage, Journal of Structural Engineering, 122(12), 1459 – 1467.

Song, J.L., & Ellingwood, B.R., 1999, Seismic reliability of special moment steel frames with welded connection: II, Journal of Structural Engineering, 125(4), 372 – 384.

Spoelstra, M.R., & Monti G., 1999, FRP confined concrete model, Journal of Composite for Construction, 3(3), 143 – 150.

Stone, W.C., & Taylor, A.W., 1993, Seismic performance of circular bridge columns designed in accordance with AASHTO/CALTRANS Standards, NIST Building Science Series 170, National Institute of Standards and Technology, Gaithersburg, MD.

Thavaraj, T., 2000, Seismic analysis of pile foundations for bridges, PhD thesis, Department of Civil Engineering, University of British Columbia.

Thoft-Christensen, P., & Baker, M.J., 1982, Structural reliability theory and its applications, Springer-Verlag Berlin, Herdelberg.
Tzavelis, C., & Shinozuka, M., 1988, Seismic reliability of rigid frame structures, Journal of Engineering Mechanics, 114(11), 1953 – 1977.

Wen, Y.K., & Kang, Y.J., 1998, Minimum life – cycle cost design criteria, Structural Safety and Reliability, Editors Shiraishi, Shinozuka & Wen, Balkema, Rotterdam, 1047 – 1054.

Whittaker, A., Constantinou, M., & Tsopelas, P., 1998, Displacement estimation for performance – based seismic design, Journal of Structural Engineering, 124(8), 905 – 912.

Williams, M.S., 1994, Inelastic damage analysis of the Oak Street and Queensborough bridge bents, Technical Report 94-03, Earthquake Engineering Research Facility, Department of Civil Engineering, University of British Columbia.

Williams, M.S., & Sexsmith, R.G., 1994, Review of methods of assessing seismic damage in concrete structures, Technical Report 94-02, Earthquake Engineering Research Facility, Department of Civil Engineering, University of British Columbia.

Wilson, J.C., & Tan, B.S., 1990a, Bridge abutments: Formulation of simple model for earthquake response analysis, Journal of Engineering Mechanics, 116(8), 1828 – 1837.

Wilson, J.C., & Tan, B.S., 1990b, Bridge abutments: Assessing their influence on earthquake response of Meloland Road Overpass, Journal of Engineering Mechanics, 116(8), 1838 – 1856.

Yashinsky, M., 1998, Performance of bridge seismic retrofits during Northridge earthquake, Journal of Bridge Engineering, 3(1), 1 – 14.

Appendix A1 As – built drawings and seismic retrofitting design drawings for Colquitz Bridge

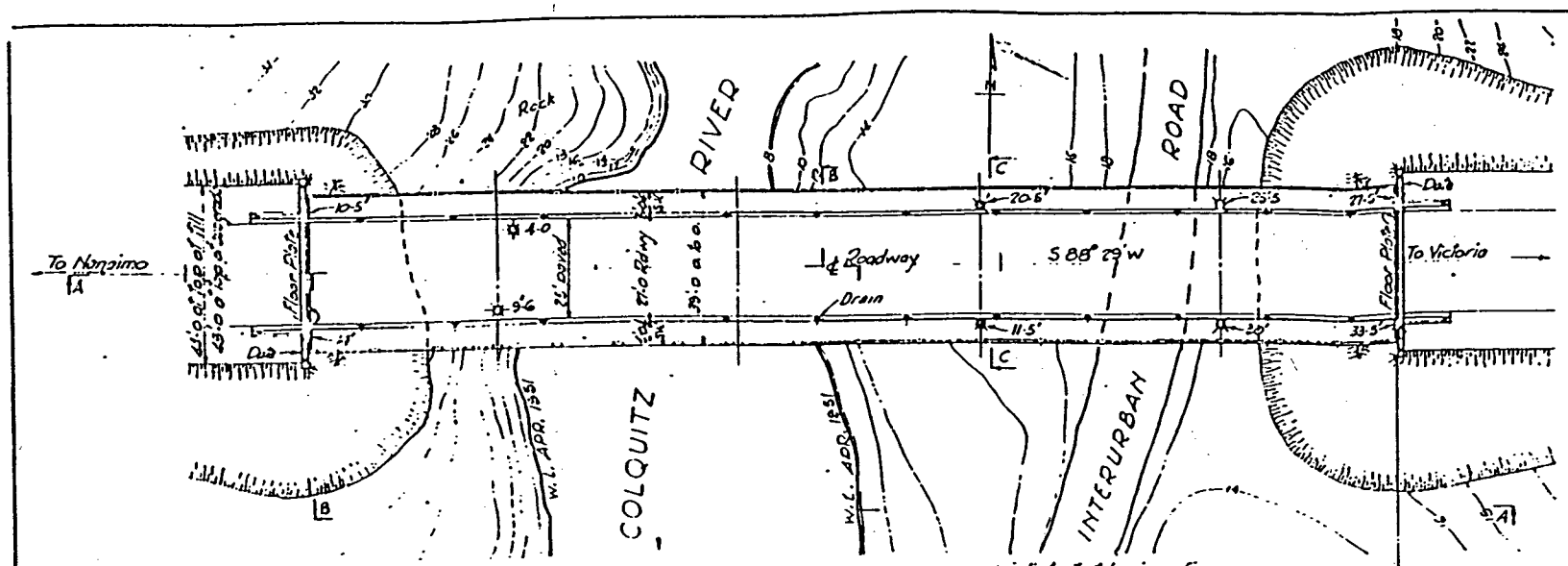

PLAN

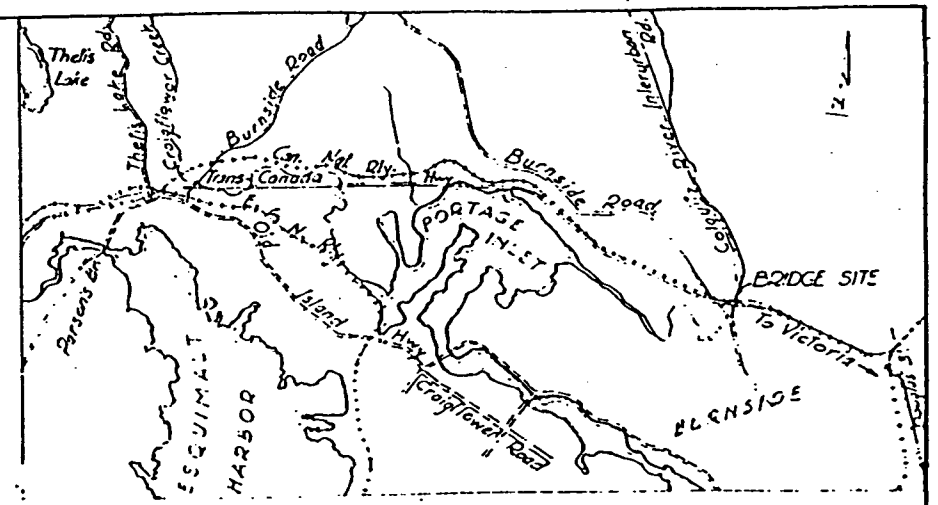

KEY MAP

Scale: 1" = 2000'±

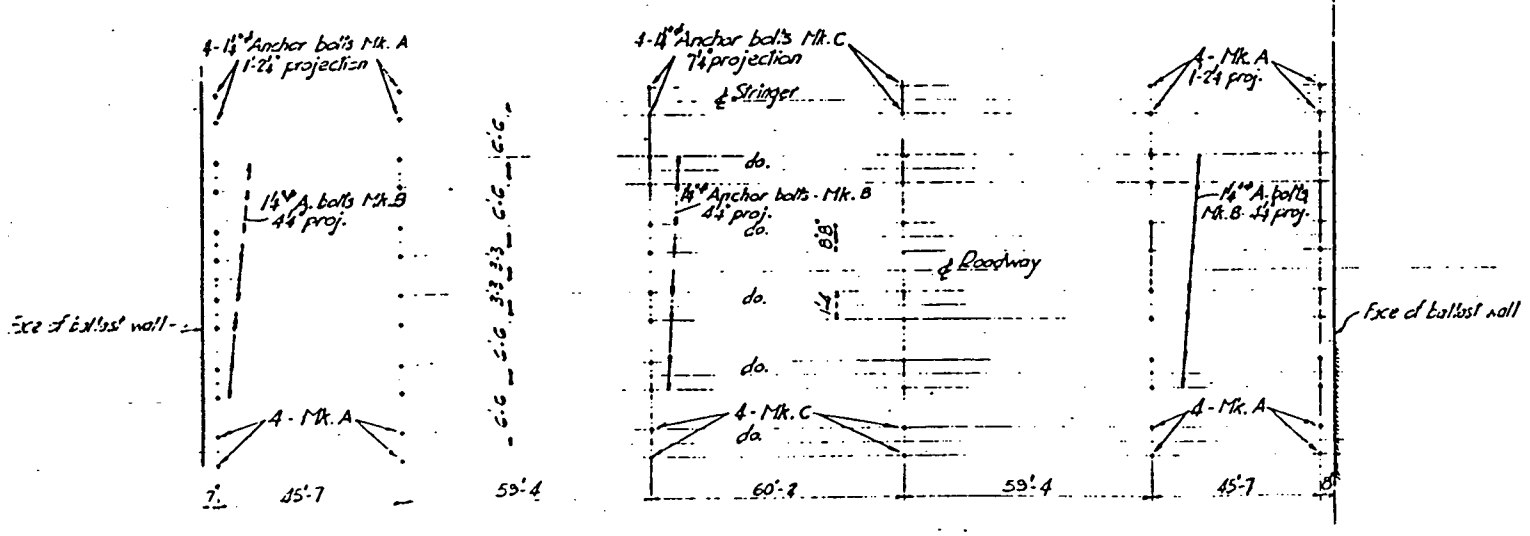

ANCHOR BOLT PLAN

See Dgs. 1378-4, 5 & 6 for details of setting of Anchor Bolts.

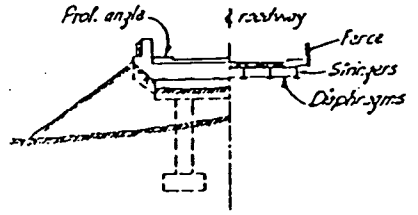

SECT. B-B

LIST OF DRAWINGS	
DDG. N°	TITLE
1378 - 3	Layout, Key Map & Anchor Bolt Plan.
- 4	West Abutment
- 5	East Abutment
- 6	Bents #2 & 3
- 7	Bents #1 & 4
- 8	Steelwork Details
- 9	Deck Details
-10	Anchor Bolt Assemblies
1310 - 537 - 7	Std. Roadway Fence

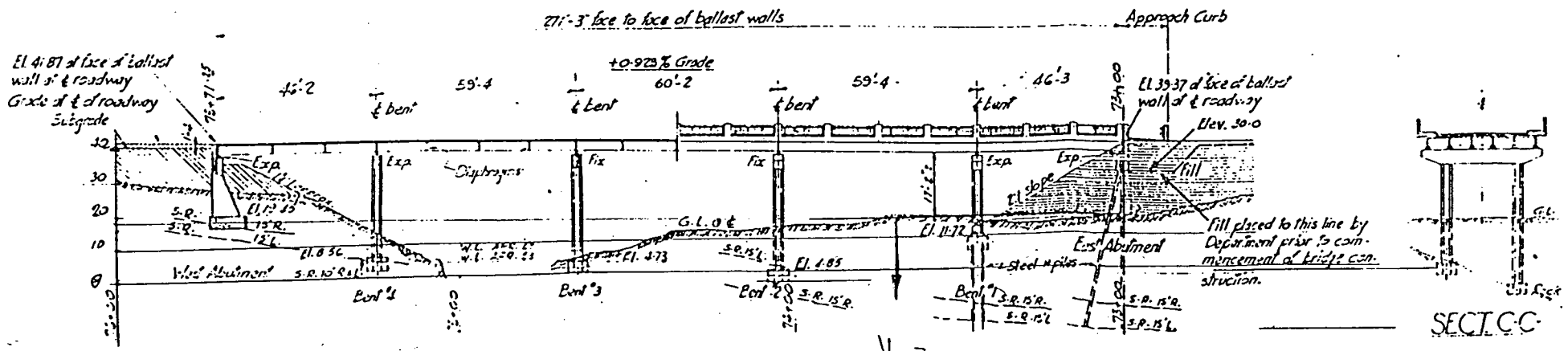

SECT. A-A

SECT. C-C

Note:
Spec: Dept of Public Works & Trans-Canada.
Live load: H20-S16.

SAANICH DISTRICT
TRANS-CANADA HIGHWAY - MILE 1.8
COLQUITZ RIVER BRIDGE
LAYOUT, KEY MAP & ANCHOR BOLT PLAN
SCALE: 1" = 20'-0 & AS NOTED

REVISIONS			
No.	Particulars	Init.	Date
A	10' added to create span	GLD	Nov/58
B	As built	AL	Aug/60

GOVT. OF BRITISH COLUMBIA
DEPT. OF PUBLIC WORKS
BRIDGE ENGINEER'S OFFICE

	Init.	Date	DRAWING NO.
Made by	YA	Oct/57	1378-3
Checked by	KDF	Nov 20/57	

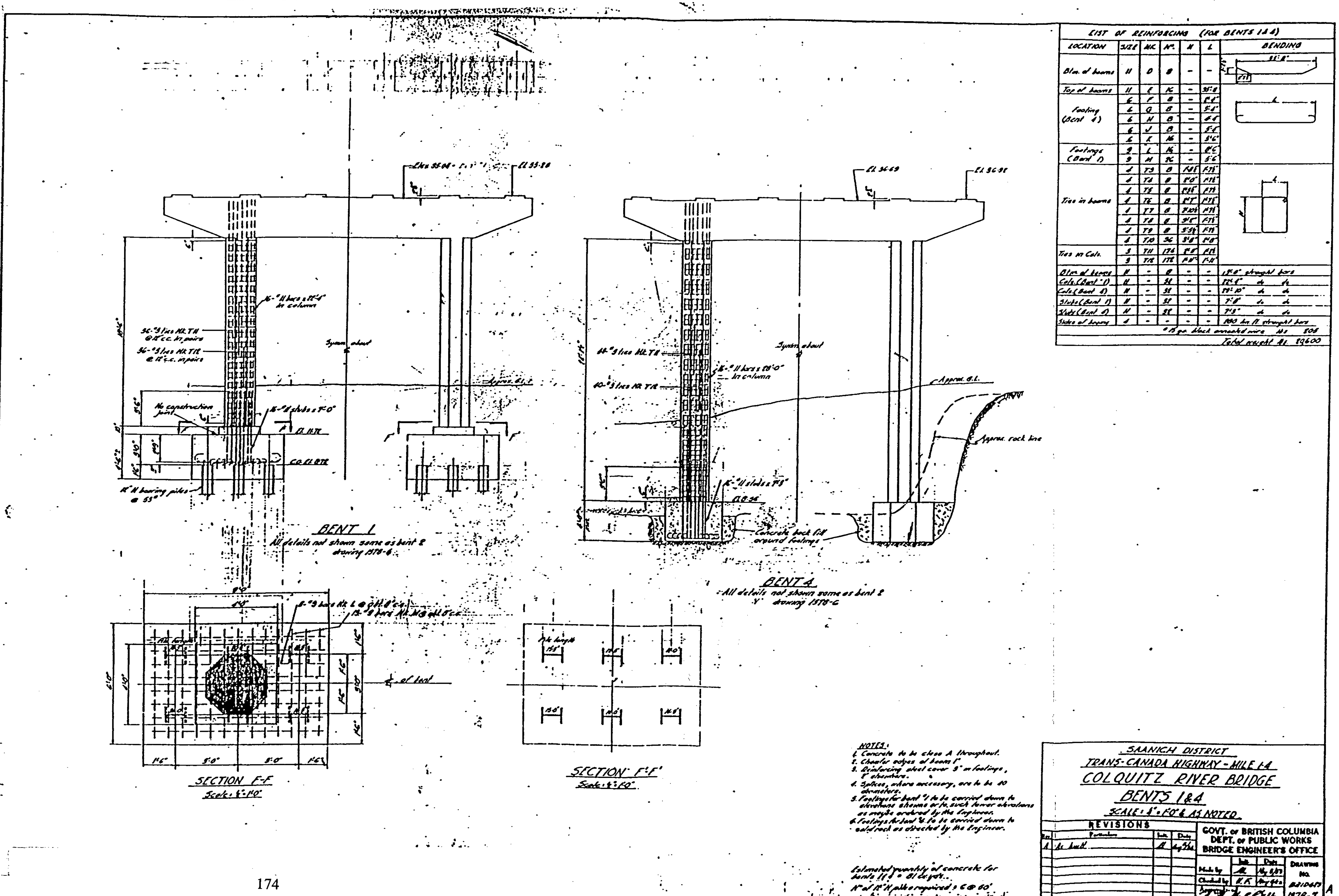
LIST OF REINFORCING (FOR BENTS 1 & 4)
BENT 1
All details not shown same as bent 2 drawing 1378-6
BENT 4
All details not shown same as bent 2 drawing 1378-6
SECTION F-F
SECTION F'-F'
Approx. rock line
Concrete back fill around footings
NOTES:
1. Concrete to be class A throughout.
2. Chamfer edges of beams 1"
3. Reinforcing steel cover 3" on footings, 2" elsewhere.
4. Splices, where necessary, are to be 40 diameters.
5. Footings for bent 1 to be carried down to elevations shown or to such lower elevations as may be ordered by the Engineer.
6. Footings for bent 4 to be carried down to solid rock as directed by the Engineer.
SAANICH DISTRICT
TRANS-CANADA HIGHWAY - MILE 1.4
COLQUITZ RIVER BRIDGE
BENTS 1 & 4
REVISIONS
GOVT. OF BRITISH COLUMBIA
DEPT. OF PUBLIC WORKS
BRIDGE ENGINEER'S OFFICE
DRAWING No.
1378-7

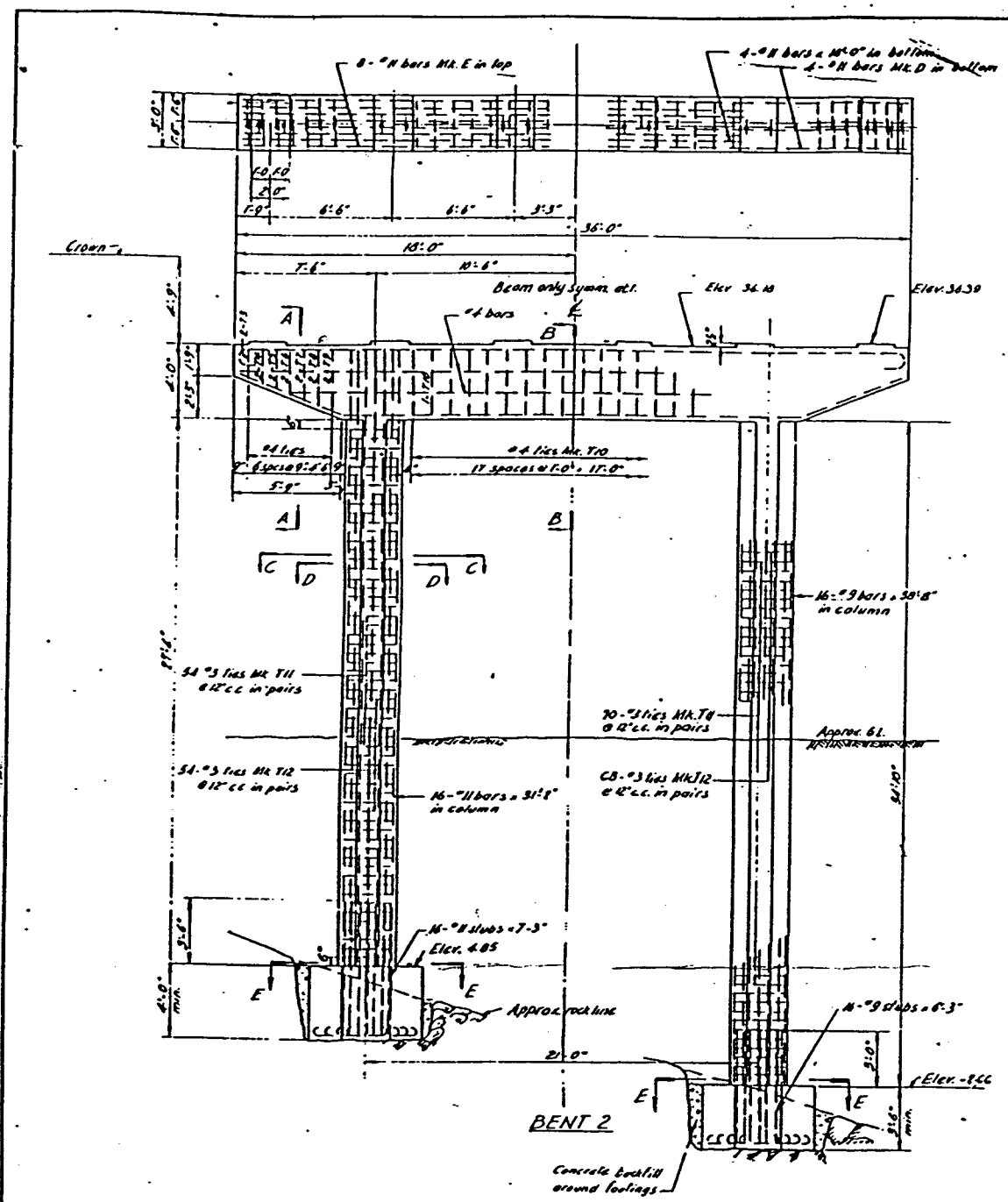

BENT 2

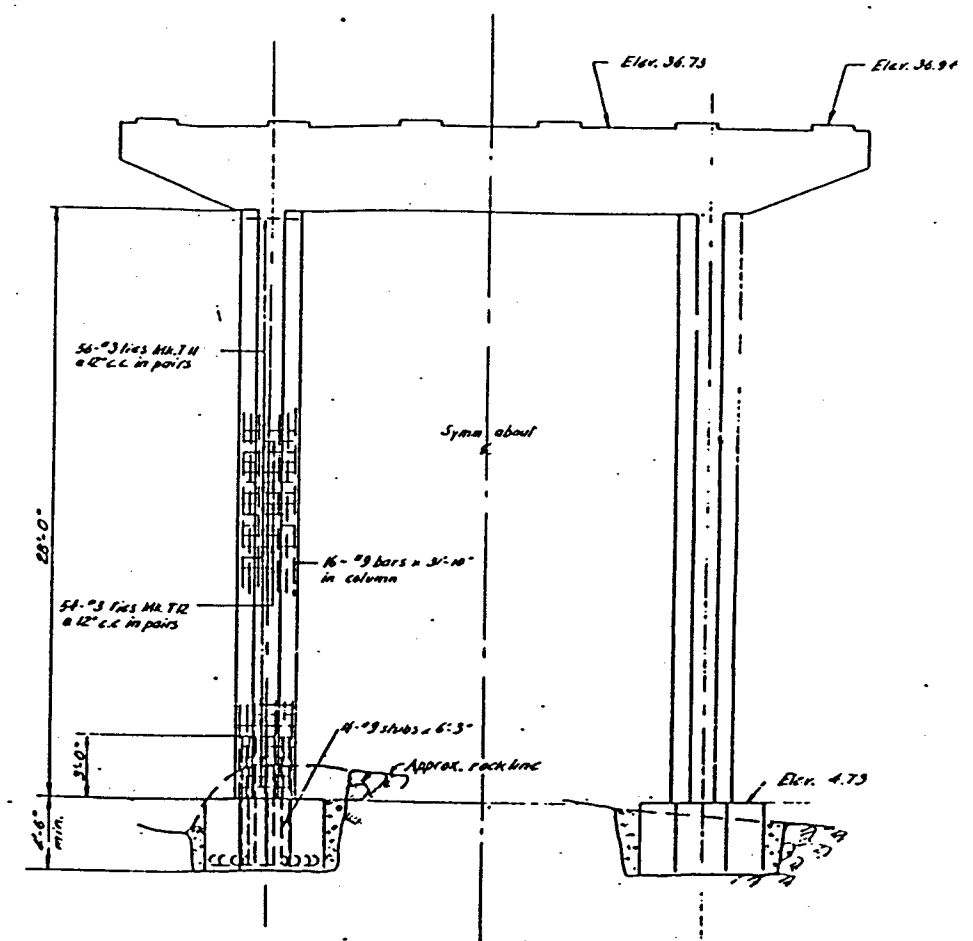

BENT 3

All details not shown same as bent 2

LIST OF REINFORCING (FOR BENT 2 & 3)						
LOCATION	SIZE	MK.	NO.	W	L	BENDING
Bim of beams	W	(D)	(8)	-	-	35'-4"
Top of beams	W	E	16	-	35'-8	
Footings	6	F	16	-	2'-4"	
	6	G	16	-	3'-4"	
	6	H	16	-	4'-4"	
	6	J	16	-	5'-4"	
	6	K	32	-	5'-6"	
Ties in beams	4	T3	6	1'-8½"	1'-1½"	
	4	T4	8	2'-0"	1'-1½"	
	4	T5	8	2'-3½"	1'-1½"	
	4	T6	8	2'-7"	1'-1½"	
	4	T7	8	2'-10½"	1'-1½"	
	4	T8	8	3'-2"	1'-1½"	
	4	T9	8	3'-5½"	1'-1½"	
	4	T10	36	3'-8"	2'-8"	
Ties in columns	3	T11	242	2'-0"	1'-2½"	
	3	T12	236	1'-11"	1'-1"	
Bim of beams	W	-	8	-	-	18'-0" straight bars
Cols. (Bent 2)	W	-	16	-	-	35'-4" " "
Stubs	W	-	16	-	-	7'-3" " "
Cols. (Bent 2)	9	-	16	-	-	39'-10" " "
Cols. (Bent 3)	9	-	32	-	-	31'-10" " "
Stubs	9	-	48	-	-	6'-3" " "
Sides of beams	4	-	-	-	-	280 lin. ft. straight bars
						#15 ga. black annealed wire lbs. 190
						Total weight lbs. 19,000

Care to be taken in setting bolts to ensure pipes are properly centered thereon. Open ends of pipes to be sealed with blocks as shown to exclude water until erection of steelwork. Use Fibregum or equal to secure watertightness.

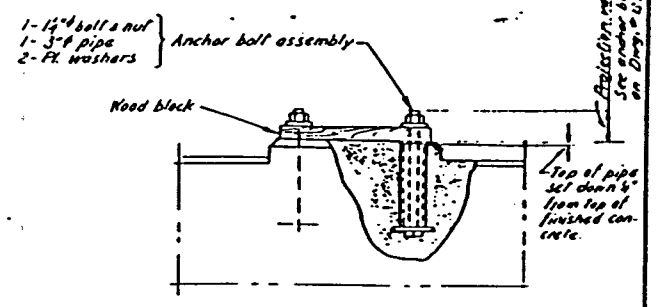

DETAIL OF BRIDGE SEATS

SCALE: 1" = 1'-0"

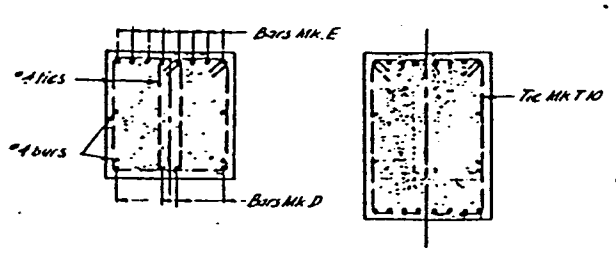

SECTION A-A

SCALE: ½" = 1'-0"

SECTION B-B

SCALE: ½" = 1'-0"

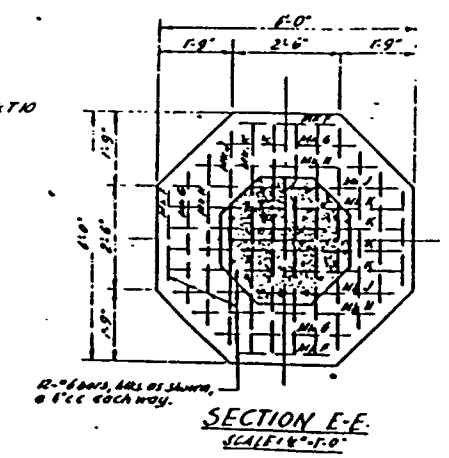

SECTION E-E

SCALE: ½" = 1'-0"

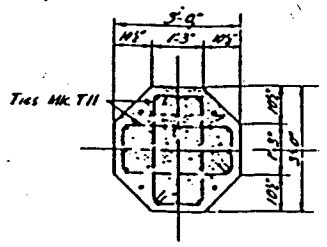

SECTION C-C

SCALE: ½" = 1'-0"

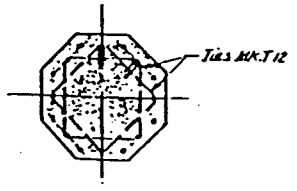

SECTION D-D

SCALE: ½" = 1'-0"

NOTES:
1. Concrete to be class A throughout.
2. Chamfer edges of beam 1".
3. Reinforcing steel cover 3" on footings, 2" elsewhere
4. Splices, where necessary, are to be 40 diameters.
5. Footings of bents to be carried down to solid rock as directed by the engineer

Estimated quantity of concrete for Bent - 2 & 3 — 73 cu. yds.

SAANICH DISTRICT
TRANS-CANADA HIGHWAY - MILE 14
COLQUITZ RIVER BRIDGE
BENTS 2 & 3
SCALE: ½" = 1'-0" & AS NOTED

REVISIONS			
No.	Description	Init.	Date
A	As built	[illegible]	Aug '54

GOVT. of BRITISH COLUMBIA
DEPT. of PUBLIC WORKS
BRIDGE ENGINEER'S OFFICE

	Init.	Date
Made by	N.F.	May '54
Checked by	[illegible]	[illegible]

DRAWING NO.

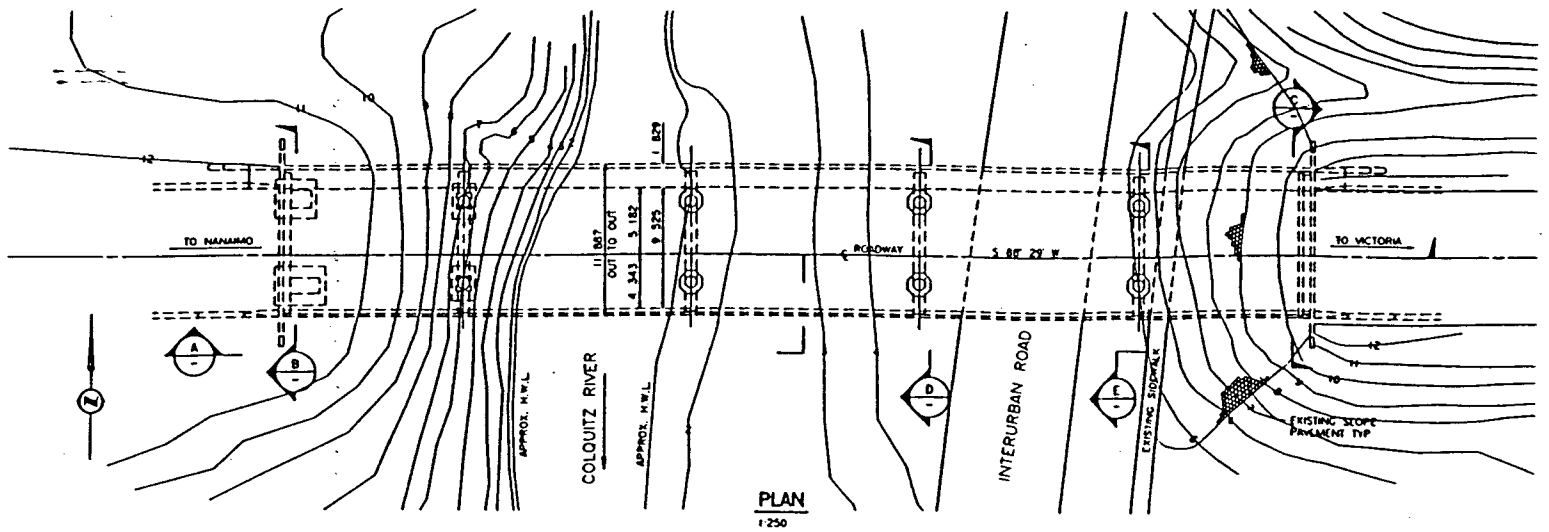

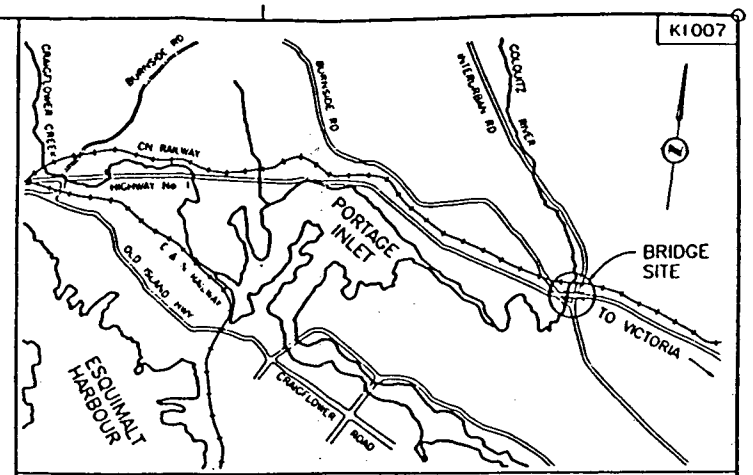

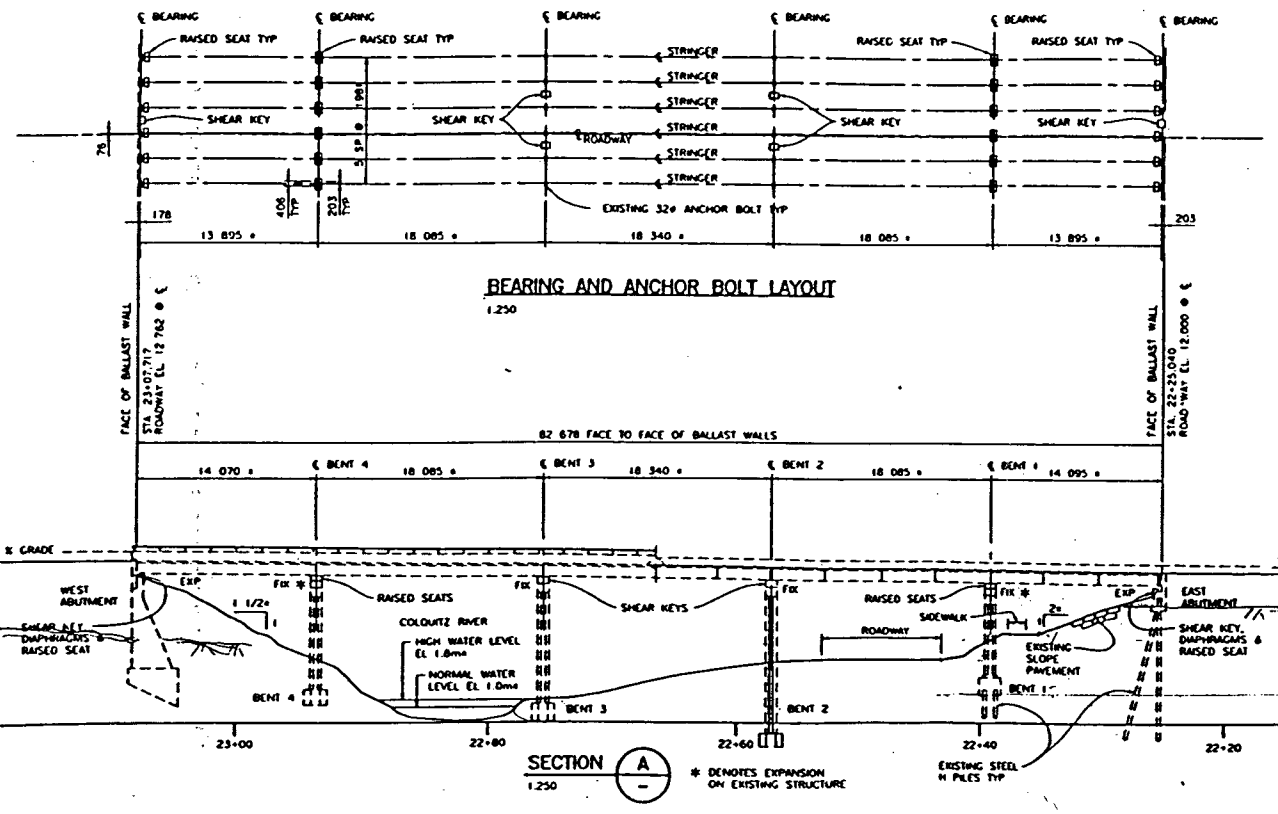

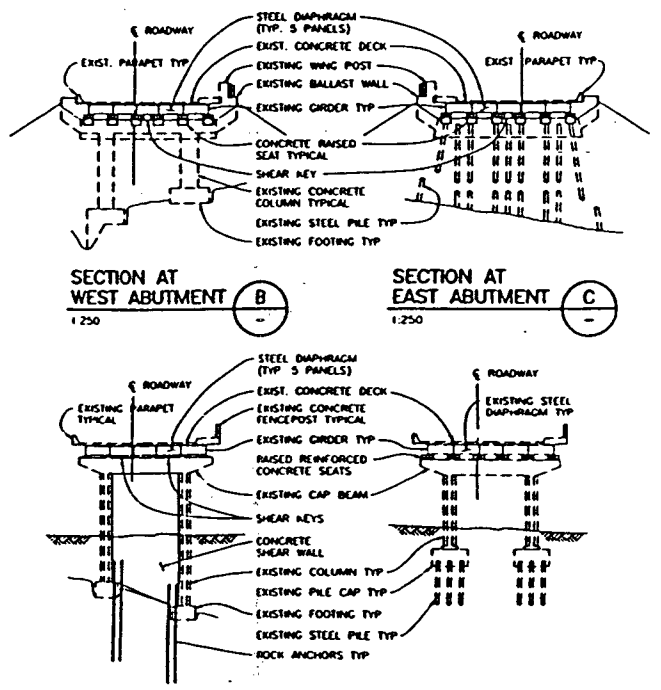

NOTES:

1. DATUM: - GEODETIC
2. SURVEY: - M.O.T.H.
3. STATIONS, ELEVATIONS AND DIMENSIONS SHOWN HAVE BEEN SOFT CONVERTED TO METRIC BASED ON EXISTING "AS BUILT" DRAWINGS. IT IS THE CONTRACTOR'S RESPONSIBILITY TO FIELD VERIFY ALL INFORMATION PERTAINING TO THE EXISTING STRUCTURE
4. FOR DETAILS OF EXISTING STRUCTURE REFER TO MINISTRY OF TRANSPORTATION AND HIGHWAYS "AS BUILT" DRAWINGS (1953) AND (1977)
5. THE STRUCTURAL IMPROVEMENTS SHOWN ON THESE DRAWINGS WERE ACCORDING TO THE "INTERIM SEISMIC ASSESSMENT AND REHABILITATION REQUIREMENTS FOR B.C. HIGHWAY STRUCTURES" (1994) FOR A SEISMIC SAFETY RETROFIT.
6. PERFORMANCE GOALS OF THE SEISMIC SAFETY RETROFIT WERE TO PREVENT COLLAPSE AND REDUCE DAMAGE DAMAGE AND/OR BRIDGE CLOSURES MAY BE EXPECTED UNDER THE DESIGN EARTHQUAKE
7. DESIGN EARTHQUAKE - 10% CHANCE OF OCCURRENCE IN 50 YEARS, OR A RETURN PERIOD OF APPROXIMATELY 475 YEARS
8. RESPONSE SPECTRA IN ACCORDANCE WITH AASHTO STANDARD SPECIFICATIONS FOR HIGHWAY BRIDGES, 1992 (DIVISION I-A, SEISMIC DESIGN)
9. SEISMIC RETROFIT DESIGN REFERENCES
   (a) SEISMIC RETROFITTING GUIDELINES FOR HIGHWAY BRIDGES, ATC-6-2. APPLIED TECHNOLOGY COUNCIL, CALIFORNIA, AUGUST, 1983
   (b) MEMO TO DESIGNERS 20-4, CALIFORNIA DEPARTMENT OF TRANSPORTATION, APRIL 6, 1992
9. (CONT)
   (c) DESIGN GUIDELINES FOR ASSESSMENT, RETROFIT AND REPAIR OF BRIDGES FOR SEISMIC PERFORMANCE; PRESTLEY, M.J.N.; SEIBLE, F.; AND CHAI, Y.H.; DEPARTMENT OF APPLIED MECHANICS AND ENGINEERING SCIENCES, UNIVERSITY OF CALIFORNIA, SAN DIEGO, STRUCTURAL SYSTEMS RESEARCH PROJECT, REPORT NO. SSRP-92/01, AUGUST, 1992, PAGES 103-180.
10. DESIGN CODE FOR NEW COMPONENTS:
    (a) CAN/CSA-S6-88
    (b) AASHTO - STANDARD SPECIFICATIONS FOR HIGHWAY BRIDGES (1992)
11. SEISMIC COEFFICIENTS: A = 0.35, S = 1.2, CLASSIFICATION = II
12. EXISTING MATERIAL STRENGTHS: (DETERMINED FROM DRAWINGS WITH MODIFICATIONS) f'_c = 30 MPa, f_y = 300 MPa (REINFORCING STEEL), F_y = 248 MPa (STRUCTURAL STEEL) (380 MPa BEARINGS AT PIERS ONLY)
13. FOR DESCRIPTION OF RETROFIT STRATEGY REFER TO SEISMIC STRATEGY REPORT DATED SEPTEMBER 1994 PREPARED BY CWMM LTD
14. RETROFIT DESIGN SUMMARY:
    (a) SUPERSTRUCTURE RETROFIT: - STEEL DIAPHRAGMS ARE ADDED AT BOTH ABUTMENTS AND NEW DIAPHRAGMS REPLACE EXISTING ONES AT BENTS 2 AND 3.
        - SHEAR CONNECTORS ARE ADDED AT ALL SUPPORTS TO TRANSFER LATERAL FORCES TO SUBSTRUCTURE.
    (b) BENT RETROFIT: - REINFORCED CONCRETE WALLS, ROCK ANCHORS AND SHEAR KEYS ADDED AT BENTS 2 AND 3 TO INCREASE LATERAL RESISTANCE.
        - REINFORCED CONCRETE RAISED SEATS ADDED AT BENTS 1 AND 4 TO PREVENT LOSS OF SUPPORT.
    (c) ABUTMENT RETROFIT: - REINFORCED CONCRETE RAISED SEATS ADDED TO PREVENT LOSS OF SUPPORT AND SHEAR KEYS ARE ADDED TO TRANSFER LATERAL FORCES TO BOTH ABUTMENTS

REFERENCE DRAWINGS	
NUMBER	TITLE
1378-3	LAYOUT, KEY MAP & ANCHOR BOLT PLAN
1378-4	WEST ABUTMENT
1378-5	EAST ABUTMENT
1378-6	BENTS #2 & #3
1378-7	BENTS #4 & #4
1378-8	STEELWORK DETAILS
1378-9	DECK DETAILS
1378-10	ANCHOR BOLT ASSEMBLIES
1378-25	MODIFICATIONS TO EXISTING DECK

LIST OF DRAWINGS	
NUMBER	TITLE
1378-30	GENERAL ARRANGEMENT
1378-31	BENT MODIFICATIONS - SHEET 1
1378-32	BENT MODIFICATIONS - SHEET 2
1378-33	ABUTMENT MODIFICATIONS - SHEET 1
1378-34	ABUTMENT MODIFICATIONS - SHEET 2

CWMM CONSULTANTS

SCALE 1:250 UNO

DESIGNED J.S. DATE JAN-17-95
CHECKED D.D.B. DATE JAN-17-95
DRAWN J.C. DATE JAN-20-95

No.	Date	Description	Init.

REVISIONS

Province of British Columbia
MINISTRY OF TRANSPORTATION AND HIGHWAYS
BRIDGE ENGINEERING BRANCH

SOUTH ISLAND HIGHWAY DISTRICT
TRANS CANADA HIGHWAY
COLQUITZ RIVER BRIDGE No. 1378
SEISMIC SAFETY RETROFIT
GENERAL ARRANGEMENT

PREPARED BY — DATE — FILE No.
RECOMMENDED — DIRECTOR OF BRIDGE ENGINEERING — DATE
ACCEPTED FOR CONSTRUCTION — CHIEF HIGHWAY ENGINEER — DATE
NEGATIVE No. — REC
DRAWING No. 1378-30

K1007

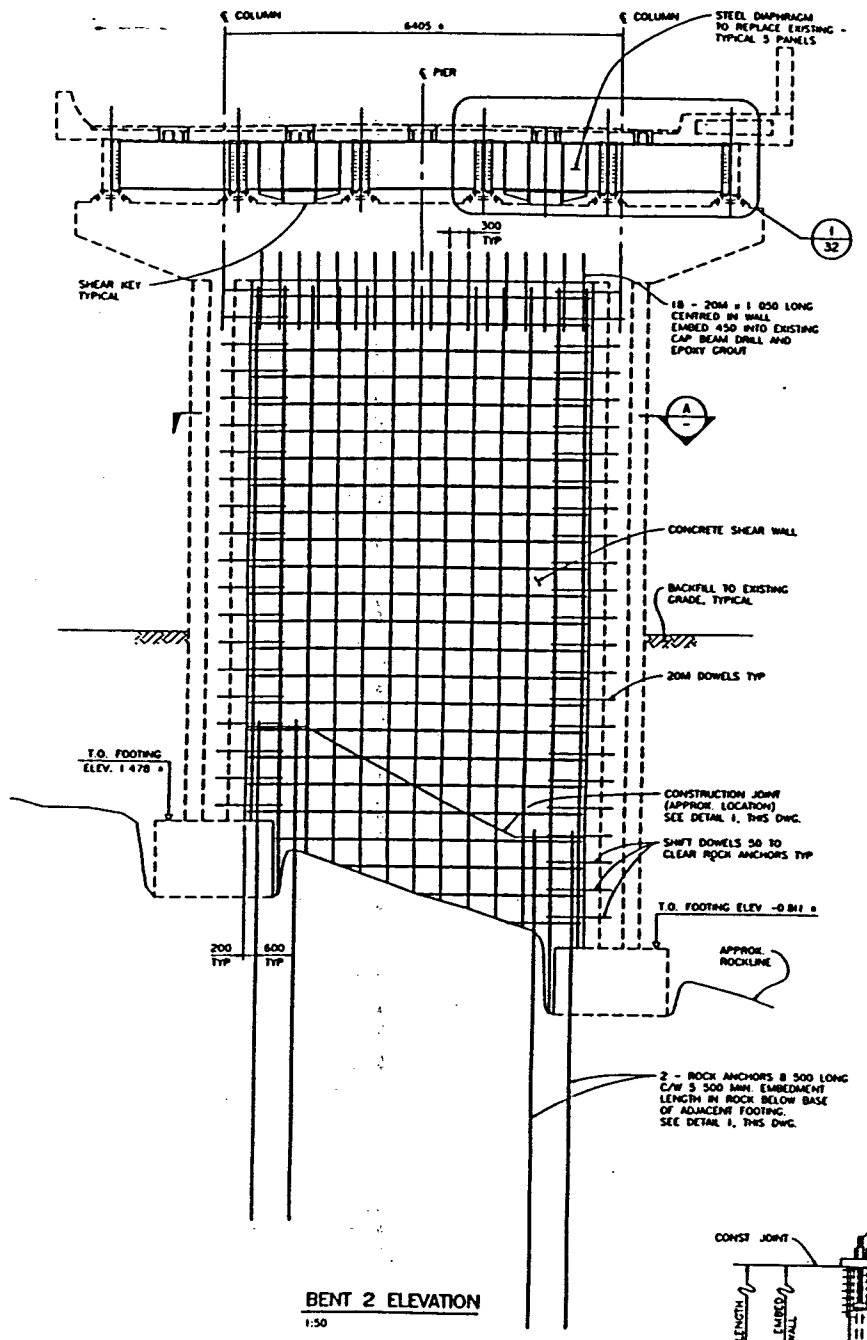

BENT 2 ELEVATION
1:50

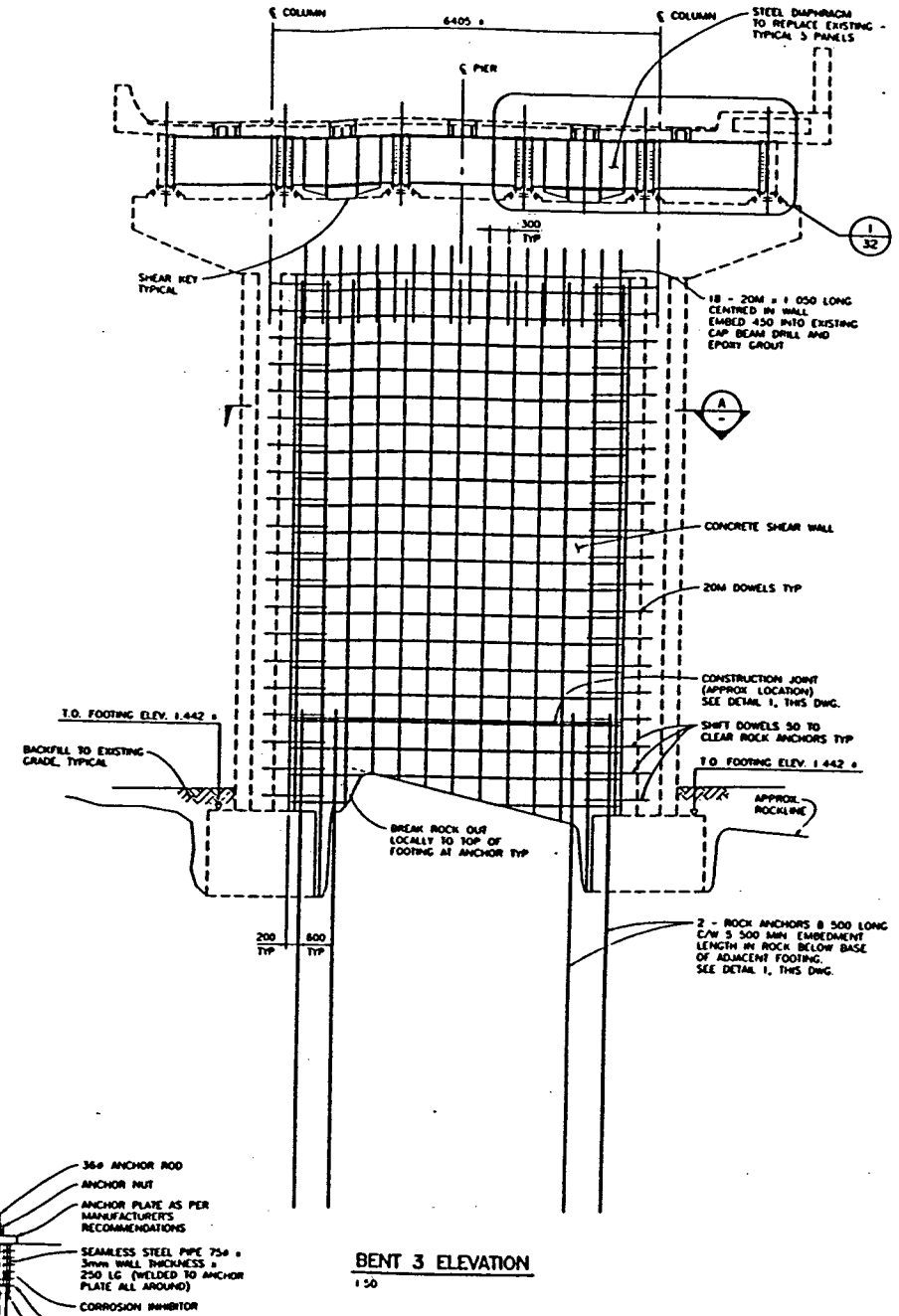

BENT 3 ELEVATION
1:50

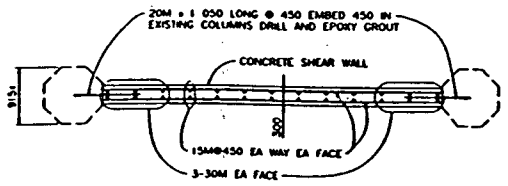

SECTION A
1:50

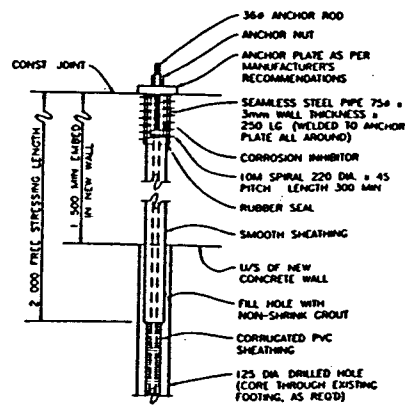

DETAIL 1
1:20

CONCRETE NOTES:

1. ALL CONCRETE SHALL HAVE A MINIMUM COMPRESSIVE STRENGTH OF 35 MPa AT 28 DAYS EXCEPT AS NOTED
2. ALL EXPOSED EDGES OF CONCRETE SHALL BE CHAMFERED 20 UNLESS NOTED OTHERWISE.
3. ALL REINFORCING STEEL SHALL CONFORM TO C.S.A. SPECIFICATION G30.18M GRADE 400R
4. ALL REINFORCING STEEL SHALL HAVE 50 COVER UNLESS NOTED OTHERWISE.
5. ALL LAPS OF REINFORCING SPLICES SHALL BE AS FOLLOWS UNLESS NOTED OTHERWISE:

BAR SIZE	LAP	LAP FOR TOP BARS (1)
10M	340	475
15M	480	675
20M	585	820
25M	905	1 265

(1) HORIZONTAL BARS WITH MORE THAN 300mm CONCRETE BELOW BARS.

6. DIMENSIONS SHOWN ARE AT 15°C UNLESS NOTED OTHERWISE.
7. CONTACT SURFACES WITH EXISTING CONCRETE SHALL BE ABRASAE OR HIGH PRESSURE WATER BLAST CLEANED TO EXPOSE EXISTING AGGREGATE AND SHALL BE COATED WITH EPOXY BONDING AGENT PRIOR TO CONCRETING. APPLICATION OF EPOXY BONDING AGENT SHALL BE IN STRICT ACCORDANCE WITH MANUFACTURER'S RECOMMENDED PROCEDURES
8. EPOXY BONDING AGENT SHALL CONFORM TO ASTM SPECIFICATION C881, TYPE V, GRADE 2, CLASS TO SUIT TEMPERATURE AND SHALL BE APPROVED BY THE MINISTRY.
9. EPOXY GROUT FOR REBAR DOWELS SHALL CONFORM TO ASTM SPECIFICATION C881, TYPE IV, GRADE 3, CLASS TO SUIT TEMPERATURE AND SHALL BE APPROVED BY THE MINISTRY. HOLES SHALL BE COMPLETELY CLEAN AND FREE OF MOISTURE. DOWELS SHALL BE INSTALLED BY AN APPROVED METHOD WHICH ENSURES COMPLETE BONDING WITHIN THE HOLE
10. THE CONTRACTOR SHALL AVOID CUTTING EXISTING REINFORCING, UNLESS NOTED OTHERWISE.
11. CONCRETE WALLS SHALL BE CAST IN PLACE TO UNDERSIDE OF EXISTING CAP BEAM, LEAVING NO CAVITIES.
12. CONCRETE WALLS SHALL EXTEND DOWN TO BEDROCK. BEDROCK SURFACE SHALL HAVE ALL LOOSE MATERIAL REMOVED AND SHALL BE BLOWN CLEAN PRIOR TO CASTING WALL.
13. DIMENSIONS INDICATED FOR LOCATIONS OF NEW DOWELS TO BE DRILLED INTO EXISTING CONCRETE ARE APPROXIMATE. IT IS THE CONTRACTOR'S RESPONSIBILITY TO ESTABLISH LOCATIONS OF EXISTING REINFORCING PRIOR TO DRILLING. REFER TO AS-BUILT DRAWINGS

ANCHOR NOTES:

1. ROCK ANCHORS SHALL BE GRADE 835/1030 AND SHALL CONFORM TO C.S.A. SPECIFICATION G279-M82. INSTALLATION SHALL BE AS PER MANUFACTURER'S RECOMMENDATIONS.
2. ALL ROCK ANCHORS SHALL BE CENTRED WITHIN CONCRETE WALLS.
3. ANCHOR SYSTEM SHALL BE DYWIDAG OR APPROVED EQUAL.
4. GROUT FOR ANCHORS SHALL BE NON-SHRINK CEMENT GROUT SUPPLIED BY AN APPROVED MANUFACTURER OF CEMENT PRODUCTS. MINIMUM COMPRESSIVE STRENGTH SHALL BE 25 MPa AT 7 DAYS AND 35 MPa AT 28 DAYS.
5. DESIGN LOAD FOR EACH ANCHOR = 667 KN.
   LOCK OFF LOAD = 100 KN.

STEEL NOTES:

1. ALL STEELWORK SHALL CONFORM TO C.S.A. SPECIFICATION CAN3-G40.21M GRADE 300W U.N.O.
2. NEW STEELWORK SHALL BE PAINTED PER SPECIFICATIONS, UNLESS NOTED OTHERWISE. ALL FAYING SURFACES SHALL BE PRIME COATED ONLY.
3. ALL DIMENSIONS PERTAINING TO THE EXISTING STRUCTURE SHALL BE FIELD VERIFIED BY THE CONTRACTOR PRIOR TO FABRICATION.
4. ALL BOLTS SHALL CONFORM TO ASTM A325 TYPE 1, WITH THREADS EXCLUDED FROM SHEAR PLANE U.N.O.
5. FIELD CONNECTIONS SHALL BE 22 DIA. BOLTS IN 24 DIA HOLES U.N.O.
6. GALVANIZING SHALL BE IN ACCORDANCE WITH C.S.A. SPECIFICATION G164, TABLE 1.
7. DIMENSIONS SHOWN ARE AT 15°C U.N.O.
8. EXISTING STEELWORK SHALL BE BLAST CLEANED TO SSPC-SP6 AND PRIME COATED LOCALLY AT ALL NEW FAYING SURFACES.
9. WHERE TOUCHUP PAINTING OF EXISTING STEELWORK IS REQUIRED LOCALLY AS A RESULT OF NEW STEEL INSTALLATION OR DAMAGE, PRIME, STRIPE, UNDCOAT AND TOPCOATS SHALL BE APPLIED AS PER THE "STRUCTURAL STEELWORK" APPENDIX.
10. SHEAR STUDS SHALL CONFORM TO ASTM SPECIFICATION A-108, GRADE C-1020, AND SHALL BE FUSION WELDED FOR COMPLETE PENETRATION.

FIELD CONFIRM ALL DIMENSIONS

C/W/M CONSULTANTS

SCALE AS NOTED

DESIGNED JJ DATE 30-12-94
CHECKED BBB DATE 30-12-94
DRAWN JC DATE 29-12-94

Rev.	Date	Description	Init.

REVISIONS

Province of British Columbia
MINISTRY OF TRANSPORTATION AND HIGHWAYS
BRIDGE ENGINEERING BRANCH

SOUTH ISLAND HIGHWAY DISTRICT
TRANS CANADA HIGHWAY
COLQUITZ RIVER BRIDGE No. 1378
SEISMIC SAFETY RETROFIT
BENT MODIFICATIONS - SHEET 1

PREPARED BY: DATE 1/12/95 FILE No.
RECOMMENDED: DIRECTOR OF BRIDGE ENGINEERING DATE 95-05-05 NEGATIVE No.
ACCEPTED FOR CONSTRUCTION: CHIEF HIGHWAYS ENGINEER DATE 25 05 08
REG
Drawing No. 1378-31

K1007

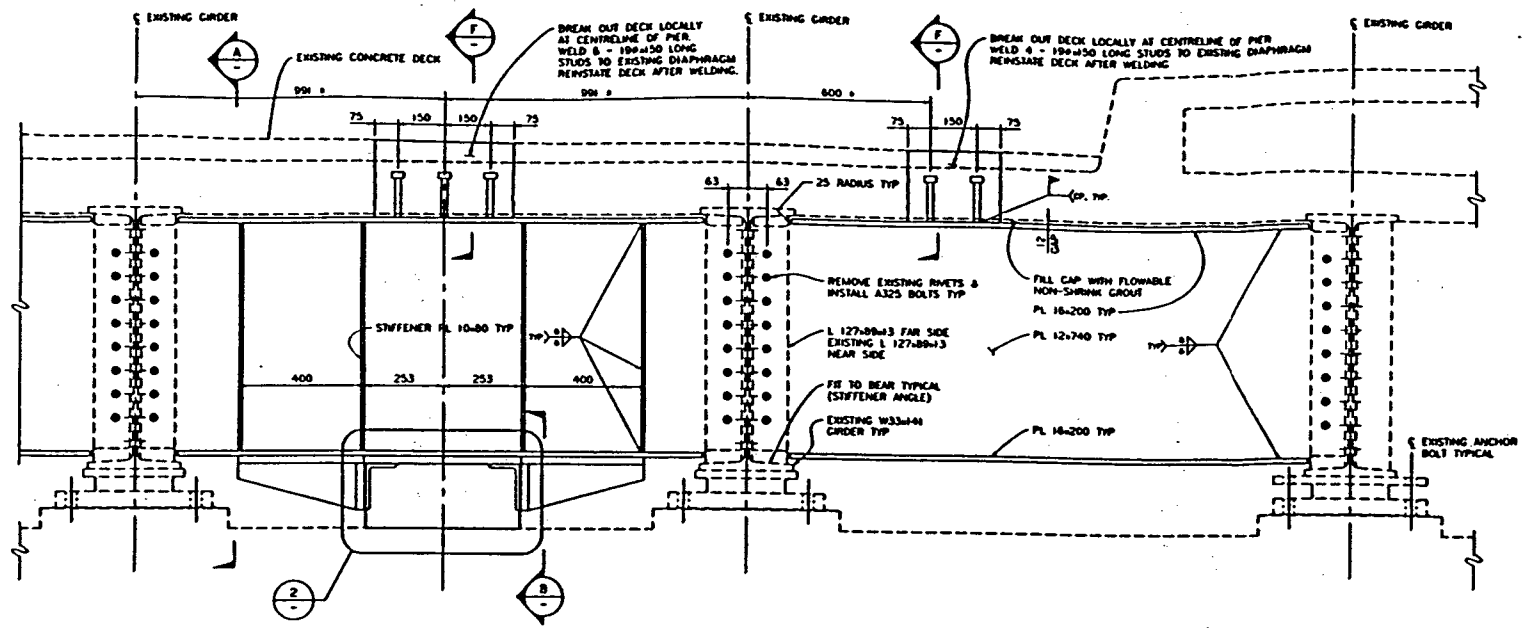

CONNECTION BETWEEN DIAPHRAGM AND EXISTING GIRDERS AT BENTS 2 & 3 — 1/31
1:10

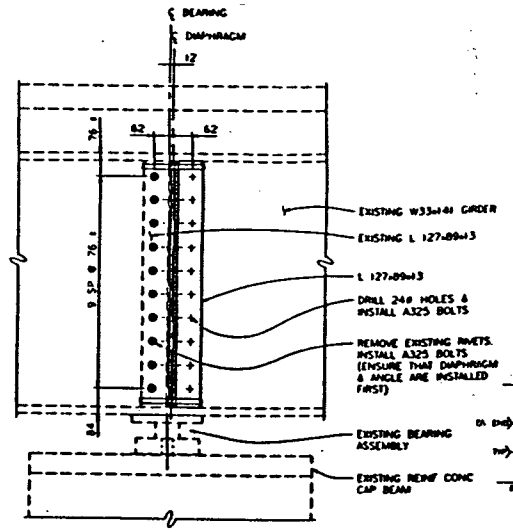

CONNECTION BETWEEN DIAPHRAGM AND EXISTING GIRDERS — A
1:10

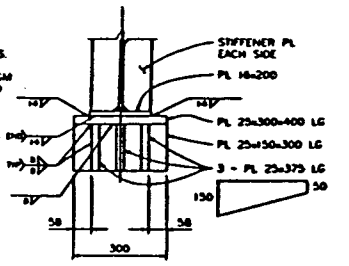

SECTION STEEL BRACKET — B
1:10

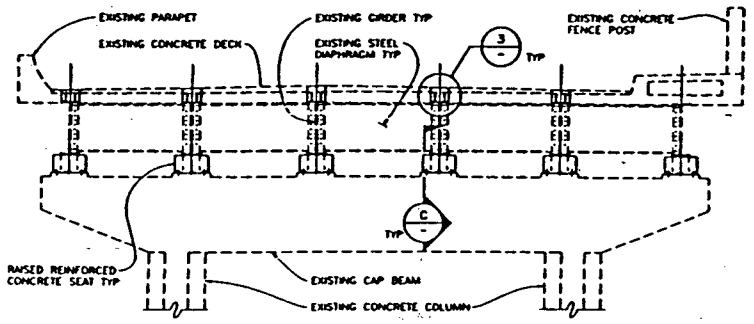

BENT 1 PARTIAL ELEVATION (BENT 4 ELEVATION SIMILAR)
1:50

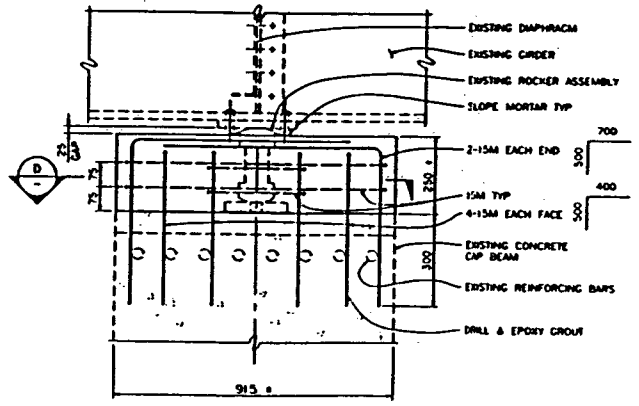

SECTION AT RAISED SEATS AT BENTS 1 AND 4 — C
1:10

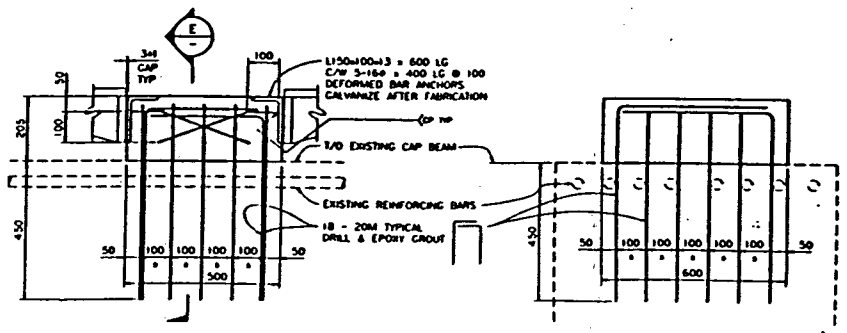

NOTE: CAST SHEAR KEYS AFTER DIAPHRAGM INSTALLATION

SHEAR KEY DETAIL AT BENTS 2 & 3 — 2
1:10

SECTION — E
1:10

KEY
- ● REMOVE EXISTING RIVETS, INSTALL A325 BOLTS.
- + DRILL 24ø HOLES, INSTALL A325 BOLTS.

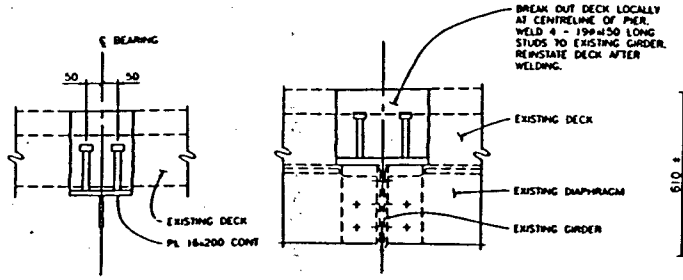

SECTION — F
1:10

DETAIL — 3
1:10

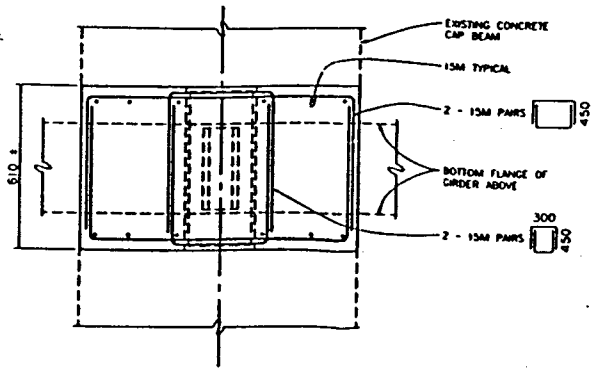

SECTION — D
1:10

FIELD CONFIRM ALL DIMENSIONS

NOTE:
SEE DRAWING 1378-31 FOR NOTES

C|W M|M CHRISTIANSEN WOLFSTEINER MCKINNEY MARKHAM CONSULTANTS

SCALE AS NOTED

DESIGNED J.S. DATE 96-12-96
CHECKED B.B.J. DATE 96-12-96
DRAWN J.C. DATE 96-10-96

No.	Date	Description	Init.

REVISIONS

Province of British Columbia
MINISTRY OF TRANSPORTATION AND HIGHWAYS
BRIDGE ENGINEERING BRANCH

SOUTH ISLAND HIGHWAY DISTRICT
TRANS CANADA HIGHWAY
COLQUITZ RIVER BRIDGE No. 1378
SEISMIC SAFETY RETROFIT
BENT MODIFICATIONS - SHEET 2

PREPARED BY	RECOMMENDED	ACCEPTED FOR CONSTRUCTION
DATE	DIRECTOR OF BRIDGE ENGINEERING DATE	CHIEF HIGHWAYS ENGINEER DATE 98 05 08
FILE No.	MEGAFILE No.	REG. DRAWING No. 1378-32

Appendix A2 Geotechnical report for Colquitz Bridge

Ministry of Transportation and Highways

SUMMARY LOG

Geotechnical and Materials Branch

TEST HOLE No. TH94-2

Project COLQUITZ BRIDGE #2655 – SEISMIC UPGRADE

Location See drawing #15-3-138-1

Elevation 4.98m

Driller MoTH – C. Sleasman Method SOLID STEM AUGER

Dates 94-03-01

Depth (m)	Sample Type	Blowcount	Recovery (m)	Shear Strength (kPa)	Gradation % Sand	Silt	Clay	Index Properties WL	WP	W	Classification	Description	Other Tests
1	S	6	.10		–	–	–	–	–	19.9	GC/SC	Loose, brown and grey, sandy GRAVEL (FILL) with some boulders; trace to some clay	
1.8m													
2												Mottled brown, silty CLAY; trace to some sand; some gravel to 50 mm diameter	
3	T	–	.54	Lv 65	18	63	19	31	20	30.1 23.7	CL		
4													
5	T	–	.57	Lv 90	20	60	20	29	18	22.0	CL		
5.2m													
6	S	–	.60	Fv 26 R 5	9	61	30	34	20	37.3	CL	Soft to firm, grey, silty CLAY; trace to some sand (in seams), medium plastic	
7													
8	T	–	.55	Lv 16 Fv 18 R 4	8	49	43	43	23	52.2 30.7	CL		
9	T	–	.60	Lv 22 Fv 23 R 4	0	47	53	51	24	48.1 45.4	CH	–trace sand (in thin layers)	
10													
11	T	–	.57	Lv 25 Fv 26 R 3	0	46	54	48	24	48.6 53.6	CH	–horizontal partings (similar to slickensides), trace of sand (in seams)	
12	T	–	.57	Lv 27 Fv 23 R 4	0	46	54	56	26	49.8 52.7	CH	–occasional sand seam	
13													
14	T	–	.60	Lv 35 Fv 34 R 6	0	48	52	55	26	51.1 44.2	CH		
15	T	–	.60	Lv 49 Fv 42 R 10	0	45	55	58	26	53.3 40.2	CH		
16													
16.5m													
17												Clayey GRAVEL	

SAMPLE TYPE
A – Auger
C – Core
D – Denison
S – Split Spoon
T – Shelby Tube
W – Wash

SHEAR STRENGTH kPa
U – Unconfined Compression
Fv – Field Vane
Lv – Lab Vane
R – Remoulded

TESTS
M – Mechanical Analysis
Q,R,S – Triaxial Compression
C – Consolidation
DS – Direct Shear
w_L,w_P – Liquid, Plastic Limits
W – Moisture Content

Blowcount – Standard Penetration Test (ASTM 1956)

FILE No.

DRAWN BY: THURBER

SHEET 01 of 02

Ministry of Transportation and Highways

SUMMARY LOG

Geotechnical and Materials Branch

TEST HOLE No. TH94-2

Project COLQUITZ BRIDGE #2655 – SEISMIC UPGRADE

Location See drawing #15-3-138-1

Elevation 4.98m

Driller MoTH – C. Sleasman Method SOLID STEM AUGER

Dates 94-03-01

Drilling Details	Depth (m)	Sample Type	Blowcount	Recovery (m)	Shear Strength (kPa)	Gradation %			Index Properties			Classification	Description	Other Tests
						Gravel	Sand	Fines	w_L	WP	w			
		S	55	0.0		–	–	–	–	–	–		Clayey GRAVEL	
	19												18.6m END OF HOLE	
	20													
	21													
	22													
	23													
	24													
	25													
	26													
	27													
	28													
	29													
	30													
	31													
	32													
	33													
	34													
	35													

SAMPLE TYPE
A – Auger
C – Core
D – Denison
S – Split Spoon
T – Shelby Tube
W – Wash

SHEAR STRENGTH kPa
U – Unconfined Compression
Fv – Field Vane
Lv – Lab Vane
R – Remoulded

TESTS
M – Mechanical Analysis
Q,R,S – Triaxial Compression
C – Consolidation
DS – Direct Shear
w_L,WP – Liquid, Plastic Limits
W – Moisture Content

Blowcount – Standard Penetration Test (ASTM 1956)

FILE No.

DRAWN BY: THURBER

SHEET 02 of 02

MOTH - COLQUITZ BRIDGE #2655
CPT TEST HOLE 94-2

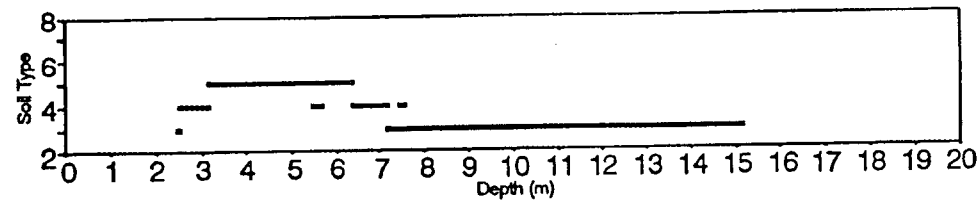

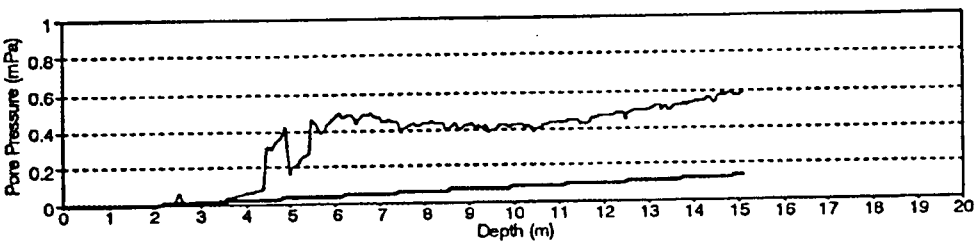

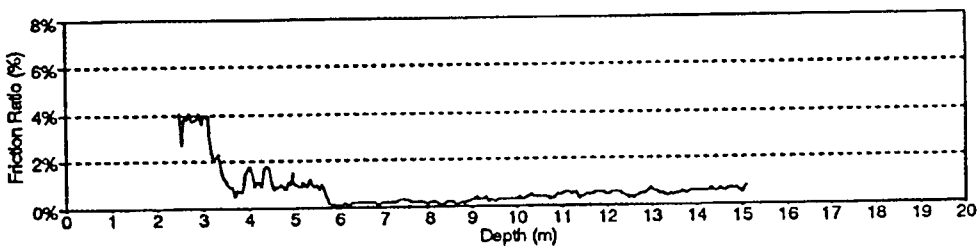

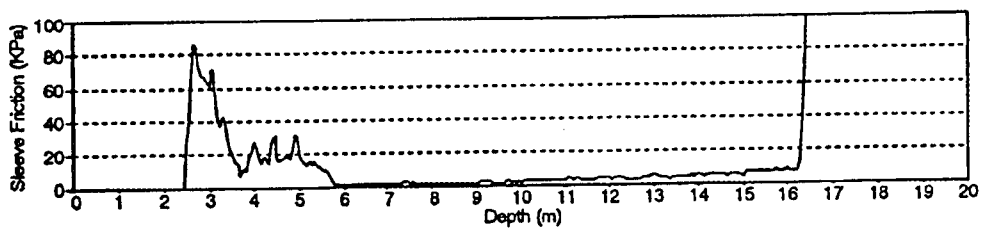

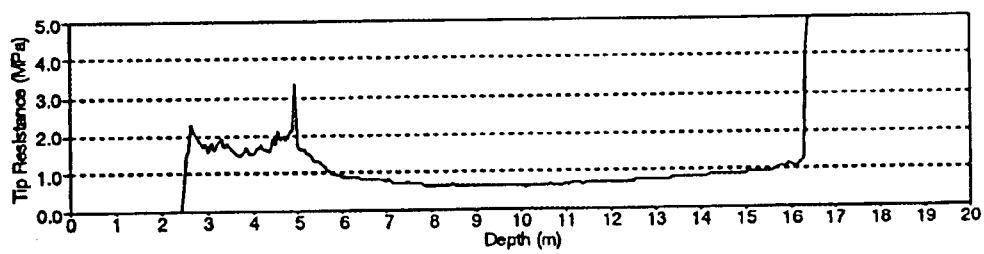

Colquitz Bridge 2655
94/03/02
Picks: D. Gillespie
Analysis: D. Gillespie
Job for Shannon Tao

OFFSET IS 1.0 m (horizontal)
Note: Depth is depth of geophone
which is 20 cm behind tip

DEPTH (m)	ARRIVAL (m/s)	CORR ARRIVAL (m/s)	AVERAGE DEPTH (m)	INTERVAL VELOCITY (m/s)
0.00	0.00	0.00		
			1.15	198
2.30	12.66	11.61		
			2.80	221
3.30	15.58	14.91		
			3.80	268
4.30	19.14	18.64		
			4.80	276
5.30	22.66	22.27		
			5.80	159
6.30	28.92	28.56		
			6.80	145
7.30	35.78	35.45		
			7.80	141
8.30	42.85	42.54		
			8.80	124
9.30	50.90	50.61		
			9.80	123
10.30	59.00	58.72		
			10.80	124
11.30	67.05	66.79		
			11.80	126
12.30	75.00	74.75		
			12.80	126
13.30	82.95	82.72		
			13.80	126
14.30	90.90	90.68		
			14.80	137
15.30	98.20	97.99		
			15.80	145
16.30	105.10	104.90		

Ministry of Transportation and Highways

SUMMARY LOG

Geotechnical and Materials Branch

TEST HOLE No. TH94-3

Project COLQUITZ BRIDGE #1378 – SEISMIC UPGRADE

Location See drawing #15-3-138-1

Elevation 11.84m

Driller MoTH – C. Sleasman Method SOLID STEM AUGER

Dates 94-03-03

Depth (m)	Sample Type	Blowcount	Recovery (m)	Shear Strength (kPa)	Gradation % Sand	Silt	Clay	Index Properties wL	wP	w	Classification	Description	Other Tests
1												Grey and brown, clayey SAND & GRAVEL (FILL); wet	
2													
3	S	24	.20		–	–	–	–	–	20.9	SC		
4													
5												5.5m	
6	S	11	.08		24	46	30	–	–	36.7	CL-CH	Firm to stiff, brown silty CLAY; trace of sand, medium plastic	
7													
8													
9	S	18	.30		6	38	56	49	25	34.3	CL-CH		
10												10.0m	
11												–transition to soft to firm, grey silty CLAY	
12	T	–	.60	Lv 35	0	58	42	47	24	34.8 38.4	CL		
13												12.5m Gravelly SAND	
14												13.5m END OF HOLE (refusal)	
15													
16													
17													

SAMPLE TYPE
A – Auger
C – Core
D – Denison
S – Split Spoon
T – Shelby Tube
W – Wash

SHEAR STRENGTH kPa
U – Unconfined Compression
Fv – Field Vane
Lv – Lab Vane
R – Remoulded

TESTS
M – Mechanical Analysis
Q,R,S – Triaxial Compression
C – Consolidation
DS – Direct Shear
wL,wP – Liquid, Plastic Limits
W – Moisture Content

Blowcount – Standard Penetration Test (ASTM 1956)

FILE No.

DRAWN BY: THURBER

SHEET 01 of 01

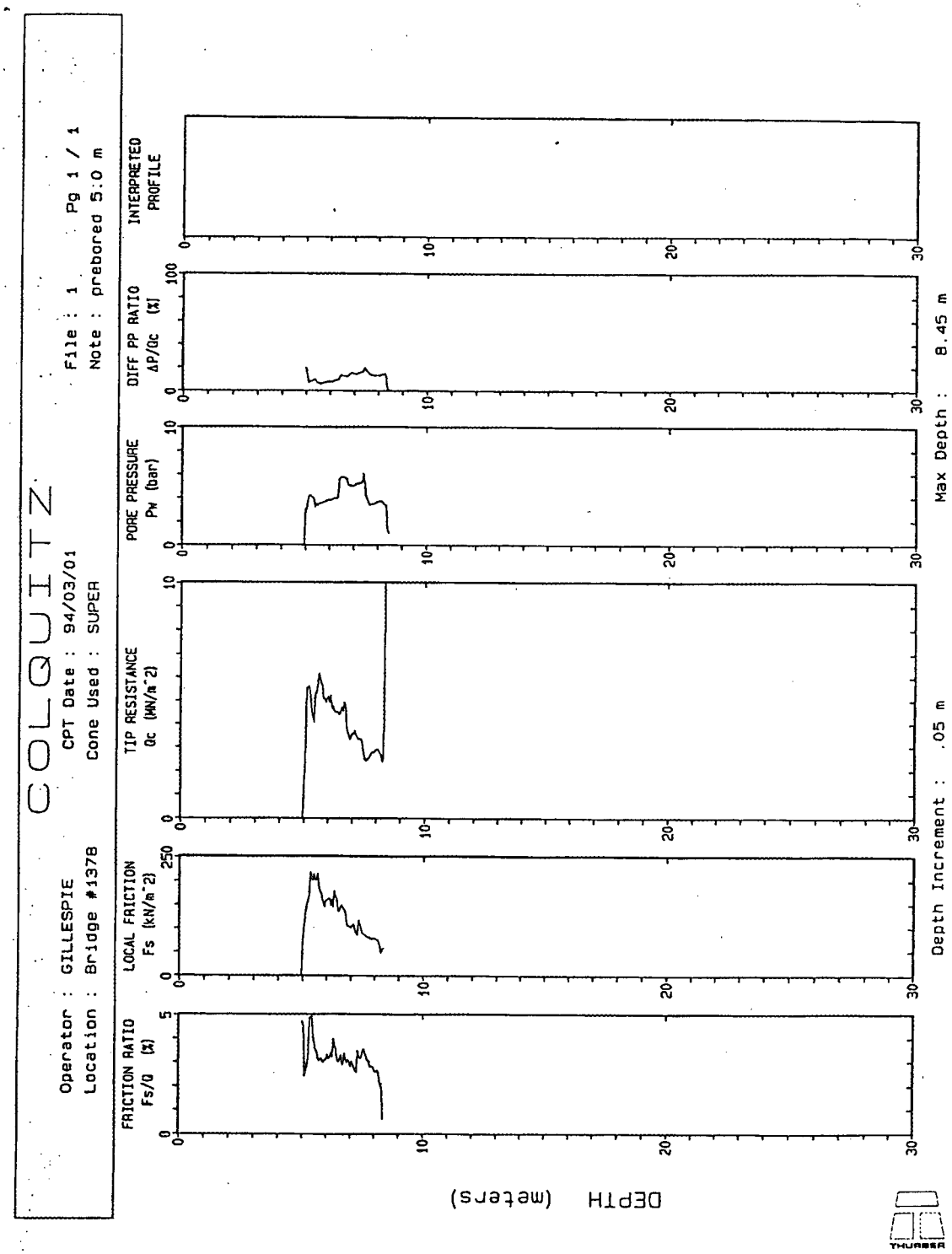
COLQUITZ
Operator : GILLESPIE
Location : Bridge #1378
CPT Date : 94/03/01
Cone Used : SUPER
File : 1
Note : prebored 5.0 m
Pg 1 / 1
FRICTION RATIO Fs/Q (%)
LOCAL FRICTION Fs (kN/m^2)
TIP RESISTANCE Qc (MN/m^2)
PORE PRESSURE Pw (bar)
DIFF PP RATIO ΔP/Qc (%)
INTERPRETED PROFILE
DEPTH (meters)
Depth Increment : .05 m
Max Depth : 8.45 m
THURBER

Colquitz Bridge #1378 OFFSET IS 1.0 m (horizontal)
94/03/01 Note: Depth is depth of geophone
Picks: D. Gillespie which is 20 cm behind tip
Analysis: D. Gillespie
Job for Shannon Tao

DEPTH (m)	ARRIVAL (m/s)	CORR ARRIVAL (m/s)	AVERAGE DEPTH (m)	INTERVAL VELOCITY (m/s)
0.00	0.00	0.00		
			2.63	180
5.25	29.65	29.13		
			5.75	192
6.25	33.00	32.59		
			6.75	227
7.25	37.35	37.00		
			7.75	238
8.25	41.50	41.20		

Appendix A3 SAP 2000 input file for response spectrum analysis

```
; File C:\My Documents\Global SAP analysis\Runs\run10.$2k saved 1/9/01 14:53:07 in
KN-m

SYSTEM
 DOF=UX,UY,UZ,RX,RY,RZ  LENGTH=m  FORCE=KN  LINES=59

COORDINATE
 NAME=CSYS1
 X=0  Y=0  Z=1
 X=1  Y=0  Z=0
 NAME=CSYS2  Z=20
 X=0  Y=0  Z=21
 X=1  Y=0  Z=20

JOINT
 1  X=10  Y=-4.05  Z=20
 2  X=14.7  Y=-4.05  Z=20
 3  X=19.4  Y=-4.05  Z=20
 4  X=24.1  Y=-4.05  Z=20
 5  X=28.6  Y=-4.05  Z=20
 6  X=33.1  Y=-4.05  Z=20
 7  X=37.6  Y=-4.05  Z=20
 8  X=42.1  Y=-4.05  Z=20
 9  X=46.7  Y=-4.05  Z=20
 10  X=51.3  Y=-4.05  Z=20
 11  X=55.9  Y=-4.05  Z=20
 12  X=60.5  Y=-4.05  Z=20
 13  X=65  Y=-4.05  Z=20
 14  X=69.5  Y=-4.05  Z=20
 15  X=74  Y=-4.05  Z=20
 16  X=78.5  Y=-4.05  Z=20
 17  X=83.2  Y=-4.05  Z=20
 18  X=87.9  Y=-4.05  Z=20
 19  X=92.6  Y=-4.05  Z=20
 20  X=10  Y=0  Z=20
 21  X=14.7  Y=0  Z=20
 22  X=19.4  Y=0  Z=20
 23  X=24.1  Y=0  Z=20
 24  X=28.6  Y=0  Z=20
 25  X=33.1  Y=0  Z=20
 26  X=37.6  Y=0  Z=20
 27  X=42.1  Y=0  Z=20
 28  X=46.7  Y=0  Z=20
 29  X=51.3  Y=0  Z=20
 30  X=55.9  Y=0  Z=20
```

```
 119 X=78.5 Y=4.05 Z=18.155
 120 X=78.5 Y=-3.2 Z=15.885
 121 X=78.5 Y=-3.2 Z=13.615
 122 X=78.5 Y=-3.2 Z=11.355
 123 X=78.5 Y=3.2 Z=15.885
 124 X=78.5 Y=3.2 Z=13.615
 125 X=78.5 Y=3.2 Z=11.355

RESTRAINT
 ADD=1 DOF=U3
 ADD=19 DOF=U3
 ADD=20 DOF=U3
 ADD=38 DOF=U3
 ADD=39 DOF=U3
 ADD=57 DOF=U3

PATTERN
 NAME=DEFAULT

SPRING
 ADD=1 U1=8131 U2=62830
 ADD=19 U1=14520 U2=25130
 ADD=20 U1=8131 U2=62830
 ADD=38 U1=14520 U2=25130
 ADD=39 U1=8131 U2=62830
 ADD=57 U1=14520 U2=25130
 ADD=71 U1=92700 U2=92700 U3=117700 R1=71760 R2=71760 R3=93260
 ADD=74 U1=92700 U2=92700 U3=117700 R1=71760 R2=71760 R3=93260
 ADD=88 U1=171900 U2=171900 U3=218300 R1=133100 R2=133100 R3=172900
 ADD=91 U1=171900 U2=171900 U3=218300 R1=133100 R2=133100 R3=172900
 ADD=105 U1=251300 U2=251300 U3=319100 R1=194500 R2=194500 R3=252800
 ADD=108 U1=251300 U2=251300 U3=319100 R1=194500 R2=194500 R3=252800
 ADD=122 U1=271800 U2=271800 U3=1384000 R1=772000 R2=329300 R3=1501000
 ADD=125 U1=271800 U2=271800 U3=1384000 R1=772000 R2=329300 R3=1501000

MASS
 ADD=2 U1=14.259 U2=14.259 U3=14.259
 ADD=3 U1=14.259 U2=14.259 U3=14.259
 ADD=4 U1=14.259 U2=14.259 U3=14.259
 ADD=5 U1=14.259 U2=14.259 U3=14.259
 ADD=6 U1=14.259 U2=14.259 U3=14.259
 ADD=7 U1=14.259 U2=14.259 U3=14.259
 ADD=8 U1=14.259 U2=14.259 U3=14.259
 ADD=9 U1=14.259 U2=14.259 U3=14.259
 ADD=10 U1=14.259 U2=14.259 U3=14.259
 ADD=11 U1=14.259 U2=14.259 U3=14.259
```

```
 ADD=12 U1=14.259 U2=14.259 U3=14.259
 ADD=13 U1=14.259 U2=14.259 U3=14.259
 ADD=14 U1=14.259 U2=14.259 U3=14.259
 ADD=15 U1=14.259 U2=14.259 U3=14.259
 ADD=16 U1=14.259 U2=14.259 U3=14.259
 ADD=17 U1=14.259 U2=14.259 U3=14.259
 ADD=18 U1=14.259 U2=14.259 U3=14.259
 ADD=21 U1=14.259 U2=14.259 U3=14.259
 ADD=22 U1=14.259 U2=14.259 U3=14.259
 ADD=23 U1=14.259 U2=14.259 U3=14.259
 ADD=24 U1=14.259 U2=14.259 U3=14.259
 ADD=25 U1=14.259 U2=14.259 U3=14.259
 ADD=26 U1=14.259 U2=14.259 U3=14.259
 ADD=27 U1=14.259 U2=14.259 U3=14.259
 ADD=28 U1=14.259 U2=14.259 U3=14.259
 ADD=29 U1=14.259 U2=14.259 U3=14.259
 ADD=30 U1=14.259 U2=14.259 U3=14.259
 ADD=89 U1=5.404 U2=5.404 U3=5.404
 ADD=90 U1=5.404 U2=5.404 U3=5.404
 ADD=99 U1=9.83 U2=9.83 U3=9.83
 ADD=100 U1=8.555 U2=8.555 U3=8.555
 ADD=101 U1=9.198 U2=9.198 U3=9.198
 ADD=103 U1=6.546 U2=6.546 U3=6.546
 ADD=104 U1=6.546 U2=6.546 U3=6.546
 ADD=106 U1=5.282 U2=5.282 U3=5.282
 ADD=107 U1=5.282 U2=5.282 U3=5.282
 ADD=116 U1=8.433 U2=8.433 U3=8.433
 ADD=117 U1=8.555 U2=8.555 U3=8.555
 ADD=118 U1=8.433 U2=8.433 U3=8.433
 ADD=120 U1=3.572 U2=3.572 U3=3.572
 ADD=121 U1=3.572 U2=3.572 U3=3.572
 ADD=123 U1=3.572 U2=3.572 U3=3.572
 ADD=124 U1=3.572 U2=3.572 U3=3.572

MATERIAL
 NAME=STEEL IDES=S
  T=0 E=1.999E+08 U=.3 A=.0000117 FY=248211.3
 NAME=CONC IDES=C
  T=0 E=1.154E+07 U=.2 A=.0000099
 NAME=OTHER IDES=N
  T=0 E=1E+10 U=0 A=.0000099
 NAME=CONC1 IDES=C
  T=0 E=1.246E+07 U=.2 A=.0000099
 NAME=CONC2 IDES=C
  T=0 E=1.344E+07 U=.2 A=.0000099
 NAME=CONC3 IDES=C
```

```
  T=0  E=1.087E+07  U=.2  A=.0000099
 NAME=CONC4  IDES=C
  T=0  E=1.087E+07  U=.2  A=.0000099

FRAME SECTION
 NAME=FSEC1 MAT=STEEL SH=R T=.5,.3 A=.15 J=2.817371E-03
I=.003125,.001125 AS=.125,.125
 NAME=GIRDER MAT=STEEL SH=R T=.381,.381 A=.0725805 J=4.807512E-04
I=1.656939E-02,.1739979 AS=.1209675,.1209675
 NAME=CROBEAM MAT=STEEL SH=R T=.192,.192 A=.036864 J=1.670801E-04
I=2.988567E-04,5.020091E-03 AS=.03072,.03072
 NAME=COL1 MAT=CONC1 SH=R T=.833,.833 A=.693889 J=6.780871E-02
I=3.835807E-02,3.835807E-02 AS=.5782408,.5782408
 NAME=COL2 MAT=CONC2 SH=R T=.833,.833 A=.693889 J=6.780871E-02
I=3.835807E-02,3.835807E-02 AS=.5782408,.5782408
 NAME=COL3 MAT=CONC3 SH=R T=.833,.833 A=.693889 J=6.780871E-02
I=3.835807E-02,3.835807E-02 AS=.5782408,.5782408
 NAME=COL4 MAT=CONC4 SH=R T=.833,.833 A=.693889 J=6.780871E-02
I=3.835807E-02,3.835807E-02 AS=.5782408,.5782408
 NAME=BRACING MAT=STEEL SH=R T=.247,.247 A=.0305045 J=5.241955E-14
I=3.101748E-14,3.101748E-14 AS=5.084083E-12,5.084083E-12
 NAME=CAPB1 MAT=CONC1 SH=R T=1.22,.915 A=1.1163 J=.168214
I=.1384584,7.788286E-02 AS=.93025,.93025
 NAME=CAPB2 MAT=CONC2 SH=R T=1.22,.915 A=1.1163 J=.168214
I=.1384584,7.788286E-02 AS=.93025,.93025
 NAME=CAPB3 MAT=CONC3 SH=R T=1.22,.915 A=1.1163 J=.168214
I=.1384584,7.788286E-02 AS=.93025,.93025
 NAME=CAPB4 MAT=CONC4 SH=R T=1.22,.915 A=1.1163 J=.168214
I=.1384584,7.788286E-02 AS=.93025,.93025
 NAME=FS1 MAT=OTHER SH=R T=1,1 A=1 J=.1408333 I=8.333334E-
02,8.333334E-02 AS=.8333333,.8333333

NLPROP
 NAME=NLPR1   TYPE=Damper
  DOF=U1  KE=0  CE=0
 NAME=BEARING   TYPE=Plastic1
  DOF=U1  KE=1E+10  CE=0
  DOF=U2  KE=1E+10  CE=0
  DOF=U3  KE=1E+10  CE=0
 NAME=BEAR2   TYPE=Plastic1
  DOF=U1  KE=1E+10  CE=0
  DOF=U2  KE=1E+10  CE=0
  DOF=U3  KE=1E+10  CE=0
 NAME=BEAR1   TYPE=Plastic1
  DOF=U1  KE=1E+10  CE=0
  DOF=U2  KE=1E+10  CE=0
```

```
  DOF=U3 KE=1E+10 CE=0

FRAME
 1 J=1,2 SEC=GIRDER NSEG=4 ANG=0
 2 J=2,3 SEC=GIRDER NSEG=4 ANG=0
 3 J=3,4 SEC=GIRDER NSEG=4 ANG=0
 4 J=4,5 SEC=GIRDER NSEG=4 ANG=0
 5 J=8,75 SEC=FS1 NSEG=2 ANG=0
 6 J=5,6 SEC=GIRDER NSEG=4 ANG=0
 7 J=6,7 SEC=GIRDER NSEG=4 ANG=0
 8 J=7,8 SEC=GIRDER NSEG=4 ANG=0
 9 J=8,9 SEC=GIRDER NSEG=4 ANG=0
 10 J=9,10 SEC=GIRDER NSEG=4 ANG=0
 11 J=10,11 SEC=GIRDER NSEG=4 ANG=0
 12 J=11,12 SEC=GIRDER NSEG=4 ANG=0
 218 J=36,18 SEC=BRACING NSEG=4 ANG=0
 219 J=18,38 SEC=BRACING NSEG=4 ANG=0
 220 J=29,11 SEC=BRACING NSEG=4 ANG=0
 221 J=11,31 SEC=BRACING NSEG=4 ANG=0
 222 J=31,13 SEC=BRACING NSEG=4 ANG=0
 223 J=13,33 SEC=BRACING NSEG=4 ANG=0
 224 J=33,15 SEC=BRACING NSEG=4 ANG=0
 225 J=15,35 SEC=BRACING NSEG=4 ANG=0
 226 J=35,17 SEC=BRACING NSEG=4 ANG=0
 227 J=17,37 SEC=BRACING NSEG=4 ANG=0
 228 J=37,19 SEC=BRACING NSEG=4 ANG=0

NLLINK
 1 J=63,60 NLP=BEAR2 ANG=0
 2 J=62,59 NLP=BEAR2 ANG=0
 3 J=61,58 NLP=BEAR2 ANG=0
 4 J=75,78 NLP=BEARING ANG=0
 5 J=76,79 NLP=BEARING ANG=0
 6 J=77,80 NLP=BEARING ANG=0
 7 J=92,95 NLP=BEARING ANG=0
 8 J=93,96 NLP=BEARING ANG=0
 9 J=94,97 NLP=BEARING ANG=0
 10 J=109,112 NLP=BEAR2 ANG=0
 11 J=110,113 NLP=BEAR2 ANG=0
 12 J=111,114 NLP=BEAR2 ANG=0

LOAD
 NAME=LOAD1

MODE
 TYPE=RITZ N=10
```

```
  ACC=UX
  ACC=UY
  ACC=UZ

FUNCTION
 NAME=VIC1 NPL=1 PRINT=Y
  .1 8.679
  .15 10.15
  .2 10.003
  .3 8.532
  .4 7.355
  .5 6.62
  1 2.942
  2 1.412
 NAME=VIC2 NPL=1 PRINT=Y
  .1 16.182
  .15 17.653
  .2 17.653
  .3 16.182
  .4 13.534
  .5 12.21
  1 5.59
  2 2.795

SPEC
 NAME=SPEC1 MODC=CQC ANG=0 DAMP=.05 DIRF=1
  ACC=U1 FUNC=VIC1 SF=1
  ACC=U2 FUNC=VIC1 SF=.4
 NAME=SPEC2 MODC=CQC ANG=0 DAMP=.05 DIRF=1
  ACC=U1 FUNC=VIC1 SF=.4
  ACC=U2 FUNC=VIC1 SF=1
 NAME=SPEC3 MODC=CQC ANG=0 DAMP=.05 DIRF=1
  ACC=U1 FUNC=VIC2 SF=1
  ACC=U2 FUNC=VIC2 SF=.4
 NAME=SPEC4 MODC=CQC ANG=0 DAMP=.05 DIRF=1
  ACC=U1 FUNC=VIC2 SF=.4
  ACC=U2 FUNC=VIC2 SF=1

OUTPUT
 ELEM=JOINT TYPE=DISP SPEC=SPEC1
 ELEM=JOINT TYPE=DISP SPEC=SPEC2
 ELEM=JOINT TYPE=DISP SPEC=SPEC3
 ELEM=JOINT TYPE=DISP SPEC=SPEC4
 ELEM=JOINT TYPE=REAC SPEC=SPEC1
 ELEM=JOINT TYPE=REAC SPEC=SPEC2
 ELEM=JOINT TYPE=REAC SPEC=SPEC3
```

```
 ELEM=JOINT  TYPE=REAC  SPEC=SPEC4
 ELEM=FRAME  TYPE=FORCE  SPEC=SPEC1
 ELEM=FRAME  TYPE=FORCE  SPEC=SPEC2
 ELEM=FRAME  TYPE=FORCE  SPEC=SPEC3
 ELEM=FRAME  TYPE=FORCE  SPEC=SPEC4

END
```

Appendix A4 CANNY input file for time history analysis

```
// analysis assumptions and output options

/* time history analysis of bent1 before retrofitting

title : BENT 1 Time History analysis (Before retrofitting)
title : Earthquake record: El Centro EQ, Magnitude 7.1
force unit = kn
length unit = m
time unit = sec

dynamic analysis in X-direction
gravity acceleration is 9.805 (default 9.8)

output of nodal displacement
output all of column response
output all of beam response
output all of support response
/*output period
output extreme response

// dynamic analysis control data

integration at time interval, 0.01
/* integration every 4 steps in the input accele. time interval
start time 0.0, end time 36.0
Newmark integration method, using Beta-value 0.25
/* Wilson integration method, using Theta-value 1.4
damping constant 0.05 to first mode
damping constant 0.05 to second mode
/* damping constant 0.05 to third mode
/* damping coefficient 0.01 to instantaneous stiffness K
/* damping coefficient 0.30 to mass matrix M
scale factor 0.00547 to X-EQ file = c:\canny\Ivalley.dat
/* scale factor 4.90 to X-EQ file = c:\canny\synthec1.dat
master DOFs for analysis control: X-translation at 8-node
response limit 1.0
check peak displacement 0.03
binary format output of analysis results at every 0-step

// node locations
node 1 , (-3.2 0 0)
node 2 , (-3.2 0 0.5)
node 3 , (-3.2 0 1.0)
node 4 , (-3.2 0 2.62)
node 5 , (-3.2 0 4.24)
```

node 6 , (-3.2 0 5.86)
node 7 , (-3.2 0 6.36)
node 8 , (-3.2 0 6.86)
node 9 , (3.2 0 0)
node 10 , (3.2 0 0.5)
node 11 , (3.2 0 1.0)
node 12 , (3.2 0 2.62)
node 13 , (3.2 0 4.24)
node 14 , (3.2 0 5.86)
node 15 , (3.2 0 6.36)
node 16 , (3.2 0 6.86)
node 17 , (-4.95 0 6.86)
node 18 , (4.95 0 6.86)
node 19 , (-2.7 0 6.86)
node 20 , (2.7 0 6.86)
node 21 , (-2.2 0 6.86)
node 22 , (2.2 0 6.86)
node 23 , (-0.99 0 6.86)
node 24 , (0.99 0 6.86)

// node degrees of freedom
general degrees of freedom : X-trans, Z-trans, X-Z rot
/* node 1 eliminate all components
/* node 2 eliminate all components

// weight at nodes
node 17 to 18 weight w = 251.5
node 23 to 24 weight w = 277.7
node 8 weight w = 323.7
node 16 weight w = 323.7
/*node 1 weight w = 46.0
/*node 9 weight w = 46.0

// element data : beam
17 8 out LU1 RU1 SU10 AU20
8 19 out LU1 RU2 SU10 AU20
19 21 out LU2 RU3 SU10 AU20
21 23 out LU3 RU3 SU11 AU21
23 24 out LU3 RU3 SU11 AU21
24 22 out LU3 RU3 SU11 AU21
22 20 out LU3 RU2 SU10 AU20
20 16 out LU2 RU1 SU10 AU20
16 18 out LU1 RU1 SU10 AU20

// element data : column
1 2 out BU50 TU51 SU60 AU70

```
2 3 out BU51 TU51 SU60 AU70
3 4 out BU51 TU51 SU60 AU70
4 5 out BU51 TU51 SU60 AU70
5 6 out BU51 TU51 SU60 AU70
6 7 out BU51 TU51 SU60 AU70
7 8 out BU51 TU50 SU60 AU70
9  10 out BU50 TU51 SU60 AU70
10 11 out BU51 TU51 SU60 AU70
11 12 out BU51 TU51 SU60 AU70
12 13 out BU51 TU51 SU60 AU70
13 14 out BU51 TU51 SU60 AU70
14 15 out BU51 TU51 SU60 AU70
15 16 out BU51 TU50 SU60 AU70

// element data : support
node 1 out TX U100
node 1 out TZ U110
node 1 out RY U120
node 9 out TX U100
node 9 out TZ U110
node 9 out RY U120

// stiffness and hysteresis parameters
/* beam flexural property (effective stiffness is 0.37 times gross section property)
/*U1 EL1 25740000.0 0.051
/*U2 EL1 25740000.0 0.051
/*U3 EL1 25740000.0 0.051
U1  CA7 25740000.0 0.051 C(500,500) Y(3000,3000)  A(1,1) B(0.00001,0.00001)
P(0.00001 2.0 0.25 0.025 1.0 0.7 0.7)
U2  CA7 25740000.0 0.051 C(500,500) Y(1665,1370)  A(1,1) B(0.00001,0.00001)
P(0.00001 2.0 0.25 0.025 1.0 0.7 0.7)
U3  CA7 25740000.0 0.051 C(500,500) Y(1866,1866)  A(1,1) B(0.00001,0.00001)
P(0.00001 2.0 0.25 0.025 1.0 0.7 0.7)

/* beam shear and axial property
U10 EL1 10730000.0 0.413
U11 EL1 10730000.0 0.413

U20 EL1 25740000.0 0.413
U21 EL1 25740000.0 0.413

/* column property
U50 CA7 25740000.0  0.019 C(500,500) Y(4000,4000) A(1,1)  B(0.00001,0.00001)
P(0.00001 2.0 0.25 0.025 1.0 0.7 0.7)
U51 CA7 25740000.0  0.019 C(500,500) Y(1863,1863) A(1,1)  B(0.00001,0.00001)
P(0.00001 2.0 0.25 0.025 1.0 0.7 0.7)
```

U60 EL1 10730000.0 0.347
U70 EL1 25740000.0 0.347

/* support: foundation spring property
U100 EL1 2.588E+6 0.1
U110 EL1 1.319E+7 0.1
U120 EL1 7.353E+6 0.1

// initial load before step and step analysis
beam 1 to 9 every 1 loade 26.2
node 17 Pz = 247.3
node 18 Pz = 247.3
node 8 Pz = 293.3
node 16 Pz = 293.3
node 23 to 24 Pz = 247.3
/*node 8 Pz = 46
/*node 16 Pz = 46
//